University of Southern Queensland
Faculty of Engineering & Surveying

A Comparison of Measured Diesel Emissions in Agriculture and Australian National Standard Emission Factors

A thesis submitted by

Ahmed Adel Naji

in fulfilment of the requirements of

Master Degree

Submitted: February, 2013

Abstract

Diesel engines used in highly mechanised agriculture can contribute a significant proportion of the total green house gas emissions generated on farm. Stringent GHG emission control legislations internationally imposed for off-road diesel engines are applied on tractors as part of off-road mobile sources. Australian national GHG emission factors (EF) are based on the Intergovernmental Panel on Climate Change Guidelines emissions factors, and in turn, those emissions factors are taken from studies conducted in 1975. The accuracy of these EFs are questioned by many researchers due to, *i*) no consideration of the transient effects of engine performance on emissions, *ii*) measurements were based on a relatively small sample of tractors and *iii*) studies were based on older tractor models with engine technology superseded by developments during the last 40 years. Inaccurate emissions factors lead to inaccurate estimates of the emission thereby over reporting in the annual emission inventory report. This research work addresses the issue related to transient effects and engine technology that affect the emission factors.

A 68.8 kW, Belarus 920 tractor was used in this study to evaluate the tractor performance and the exhaust gas emission component such as CO, CO_2 and NO_x. This study aims to evaluate Australian emission factors for agricultural tractor

considering the transient effects on tractor operating condition. Steady-state test (ECE R-49) and the European Stationary Cycle Test were used to assess the emission factors. The experimental apparatus consists of PTO dynamometer, fast response portable gas analyser type CODA, speed sensors, flow rate measuring systems, thermocouples and pressure transducers.

Transient test result was compared with steady-state test result. The experimental results demonstrated that transient produce higher emission for CO_2 and NO_x (3.73% and 33.58% respectively). CO emission of transient test was lower by 44.26% than steady-state emission.

CO_2-equivalent emissions were calculated for the ECE R-49 , ESC, and Constant Speed tests based on time integrated fuel consumption using the Australian emission factors. The calculations resulted in 11.8 % (on average) less emissions than real measurements indicating there is a need for revising the emission factors or the followed methodology.

Certification of Dissertation

I certify that the ideas, designs and experimental work, results, analyses and conclusions set out in this dissertation are entirely my own effort, except where otherwise indicated and acknowledged.
I further certify that the work is original and has not been previously submitted for assessment in any other course or institution, except where specifically stated.

Ahmed Adel Naji

0061009457

_____

Signature of Candidate

_____

Date

ENDORSEMENT

_____	_____
Signature of Principle Supervisor	Signature of Associated Supervisor
_____	_____
Date	Date

Acknowledgments

First and foremost I would like to express my sincere appreciation and gratitude to Associate Professor Talal Yusaf, my principle supervisor and friend, for his insight. My associate supervisor, Mr. Craig Baillie also provided valuable contribution in shaping this work. I am truly appreciative for their support and guidance throughout my study. I am also grateful to them for giving me the opportunity to work on this research project which has helped me to broaden my knowledge and develop new skills.

I would like also to acknowledge the great contribution to this project by Dr Paul Baker, Dr Troy Jensen and Dr Lez Bowtail in calibrating the experimental set-ups. I would like to thank all the technical staff in the faculty of engineering and surveying especially: Dean Beliveau, Victor Skowronski and Richard Landers in developing the data acquisition system and Yi Jiang (Jack), Adrian Blokland, Daniel Eising and Mohan Trada for their technical assistance. A special thank you for Terry Byrne and Graham Holmes for helping in providing the required resources.

I would like to extend my gratitude to my friend Dr Saddam Al-Lwayzy for his assistance in the experiments and for providing generous consultations in the agricultural part of the project. And also I would like to thank my friend Sinan

Al-Harjani for helping in recording the measurements and Dr Ahmed Al-sabawy for performing the statistical analysis using SPSS software.

As a part of my appreciation, I extend my gratitude to Mr James Binnie who generously agreed to tackle the arduous task of proof reading the manuscript.

I am very grateful to my parents and my sisters Rana and Rusol for their support during my study. And a big thank for all my friends Mei Ling Lau (Sindy) and Ibrahim Al-Jobori for their support through toughest stage of my study, writing the dissertation.

Finally, my greatest appreciation and gratitude is to the Iraqi government which sponsored my study and provided me the opportunity to fulfil my dream.

Ahmed Adel Naji

University of Southern Queensland

February 2013

Contents

List of Figures

List of Tables

Notation

C_a	Percentage of carbon to the mass of a fuel
C_i	Density of the measured fuel (kg/kL)
C_{jct}	Proportion of gas type (j) in the volume of the gas stream
$\overline{\mathrm{CO}}$	CO weighted specific emission (g/kWh)
$\mathrm{CO}_{(\mathrm{conc})}$	CO concentration (ppm)
$\mathrm{CO}_{(\mathrm{mass})}$	CO mass flow rate (g/h)
$\overline{\mathrm{CO}_2}$	CO_2 weighted specific emission (g/kWh)
$\mathrm{CO}_{2(\mathrm{conc})}$	CO_2 concentration (ppm)
$\mathrm{CO}_{2(\mathrm{mass})}$	CO_2 mass flow rate (g/h)
E_{ij}	Emissions of gas j of fuel i (kg CO_2-e)
e_{ij}	Average litres consumed per kilometre travelled
EC_i	Energy content (GJ/kL)
$EF_{ij,ox,ec}$	Emission factor of gas j (kg CO_2-e/GJ)
$EF_{i,\mathrm{CO}_2,ox,kg}$	Emission factor of CO_2 (kg CO_2-e/kg of fuel)
$EF_{i,\mathrm{CO}_2,ox,ec}$	Emission factor of CO_2 (kg CO_2-e/GJ)
FR_{ct}	Flow rate of the gas stream (m^3/s)
$\mathrm{H_a}$	Humidity of the air (g of water per kg dry air)
K_d	Engine power correction factor
k_{ij}	Annual kilometres travelled per vehicle

$K_{H,D}$	NO_x correction factor for humidity an temperature
M_{jct}	Mass of emissions of gas type (j) (ton/s)
MM_j	Molecular mass of gas type (j) (ton/kilomole)
$\dot{m}_{exhw}$	Wet exhaust gas mass flow rate (kg/h)
$\dot{m}_{aird}$	Dry intake air mass flow rate (kg/h)
$\dot{m}_{fuel}$	Fuel mass flow rate (kg/h)
n_{hi}	High engine speed (rpm) for ESC test
n_{ij}	Number of vehicles type i fuel type j
n_{lo}	Low engine speed (rpm) for ESC test
$\overline{NO_x}$	NO_x weighted specific emission (g/kWh)
$NO_{x(mass)}$	NO_x mass flow rate (g/h)
$NO_{x(conc)}$	NO_x concentration (ppm)
OF_i	Oxidation factor
P_a	Saturation vapour pressure of the air (kPa)
P_B	Total barometric pressure (kPa)
P_{ct}	Pressure of the gas stream (kPa)
$P(n)_i$	Engine power for mode number i
P_s	Ambient pressure (kPa)
Q_i	Quantity of the combusted fuel i (kL)
R_a	Relative humidity of the air (%)
T, T_a, T_{ct}	Temperature (K)
WF_i	Weighting factor for mode number i
λ	Lambda – normalized A/F ratio

Acronyms & Abbreviations

CH_4	Methane
CI	Compression Ignition
CO	Carbon Monoxide
CO_2	Carbon Dioxide
CO_2-e	Carbon Dioxide Equivalent
COP 3	Third Conference of Parties
CUEDC	Composite Urban Emissions Drive Cycle
DCCEE	Department of Climate Change and Energy Efficiency
EC	Energy Content
EEA	European Environment Agency
EF	Emission Factor
EGR	Exhaust gas recirculation
ESC	European Stationary Cycle
ETC	European Transient Cycle
EUD	European Union Directive
GHGs	Greenhouse gasses
H_2O	Water
HC	Hydrocarbons and Total Hydrocarbons
HD	Heavy-Duty Diesel Engine

IPCC	Intergovernmental Panel on Climate Change
KP	Kyoto Protocol
NEPC	National Environment Protection Council
NGA	Australian National Greenhouse Accounts
NGERD	National Greenhouse and Energy Reporting (Measurement) Determination
N_2O	Nitrous Oxide
NO	Nitrogen Monoxide
NO_2	Nitrogen Dioxide
NO_x	Oxides of Nitrogen (refer to NO and NO_2)
O_2	Oxygen
O_3	Ozone
PM	Particulate Matter
ppm	part per million
PTO	Power-Take-Off
rpm	Revolution per minute
SFC	Specific fuel consumption
SI	Spark Ignition
THC	Total Hydrocarbons
UNFCCC	United Nations Framework Convention on Climate Change

Chapter 1

INTRODUCTION

1.1 Overview

The growing dependence on fossil fuel-based energy input in the agricultural practices to enhance the productivity has contributed significantly to the total emission of greenhouse gases (GHGs) emitted per year. The GHG emissions have a major impact on global warming and subsequently influence the climate change. In order to reduce the GHG emissions in Australia, regulations were enforced by central and local governments and they are designed to be consistent with the international regulations. Various studies have questioned the adequacy of these regulation to the Australian agricultural practices (Dalal et al., 2008).

1.1.1 The issue of climate change

Substantial increases in the major greenhouse gases have taken place during the industrial era. A wide range of studies involving direct and indirect measurements

confirms that the amount of CO_2 has dramatically risen in the atmosphere. Over the last two and half centuries, CO_2 concentration has increased by 38% induced primarily by humans (Raupach and Fraser, 2011). It reached a 100 ppm increase in 2005 (Forster et al., 2007; Dalal et al., 2008) and a 110 ppm in 2009 (Raupach and Fraser, 2011); it became 386 ppm after it was at the normal level of 280 ppm before 1750 (Houghton et al., 1996; Forster et al., 2007; Le Treut et al., 2007). Fifty five percent of the change in CO_2 atmospheric concentration has occurred in the last 50 years and can be directly attributable to human activities (Forster et al., 2007). Whereas, the absolute growth for the first 50 ppm above the pre-industrial value occurred slowly in the atmosphere for more than 200 years until the 1950s. The highest average increase rate of CO_2 recorded, has occurred over the period from 1958 to 2005 is 1.4 – 1.5 ppm per annum (Lacis et al., 1990; Forster et al., 2007).

1.1.2 Future impact of the current use of energy

The current total energy consumption and the structure of energy supply will determine the future Earth's climate (Nakicenovic et al., 2000). CO_2, methane (CH_4) and Nitrous Oxide N_2O, which are known as long-lived greenhouse gas emissions, remain in the atmosphere for about a century until they dissipate. In 1990, the total anthropogenic emission of CO_2 was estimated to be 7.1 GtC/yr (5.5 GtC/yr is from fossil fuel production and combustion) where 3.3 GtC/yr is stored into the atmosphere (Houghton et al., 1996). For the period between 1999 to 2005, a linear averaged increase at a rate of roughly 3% per year occurred in

the global emissions from fossil fuel and cement production (Forster et al., 2007). It takes 30 years for 40-60% of the currently emitted GHGs to be consumed by the environment and nearly a hundred years for full removal (Houghton et al., 1996).

1.1.3 Australian agriculture reliance on fossil based energy

According to Dalgaard et al. (2001), 5% of the total global energy is consumed in the agriculture sector. The use of fossil energy in agriculture has become to the focus of many studies not only because fossil energy is an unsustainable resource and cannot be conserved for the future, but mainly because of its enormous contribution into the atmospheric greenhouse gas emissions and the ever-increasing cost (Chen and Baillie, 2007; Dalgaard et al., 2001). The combustion of fossil fuel (diesel fuel) in agricultural activities is responsible for producing 25% of the annual global CO_2 emissions (Salam et al., 2010) and represents 40% of the total emissions from on-farm activities as reported by Garnett (2011). These percentages illustrate the significant contribution of on-farm energy use emissions to the total GHGs from anthropogenic activities.

Australia is one of the largest exporters of agricultural commodities. In 2011, Australian agricultural land occupied about 53% of Australia's total mainland where the area planted to crops rose to 32.1 million hectares. On state-level measures, Queensland, with 81% of its land used for the farming, contributes 34% of Australia's total agricultural land (ABS, 2012). Chen and Baillie (2009)

pointed out that Australian agriculture growth is associated with intensive use of mechanised farming techniques. The utilised machines are mostly operated by fossil fuels (diesel) (Dyer and Desjardins, 2003; Baillie and Chen, 2011).

1.1.4 Diesel engine contribution

In the middle of the 20th century, mobile sources were recognised as one of the major inducers to the problem of air pollution (Pulkrabek, 2004; Wark et al., 1998). They accounted for one-fifth of the total energy use in 1990 (Nakicenovic et al., 2000). However, the first regulation regarding diesel gaseous pollutant was introduced in 1988 (Fritz and Pitchon, 1997).

The compression ignition (CI) engine is preferred in heavy duty equipment due to several characteristics (Chow, 2001). The most attractive feature is that it can demonstrate excellent fuel efficiency, which may exceed 40% in some vehicular applications resulting in desirable expenditure savings over the vehicle's lifetime (Rakopoulos and Giakoumis, 2009; Desantes et al., 2005). According to Wark et al. (1998), it can operate at a wide range of fuel-air mass ratios (0.01–0.06) which gives diesel engines the merit of lower sensitivity for load changes.

1.2 Background and Hypothesis

Agricultural diesel engine's contribution to the air pollution problem has captured the public attention in the recent years. It is generally accepted that the pop-

ulation of diesel-engine-powered vehicles has an increasing tendency (Al-lwayzy et al., 2012). The first agricultural mobile machinery powered by a diesel engine was a power plough produced by Benz-Sendling in 1922 (Lindgren, 2004). Since then, the use of diesel engine equipment, especially self-propelled equipment (tractors in the majority), has become dominant since the 50s of last century and almost all on-farm diesel fuel is consumed by these vehicles (Weaver, 1988; Dyer and Desjardins, 2003; Nelson et al., 2009).

Agricultural Industries within Australia are highly mechanised and dependent on fossil fuel (Chen and Baillie, 2009). within these industries a large component of GHGs is likely to come from fossil fuels. Therefore, the accuracy of how this is determined needs consideration.

Accounting for all the discussed facts regarding the role of agricultural machinery in enhancing the problem, emissions of those sources were incorporated (on the Australian national and the international level) when the estimate of the total annual GHGs was made. Moreover, the emission factors which are used in the calculations are derived from old studies and for other mobile sources which differ in the nature of their application from agricultural applications. This includes the IPCC's (1997*a*; 2006) and DCCEE's (2011) emission factors. Weaver (1988) reported that emission factors were extracted from an Environmental Research and Technology (ERT) report in 1982. The use of these emission factors was criticized as they were no longer representative because they had been measured in the early 70s from testing old tractor models which is no longer in use.

It may be argued that there have been significant advancements in technology

resulting in the development of cleaner diesel engines than those thirty years ago (Chow, 2001). Some of these techniques targeted engine efficiency and eventually improved fuel economy. Others explored the possibility of using alternative fuel sources with lower emissions. Some improved the methods of post-combustion treatment (e.i. EGR) for the exhaust products. However, the knowledge about the engine operational characteristics has expanded significantly mainly after espousing transient behaviour in the testing regimes which may indicate accordingly a variation in the measured emissions.

The heavy toll of climate change on the Earth's environment drives regional and international policy makers to impose stringent emissions regulations in response to this issue. Generalised regulations which comprise a wide range of engine categories are increasing the burden on the economic sector performance of countries by adding extra costs to product prices. Therefore, to propose a proper GHG concentration abatement strategy for a clean future environment, the quantity of the main GHG emissions arising from all anthropogenic activities each year should be estimated accurately.

1.3 Research Objectives

The objectives of this study are:

1. Determine how exhaust gas emissions from transient testing differs from steady-state.

2. Determine how emission factors vary with machinery applications.

3. Compare emissions determined from Australian emission factors for agriculture versus measured emission factors.

4. Revise or confirm emission factors for diesel fuel in agriculture.

1.4 Overview of the Dissertation

This dissertation is structured in 6 chapters and they are as follows:

- **Chapter 1** gives a brief introduction to the issue of emission estimation accuracy level. It contains the hypothesis behind this study and lists the targeted objectives.

- **Chapter 2** comprises a literature survey for three major areas of the knowledge related to this study. Section 2.2–2.3 examine the effects of GHGs on the Earth's climate and their major source in Australia. Then, in Section 2.4, the composition and combustion characteristics of diesel is discussed by covering the emissions from diesel combustion in different applications and conditions. Finally, Section 2.5 reviews the current methodologies relating to diesel engine certification and its emission regulation as well as diesel emission accounts in agriculture for the national inventories. The chapter outlines the difference between emission testing procedures currently in use.

- **Chapter 3** presents the methods and the equipment that were utilised in this research to achieve research objectives. It defines the research areas that are yet to be examined and explains the reasons behind omitting some areas. The chapter describes the specifications of the experimental apparatus and its commissioning and calibration. The experimental set-ups are described and presented as schematic diagram.

- **Chapter 4** presents the test procedures. The chapter also presents the experimental results of engine performance testing and steady state tests. It is then explained with a justification drawn from the literature for the acquired results.

- **Chapter 5** presents the experimental results of the transient test and the constant speed test. It is then explained with a justification drawn from the literature for the acquired results.

- **Chapter 6** concludes the dissertation by summarising the findings of the experimental results. It also includes recommended future work for researchers.

Chapter 2

LITERATURE REVIEW

2.1 Introduction

The first part of this chapter identifies the effect of changes in GHGs' percentages on the climate. It pinpoints the significance of studying the increasingly occurring changes. It is also of vital importance to review the international and national responses. Focusing more narrowly, the second part reviews the regulations that were put in place to control the emissions of human activities. The key objective of this thesis is to revise the Australian emission factors of agricultural machinery. Therefore, the last part of this chapter (2.4) is dedicated to reviewing the contribution of diesel engines to the problem of air pollution and how they are tested and certified by the major organizations.

2.2 Greenhouse Gas Emissions

Climate change science has been accumulated over centuries of careful observation of phenomena. The first weather observations started in Italy shortly after the invention of the thermometer in the early 17^{th} century (Seinfeld and Pandis, 2006; Le Treut et al., 2007). Thereafter, the early scientific understanding of the earth's greenhouse effect emerged in 1824 when Joseph Fourier stated that the regional climate changes are induced, in addition to the natural drivers, by the effects of human industry (cited in Fleming, 1998, p. 61). Pouillit, in 1836, followed up with an argument that the atmospheric layer plays a significant role in absorbing the solar heat (cited in Le Treut et al., 2007, p. 103). Induced by these findings, Tyndall (1861) conducted an experiment to study the heat absorption of different gasses and he inferred that changes in CO_2 and water (H_2O) in the atmosphere cause changes in the absorbed solar heat.

The knowledge about climate forcing-agents remained the same for a considerable time after Tyndall's experimental outcomes. More than a century later, in the 1970s, other greenhouse gasses such as CH_4 and N_2O were widely recognised and placed in perspective (Le Treut et al., 2007).

2.2.1 The impact on the climate

The Earth radiates all energy that reaches it surface from the Sun. This amount is estimated to be approximately 240 $W.m^{-2}$ and is radiated, in long-wave form, back to the space (Seinfeld and Pandis, 2006; Le Treut et al., 2007). In this

case the global mean temperature for the Earth would be −19 ℃, whilst the actual global mean temperature is 14 ℃. The presence of carbon dioxide and other greenhouse gases including aerosols have a blanketing effect on the long-wave radiated back from the Earth's surface by absorbing its energy leading to raise the Earth's temperature (Le Treut et al., 2007). Thus, human activities by which greenhouse gases are released intensify the blanketing effect and thereby warming the climate.

2.2.2 Methods of assessment and quantifying

As the climate science evolved over centuries, several metric measures were deployed to assess and compare the influence of external drivers of climate change. After years of studying the climate response to changes in CO_2 and solar insulation, the 'radiative forcing' concept arose and was employed to denote any perturbation caused by radiatively active constituents (Forster et al., 2007; Myher et al., 1998).

Ramaswamy et al. (2001) referred to the importance of counting the life span of a substance removal from the atmosphere, not only the radiative properties. They further explained that radiative properties are characterising the radiation absorption of a specified mass unit of a gas at any time, whereas a substance lifetime is a reflection of how long will continue to influence the thermal budget. It is also important to consider the lifetime of greenhouse gas emission in relation to a reference greenhouse gas in order to have a unified and simple means for emission trade-off (Forster et al., 2007). Global warming potentials (GWP) are the tool

to measure the time-integrated relative impact of a gas compared to a reference gas which is often CO_2 (Shine et al., 1990; Ramaswamy et al., 2001; Forster et al., 2007). Table 2.1 lists the values of GWPs for CO_2, CH_4 and N_2O quoted from different references.

Table 2.1: Primary GHGs' global warming potential for 100 years time span.

Gas	**Chemical formula**	**Global Warming Potential**		
		NGA & SAR[1]	**TAR**[2]	**AR4**[3]
Carbon dioxide	CO_2	1	1	1
Methane	CH_4	21	23	25
Nitrous oxide	N_2O	310	296	298
Carbon monoxide	CO	—	1 – 3	—

2.3 Greenhouse Gases Inventory Reporting

There are several methodologies to estimate the emissions of GHGs. They vary in the complexity and the accuracy of the calculation depending on the purpose behind the estimation. Traditionally, estimations have been conducted for the Australian national and the international emission inventories. Emission factors for various fuels have different levels of accuracy due to the significance of their contribution to GHG global concentrations and the cost of conducting the measurements. The accuracy of emission estimates is a function of how they have been determined. Factors such as kilometres travelled/actual working hours, load,

[1]IPCC Second assessment report.
[2]IPCC Third assessment report.
[3]IPCC Forth assessment report.

speed and the age of the engine also play a vital part in the accuracy of the result.

2.3.1 The UNFCCC and the Kyoto protocol

Imposing globally implemented legislations were believed to be the mitigation for the ever-increasing atmospheric concentrations of greenhouse gasses. In 1992, in Rio de Janeiro, approximately 160 countries ratified the United Nation Framework Convention on Climate Change (UNFCCC), where the principal objectives were to stabilise GHG concentrations and reduce them to harmless levels (IPCC, 1997*a*; Hediger, 2006; Filipovic et al., 2006). In the third conference of parties (COP 3), Kyoto Protocol was adopted with a principal target of 6% reductions in GHG emissions under the 1990 concentrations for the period between 2008 and 2012 (Srivastava and Oyama, 2009). The parties were committed to providing annual emissions data in the form of a periodical national inventory in order to achieve that target. Therefore, the Revised 1996 IPCC Guidelines for National Greenhouse Gas Inventories (1996 IPCC guidelines) accepted by the Intergovernmental Panel on Climate Change (IPCC) was intended to help the participants to report GHG emissions by using comparable methodologies (IPCC, 1997*a*). The 1996 IPCC guidelines came in a series of three books and were then followed by 2006 guidelines.

2.3.2 Australian national greenhouse accounts (NGA)

Ratifying the Kyoto Protocol (KP) in 2007, committed the Australian Government to submitting an annual greenhouse gas emissions inventory report for all sectors mentioned in the Intergovernmental Panel on Climate Change (IPCC) guidelines. The National Greenhouse Accounts (NGA) factors are organised and published by the Department of Climate Change and Energy Efficiency (DCCEE). It is aimed to assist Australian registered corporations and facilities to estimate and report the greenhouse gas emissions they release to the environment annually (DCCEE, 2010*a*). Australian Government has to compile those final numbers of the total emissions quantity and submit them in a national inventory report to the United Nations Framework Convention on Climate Change (UNFCCC) in accordance with the Kyoto Protocol.

The NGA factors are derived from National Greenhouse and Energy Reporting (Measurement) Determination 2008 (DCCEE, 2010*b*) which contains four methods of calculating the emissions released from the combustion of liquid fuels.

The first method is reasonably straightforward. It is about substitution of default emission factors (EF) of CO_2, methane (CH_4) and nitrous oxide (N_2O) and energy content (EC) for every fuel type using Equation 2.1 (DCCEE, 2010*b*):

$$E_{ij} = \frac{Q_i \times EC_i \times EF_{ij,ox,ec}}{1000}, \tag{2.1}$$

where:

$\boldsymbol{E_{ij}}$ is the emissions of CO_2-e measured in tonnes which is released from the combustion of fuel type (i) from a facility per year,

$\boldsymbol{Q_i}$ is the quantity of the fuel (i).

$\boldsymbol{EC_i}$ is the energy content of fuel (i).

$\boldsymbol{EF_{ij,ox,ec}}$ is the emission factor for emission (j) emitted from fuel (i) which includes the effect of an oxidation factor and expressed in kg CO_2-e/GJ.

EC and EF, for this methodology, are calculated for ideal conditions according to fuel type regardless to the combustion mechanism. The emission factors of heavy-duty diesel engines for this method are listed in Table 2.2.

Table 2.2: Emission factors for heavy duty diesel engines used for transportation and generalised for all heavy duty vehicles (DCCEE, 2011).

Transport equipment type	**Fuel**	**Energy content factor (GJ/kL)**	**Emission factor (kg CO_2-e/GJ)**		
			CO_2	**CH_4**	**N_2O**
Euro iv or higher	Diesel oil	38.6	69.2	0.05	0.5
Euro iii	Diesel oil	38.6	69.2	0.1	0.5
Euro i	Diesel oil	38.6	69.2	0.2	0.5

In Method 2, EC and EF have to be calculated for CO_2 by using equations 2.2 and 2.3 (DCCEE, 2008):

$$EF_{i,\mathrm{CO}_2,ox,kg} = \frac{C_a}{100} \times OF_i \times 3.664, \tag{2.2}$$

$$EF_{i,\mathrm{CO}_2,ox,ec} = EF_{i,\mathrm{CO}_2,ox,kg} \div \left(\frac{EC_i}{C_i}\right), \tag{2.3}$$

where:

$\boldsymbol{EF_{i,CO_2,ox,kg}}$ is the emission factor of CO_2 released from the combustion of fuel type (i) expressed in kg CO_2-e per kg of fuel.

$\boldsymbol{EF_{i,CO_2,ox,ec}}$ is the emission factor of CO_2 released from the combustion of fuel type (i) expressed in kg CO_2-e/GJ.

$\boldsymbol{C_a}$ is the percentage of carbon to the mass of the fuel

$\boldsymbol{OF_i}$ is the oxidation factor (For diesel is 0.99)

$\boldsymbol{EC_i}$ is the energy content

$\boldsymbol{C_i}$ is the density of the measured fuel in kg/kL.

The fuel is to be analysed for EC, C_a and C_i (which are important for calculating emission factors) in accordance with Australian standards (Australia follows ASTM D 240-02, 4809-06, 5291-02 (2007) and ASTM D 1298-99 (2005) for analysing diesel oil) (DCCEE, 2008; DCCEE, 2010*b*)

Method 3 is the same as method 2 except fuel sampling should be conducted according to specific standards. However, according to DCCEE (2010*b*) method 3 is not applicable for estimating the emissions of methane and nitrous oxide.

Method 4 is the direct measurement of emissions using equation 2.4 (DCCEE, 2010*b*):

$$M_{jct} = \frac{MM_j \times P_{ct} \times FR_{ct} \times C_{jct}}{8.31 T_{ct}}, \tag{2.4}$$

where:

$\boldsymbol{M_{jct}}$ is the mass of emissions of gas type (j) expressed in (tonnes/second).

$\boldsymbol{MM_j}$ is the molecular mass of gas type (j) measured in tonnes per kilomole and

they are listed in table 2.3

$\boldsymbol{P_{ct}}$ is the pressure of the gas stream in kPa at the time of measurement.

$\boldsymbol{FR_{ct}}$ is the flow rate of the gas stream in cubic metres per second at the time of measurement.

$\boldsymbol{C_{jct}}$ is the proportion of gas type (j) in the volume of the gas stream at the time of measurement.

$\boldsymbol{T_{ct}}$ is the temperature, in Kelvin, of the gas at the time of measurement.

Table 2.3: Molecular mass of gasses.

Gas type	**Molecular mass kg/mol**
methane	16.04×10^{-3}
carbon dioxide	44.01×10^{-3}
nitrous oxide	44.01×10^{-3}

Direct measurement as mentioned in method 4 is not used to calculate the emission of mobile sources including agricultural machinery because of its high cost (DCCEE, 2011). Method 1, 2 and 3 emission factors for off-road mobile sources (agricultural tractors) are calculated based on the IPCC guidelines emission factors.

2.3.3 IPCC Methodology for emission reporting

Emission factors of fossil fuel based GHGs in the IPCC guidelines are disaggregated according to the sectors, source/activity and fuel type. This classification has been adopted in the national methodologies of many countries to achieve consistency and a comparable result. The Australian national account follows

this classification to classify emissions generated by human activities. Estimations of agricultural machinery emissions are covered in sector 1A4cii (off-road vehicle and other machinery) (IPCC, 1997*b*). In this classification, (1A) stands for energy produced by the combustion of fuel and (4) stands for sectors other than energy such as manufacturing, construction and transport industries. The letter (c) stands for agriculture/forestry/fishing, which includes the usage of agricultural machinery.

It is very necessary to classify emissions sources into categories and subcategories. The reason behind this is to avoid the possibility of double counting. For instance, emissions emitted from electricity generation in power plants can be double counted, first at power plants during the process of generating the electricity and second at corporations and factories where the power is consumed. The other important reason is that non-CO_2 emissions vary strongly from one activity to another according to 'combustion technology and operating conditions' (IPCC, 1997*b*, p. 1.17).

To ensure accurate estimates of CH_4 and N_2O emissions, IPCC (2000) used two methods depending on engine technology, fuel characteristics and operation conditions.The first method ('top down' approach) is based on distance travelled by a specific vehicle type and it is represented by Equation 2.5 (IPCC, 2000).

$$\begin{aligned} \text{Emissions} = \sum_j [&(\text{Emission Factors}_j \times \text{Fuel Consumed}_j) \\ &- \text{Carbon Stored}] \times \text{Fraction Oxidised}_j \times \frac{44}{12} \ , \end{aligned} \tag{2.5}$$

where: j is the fuel type.

The second method ('Bottom-up' approach) is based on the amount of fuel consumed and consists of two steps to calculate the emissions. Estimating fuel consumed according vehicle type is determined in the first step by equation 2.6 (IPCC, 2000):

$$\text{Fuel Consumption}_{ij} = n_{ij} \times k_{ij} \times e_{ij} \ , \tag{2.6}$$

where:

$\boldsymbol{n_{ij}}$ number of vehicles type i using fuel type j

$\boldsymbol{k_{ij}}$ annual kilometres travelled per vehicle (km),

$\boldsymbol{e_{ij}}$ average litres consumed per kilometre travelled (L/km).

The second step is to calculate the emissions of CO_2 by equation 2.7 (IPCC, 2000)

$$\text{Emissions} = \sum_i \sum_j (\text{Emission Factor}_{ij} \times \text{Fuel Consumption}_{ij}), \tag{2.7}$$

The selection of the method for inventory preparation should be based on data availability and quality. These approaches are applicable for calculating emissions from road transport which significantly differ in operating characteristics from off-road vehicles, however they are used for non-road transport. Dalgaard et al. (2001) identified that these methods are not adequate for calculating the emission of fossil fuels-based CO_2 in agriculture.

In IPCC guidelines, it is recommended that country-specific emissions factors are used for estimating CO_2 emissions rather than using default emission fac-

tors that are provided by IPCC. IPCC Good Practice Guidance covers estimates development for only the direct GHGs CO_2, CH_4 and N_2O.

2.4 Diesel Engines' Characteristics

2.4.1 Fuel consumption

Fuel consumption increases as the load or the speed increases in all internal combustion engines. However, the principle of how the fuel is burned differs from compression ignition (CI) engine to spark ignition (SI) engine. Apart from the method of igniting the fuel, the air to fuel ratio is the major difference. In gasoline engine, air-fuel ratio is kept, as practically as possible, close to the stoichiometric, so the air is increased as the fuel is needed to be increased. In contrast, a fixed amount of air is compressed in the combustion chamber of a diesel engine in every cycle yet the fuel is changed to produce the required torque.

2.4.2 Operating characteristics

2.4.2.1 Norms of agricultural operations

Actual operating conditions for compression ignition (CI) diesel engines in the agriculture industry are more likely transient. The majority of daily operating hours involve transient operating conditions where engine rarely operates in a steady state (Rakopoulos and Giakoumis, 2009). However, stationary per-

formance of the engine is conventionally tested in most of the previous studies (Nagendran, 2003; Lindgren and Hansson, 2004).

Hansson et al. (2003) studied the effects of transient loads of the front-end loading and the on-farm driving operating conditions on fuel efficiency of the tractor engine. They found that 13 % and 7 % decrease in fuel efficiency for front-end loading and on-farm driving respectively, corresponding to the emissions calculated based on steady state testing.

Diesel consumption for the same tractor varies notably according to the type of the operation. In general, a crop growing process undergoes many different stages varying in load requirements depending on the utilised implement. Dalgaard et al. (2001) stated that ploughing at a depth of 21 cm during the spring season requires 17 L/ha, while seedbed harrowing requires 6.5 L/ha. Moreover, according to Dalgaard et al. (2001), ploughing during autumn varies from spring for the same depth (21 cm). Chen and Baillie (2009) indicated that the variation in the fuel consumption for different tillage methods in Australian cotton farming: subsoiling (which is the highest) requires 18 L/ha and light harrowing (which is the lowest) requires 4 L/ha. The variability in torque for these operations results in the fuel consumption variations. Normally, when high load is applied, air-fuel ratio decreases from the optimum and leads to undesirable smoke emissions and higher NO_x concentrations due to the increase in engine temperature (Rakopoulos and Giakoumis, 2009).

2.4.2.2 Engine characteristics during transient conditions

Results of many studies (Hansson et al., 2003; Lindgren and Hansson, 2004) conducted on transient loads effects show that fuel consumption is strongly affected by the fast changes that occur in the applied torque on the engine. Transient loads increase the fuel required for carrying out specific work. Hansson et al. (2003) recommend that exhaust gas emissions have to be measured in real driving conditions because they are strongly influenced by transient loads. Lindgren and Hansson (2004) have studied the impact of transient effects such as fast increases in engine load and speed on the emissions for off-road diesel engines. Results indicated that fuel consumption was double the corresponding stationary test.

According to Hansson et al. (2003), several factors cause the decrease in fuel efficiency due to transient loads. First, rapid changes in engine speed and torque hamper the fuel injection system resulting in a rich air-fuel mixture. This case occurs especially in engines equipped with turbochargers and injection systems that are mechanically controlled. The second factor is the thermal inertia of the engine. A delay in thermal equilibrium, caused by the increase in the amount of burning fuel, lasts for several hundred seconds until the thermodynamic equilibrium is reached again (Lindgren, 2004). The third reason that is mentioned by Lindgren (2004) is that the turbocharger requires at least 5 seconds to reach a steady state after sudden changes in either speed or load.

2.4.3 Emissions of diesel engine

Combustion of the fuel in a diesel engine is a process by which the fuel's chemical energy is reproduced as mechanical power. This process results in producing carbon dioxide (CO_2) and water (H_2O) in a theoretically complete combustion (Tschoeke et al., 2010). In practice, a diesel engine's combustion efficiency is near to the complete combustion, i.e. 98% of the fuel is combusted inside the chamber (Pulkrabek, 2004). The two percent left is unburned fuel, where carbon monoxide (CO), total hydrocarbons (THC) and particulate matter (PM) are the main by-products. Oxides of nitrogen in the exhaust gas are formed from the atmospheric nitrogen (which is the main constituent of the air and accounts for 79% by volume) as it enters the combustion chamber.

Two of the diesel engine exhaust emissions, diesel particulate matter (PM) and NO_x, are the highest potentially harmful components that affect human health (Nagendran, 2003). Schimel et al. (1996) related the chemical production of ozone in the troposphere to NO_x, CO and HC. A wide range of criteria influences emissions forming inside the combustion chambers. The most influential factors are engine speed, engine load and patterns of changing loads such as steady, quasi-steady and unsteady (transient) (Rakopoulos and Giakoumis, 2009). The formation of these components inside the combustion chamber is described in the following sections with a brief general discussion of there impact.

2.4.3.1 Carbon dioxide

Theoretical combustion of diesel fuel would produce CO_2, hence, the calculation of CO_2 is straightforward. The chemical composition of diesel fuel is $C_{12}H_{26}$ (Giakoumis and Alafouzos, 2010), the resulted amount of CO_2 shall be determined (for normalized air-fuel ratio (λ)=3 and air-fuel mass ratio is 1:14.5) as stated in Tschoeke et al.'s (2010) work in the following reaction:

$$\begin{aligned} 1\text{kg } C_{12}H_{26} + 3(3.3\text{kg } O_2 + 11.2\text{kg } N_2) \longrightarrow \\ 3.2\text{kg } CO_2 + 1.2\text{kg } H_2O + 6.6\text{kg } O_2 + 33.6\text{kg } N_2 \end{aligned} \tag{2.8}$$

In this reaction the conversion factor is 2.72 kg CO_2/L fuel if diesel density is assumed to be 0.85 kg per litre of fuel. Baillie and Chen (2011) have employed 2.89 kg CO_2-e/L (which was quoted from DCCEE (2010*a*)) in their software to calculate the on-farm energy use CO_2 from fuel consumption in Australian cotton farming. This value ranged widely in the literature; 2.75 kg CO_2/L was quoted by (Filipovic et al., 2006) when they investigated the possibilities of fuel saving in Croatia and it was higher (2.764 kg CO_2/L) in Dyer and Desjardins's (2003) study in Canada. These differences are attributable to the variations in fuel density and carbon content.

2.4.3.2 Carbon monoxide

Oxygen deficiency is the primary cause of CO forming in the exhaust. Although the fuel in CI engines is burned in the abundance of air, some regions in the

combustion chamber such us the core of the fuel jet are fuel-rich due to the heterogeneous mixture (Wark et al., 1998). However, according to Lindgren (2004) and Stone (1999) emission of CO is not a significant problem as the air feeding control i.e. swirl can enhance the air fuel mixing and thereby result in a reduction in CO. An additional reason that leads to CO forming is that CO_2 dissociates at high temperatures as follows (Lindgren, 2004):

$$CO_2 \overset{\text{heat}}{\rightleftharpoons} CO + \tfrac{1}{2}\, O_2 \tag{2.9}$$

Alongside with the adverse effect on human health, CO has indirect effects on the climate. Forster et al. (2007) indicated that the effects of CO occur through reduction in OH levels which lead to enhanced concentrations of CH_4 and increasing ozone.

2.4.3.3 Nitrogen oxides NO_x

Nitrogen oxides (NO_x) in the exhaust consist of nitrogen oxide (NO) and a small portion of nitrogen dioxide (NO_2) (Pulkrabek, 2004). Formation of NO_x is explained by Zeldovich (cited in Fritz and Pitchon, 1997) in Equation 2.10 – 2.13. NO_x emissions formation is a function of load and engine speed (Klingstedt et al., 2006). NO_x emission tends to increase as diesel engine's operation approaches the stoichiometric condition to overcome the load increase (Wark et al., 1998). Giakoumis and Alafouzos (2010), related the increase in the in-cylinder temperature due to over-fuelling to the enhanced amount of NO_x. The data indicates

that off-road diesel equipment accounts for 25% of NO_x emissions from mobile sources (Kean et al., 2000).

$$\left.\begin{array}{l} N_2 + \frac{1}{2}\,O_2 \rightarrow NO + \frac{1}{2}\,N_2 \\ O_2 + \frac{1}{2}\,N_2 \rightarrow NO + \frac{1}{2}\,O_2 \end{array}\right\} N_2 + O_2 \xrightarrow{2500\text{-}3000\,K} 2\,NO \tag{2.10}$$

$$N + OH \longrightarrow NO + H \tag{2.11}$$

$$NO + H_2O \longrightarrow NO_2 + H_2 \tag{2.12}$$

$$NO + O_2 \longrightarrow NO_2 + O \tag{2.13}$$

$$NO_2 \xrightarrow{\text{sunlight}} NO + O + somg \tag{2.14}$$

$$O + O_2 \longrightarrow O_3 \tag{2.15}$$

There are two opposing indirect effects of NO_x on the global warming. First of all, NO_x is enhancing ozone in the troposphere and forming the photochemical smog as in Equation 2.13 to 2.15 (Pulkrabek, 2004). Secondly, it leads to the reductions in CH_4 (Forster et al., 2007).

2.4.3.4 Total hydrocarbons (HC)

Unburned hydrocarbons (HC) in diesel engines occur for two reasons. Firstly, some zones inside the chamber are too lean to burn therefore unburned fuel appears in the exhaust components. The second source is that some fuel residue remains in the spray holes of the injectors. In this case, production of HC emis-

sions is due to the fuel entering the combustion chamber late in the cycle and remains unburned or partially burnt (Stone, 1999). The amount of HC in diesel engines is influenced by cylinder geometry, injection method and injection timing.

2.5 Agricultural and Off-Road Diesel Engine Testing

Since the 1990s, diesel engine emissions have reduced dramatically due to the inclusion of new technologies such as turbocharging, aftercooling and common rail injection systems to the engine design (Jokiniemi and Ahokas, 2011). These technological advances resulted in a remarkable increase in the engine power output of up to four times and consequently emissions reduction with no significant changes in the engine dimensions (Nagendran, 2003; Rakopoulos and Giakoumis, 2009). Therefore, diesel engine emission regulations are becoming more stringent because of the high expectations to bring the emission levels below 2000 levels (Nagendran, 2003) (see Fig 2.1).

Diesel engine emission testing has witnessed different stages as the knowledge about the combustion characteristics evolved. In Europe, two test cycles were employed to certify diesel engines before the current transient cycle comes into practice. It was firstly tested for smoke levels starting in 1972 by performing a full load at a steady speed. CO, HC and NO_x emissions were first controlled in 1988, yet a new test cycle was performed. Both methods are described in this section.

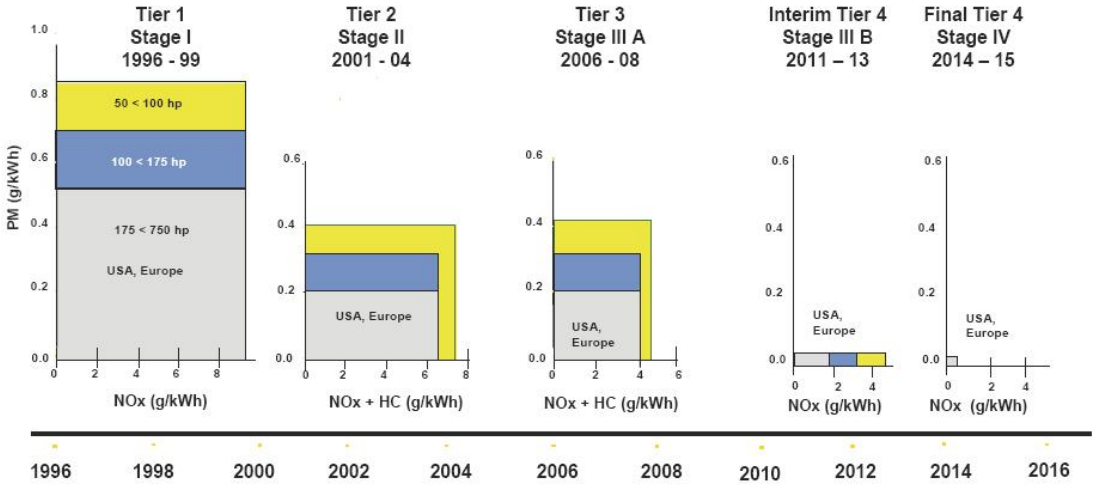

Figure 2.1: HC, NO_x and PM regulations in the US and Europe (Xinqun et al., 2010).

2.5.1 Steady-state testing

In Europe, the steady-state testing started in 1988 (ECE R-49 test). The test's purpose and parameters were addressed in Directive 88/77/EEC for the European Union emission standards. This test comprises 5 modes of steady loading at intermediate speed followed by unloading 5 modes at rated speed. These ten modes are separated, preceded and ended by low idle mode (see Table 4.1). It continued in practice until 2000 when it was then superseded by the European Stationary Cycle (ESC) and Transient Cycle (ETC) tests.

2.5.2 Transient cycle testing

2.5.2.1 European stationary cycle (ESC)

The European Stationary Cycle is used in Europe for type approval for off-road heavy-duty (HD) diesel engines since July 2000. Agricultural machinery is one of

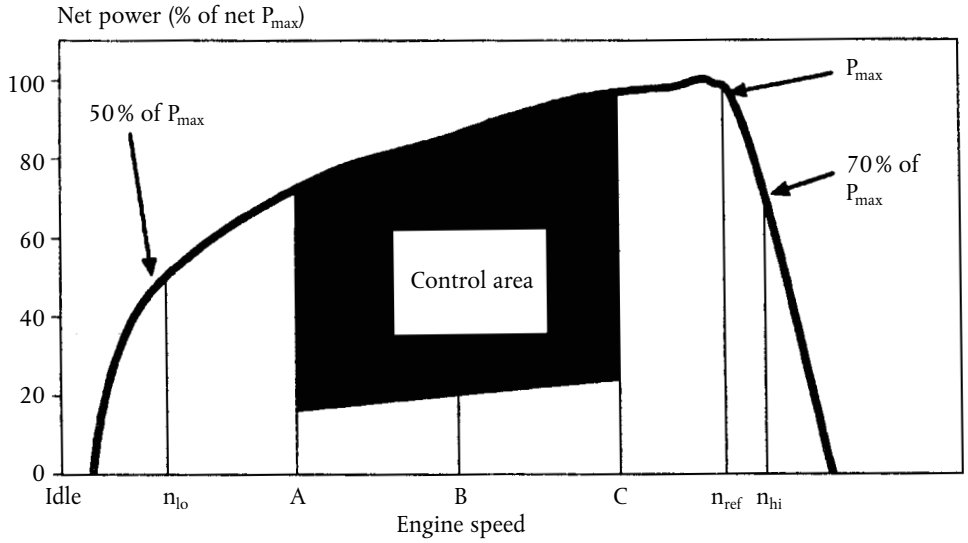

Figure 2.2: The area of controlled loads.

the types of HD vehicular application considered in the test (EEA, 2006). This cycle consists of 12 dynamic loading and speed modes proceeded by a low idle mode. The cycle does not include cold start (Bünger et al., 2007). The area of controlled loads in this test is shown in Fig. 2.2.

2.5.2.2 European transient cycle (ETC)

The European Transient Cycle (ETC) test has been in practice for emission certification of HD diesel engines since 2000. It is also known as the FIGE transient cycle yet the final ETC cycle is an edited and slightly enhanced version of the original FIGE proposal. FIGE Institute, Aachen, Germany, developed a 1800 second duration cycle test representing three different driving conditions urban, rural and motorway driving cycles depending on real road cycle measurements of heavy-duty vehicles, see Fig. 2.3 (*Diesel Net: Emission Test Cycle, European Transient Cycle*, 2010). From the figures, it can be seen that the transients govern

engine performance. However, the cycle does not represent the transient nature of agricultural on-farm applications.

According to Directive 1999/96/EC (2000), the ETC test is designed for testing heavy-duty engines on the bases of road-type-specific driving patterns of buses and trucks. The ESC test is designed to represent the wider range of the off-road diesel engine operations.

2.5.2.3 Composite Urban Emissions Drive Cycle (CUEDC)

The Composite Urban Emissions Drive Cycle test Has been developed in Australia by the National Environment Protection Council (NEPC) to provide a method of testing vehicles that closely replicates actual on-road driving conditions. The test design is based on NEPC's study in 1998 (DNEPM Project 2.1) in which different vehicles' actual speed/acceleration profiles in congested, minor roads, arterial and highway driving conditions were recorded. Six different CUEDC,s were developed; Each cycle covers the varying driving patterns of six major vehicle categories (MC, NA, NB, ME, NC and NCH) (Yastreboff, 2013).

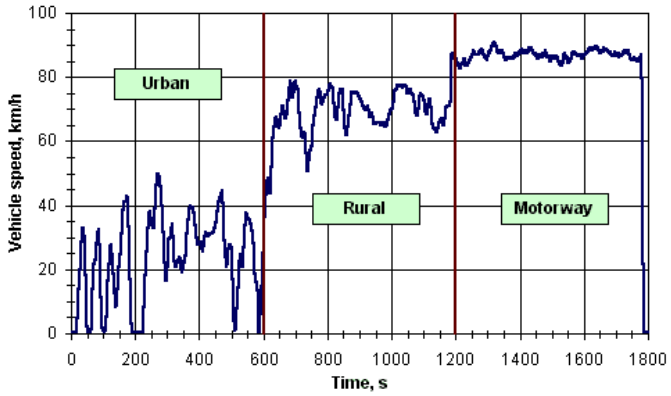

(a) Vehicle speed

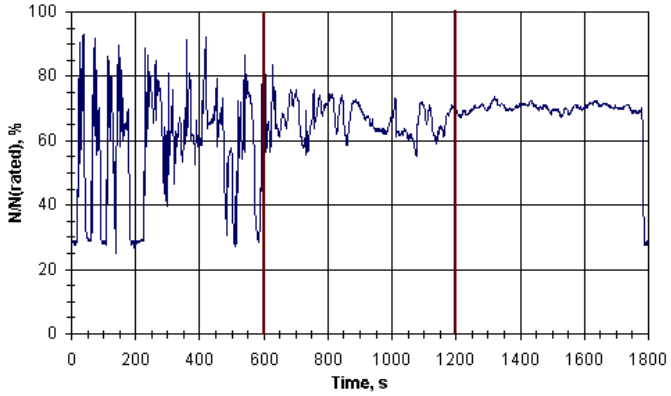

(b) Engine speed

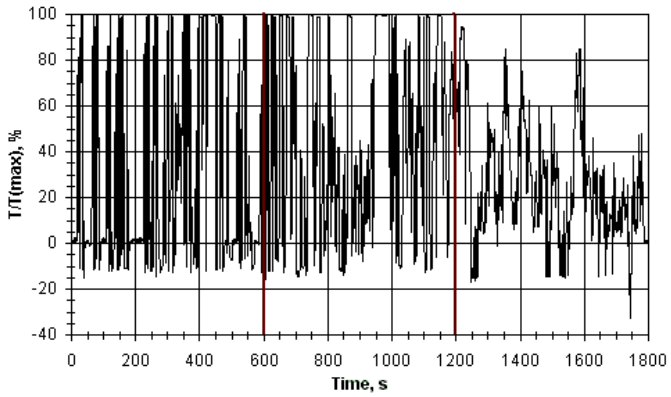

(c) Engine torque

Figure 2.3: ETC test cycle. (source: *Diesel Net: Emission Test Cycle, European Transient Cycle*, 2010).

2.6 Summary

The Earth future is influenced by the current control techniques. Emission factors that are used to estimate the annual anthropogenic emissions play the key role in determining the accuracy of the estimates. The Australian emission factors of diesel for agricultural tractors were found out-dated, derived from testing off-road vehicles other than tractors and based on steady state tests. Therefore, the need for up-to-date study which is tractor-specific and includes the transient effect is a paramount importance.

Chapter 3

RESEARCH METHODOLOGY

3.1 Introduction

This chapter presents the trial design and the materials of the methodology to undertake experimentation. The chapter also describes the instrumentation developed to monitor, measure and record the data of the variables in the experiments.

3.2 Experimental Methods and Materials

3.2.1 Experimental design criteria

Considering every engine has unique combustion characteristics and may exhibit a considerably different performance if mounted on different vehicles. This study compared different sequences of engine loading one engine via power take off (PTO) mounted dynamometer.

When executing the tests through the PTO, some advantages are gained. The effective net power of the tractor (engine) is obtained and thereby, its emission is tested. According to Dyer and Desjardins (2003) the power at PTO is about 4 % less than the power at the drive shaft. In the draw-bar test as an alternative, there are multiple factors associated with this test. Part of the engine power is lost in overcoming the rolling resistance of the soil and wheel slippage. If the draw-bar test is implemented, the effect of the operator skills is an another factor that has to be considered. All these factors, as they cannot be included in this study due to time constraints, were avoided. Another advantage of testing the tractor (engine) through the PTO is that the test is executable inside the laboratory where some parameters were preconditioned and others were controlled. Thus, it is believed that the power at the PTO, if used for testing the emission of the tractor, is more representative in calculating the emission factors. All the measured variables in this study and the employed methods to measure them are summarised in Table 3.1.

3.2.2 Fuel Specification

It has been recognised that the quality of diesel in Australia varies from supplier to supplier and has not been the focus of up-to-date literature. Therefore, there could be a scope for researching the effect of considerable variation in composition on the emissions. However, it is agreed that studying the effects of variation in diesel quality is outside of the scope of this thesis. In addition, it was one of the intentions to include within the scope the testing of a range of biodiesel

Table 3.1: The measured variables.

Measured Variables	**Unit**	**Measurement**
Engine Speed	rpm	BDM 300 speed censor
PTO Speed	rpm	tachometer
PTO Torque	Nm	load cell
Fuel Mass Flow Rate	g/min	volumetric buret
Exhaust Temperature	℃	thermocouple
Intake Air Temperature	℃	thermocouple
Ambient Barometric Pressure	kPa	via exhaust gas analyser
Relative Humidity	%	via exhaust gas analyser
CO Emissions	%	via exhaust gas analyser
CO_2 Emissions	%	via exhaust gas analyser
NO_x Emissions	ppm	via exhaust gas analyser
O_2	%	via exhaust gas analyser
Lambda	—	via exhaust gas analyser

blends because biodiesel fuel has tremendous potential to be the fuel of the future. Conversely, due to the multiplicity of biodiesel sources, (e.g. waste cooking oil, cotton seed oil, rapeseed oil etc.), and the time constraints, it is accepted that the research will concentrate on conventional type of diesel only.

The specifications of the selected fuel had to be comparable to that specified by European Union standards (Directive 1999/96/EC). The difficulty in obtaining unified commercial diesel fuel specifications, led to the decision to use only commercial diesel that is procured from Shell Australia Limited. The choice was

made after comparing different options. The closest option to the fuel properties that are specified by the European Union Directive (EUD) and is commercially popular was Shell low sulphur. Its full specifications are shown in Table 3.2 (refer to Appendix C for more details about the properties of other fuel types for comparison).

Table 3.2: Shell diesoline 10 automotive diesel fuel properties (Shell, 2009).

Description	**Units**	**Typical**
Density @15 ℃	kg/L	0.830
Viscosity @40 ℃	mm^2/s	3.05
Flash point	℃	79
Sulphur	mg/kg	8
Cetane Index	—	49
Distillation - 95%	℃	340
Water	% volume	< 0.05
Ash	% mass	< 0.01
Sediment	% mass	< 0.01
Filterability Test	% mass	1.05
Strong Acid Number	mg KOH/g	Nil
Total Acid Number	mg KOH/g	< 0.1
Copper Corrosion	—	1a
Lubricity (HFRR test)	Microns	400

3.2.3 Fuel consumption

Fuel consumption was identified as being an important factor in measuring the commercial success of a tractor (Baillie and Vasey, 1969). For a given fuel amount, a great deal of parameters affect the extracted energy. For example, the age of the engine affects fuel consumption. It is not an intended consideration in this thesis because it was studied intensively in the literature. Moreover, the purpose of the study is to compare relative differences in testing procedures, therefore, some of the factors influencing engine performance are not relevant when using the same engine.

3.2.4 Emissions measurement

One of the underlying assumptions of this research is the advances in diesel engine technology which promises a significant reduction in emissions compared with old technology. In contrast, presumingly embracing the transient cycle test in the recent testing cycles in regulating diesel emissions would better represent the real-time operations and might indicate an increase in the emission. To prove this, it is proposed to test within the normal operating range of the selected tractor's engine deploying the conventional steady-state test and a transient cycle. Both the observed emission trends and the specific emission values for each test will be compared against the calculated emissions from the Australian emission factors.

As these tests were performed, the number of the exhaust gas emission to be measured was limited to include NO_x, CO_2 and CO only because of advances

in engine design as a response to the current regulation have almost eliminated smoke emissions from modern diesel engines. It is also due to equipment availability (see section 3.3.2).

In previous research projects (Dyer and Desjardins, 2003; Lindgren, 2004; Filipovic et al., 2006; Nelson et al., 2009), total annual CO_2 emissions (per **ha** or **kg** of product) for crops production were combined in accounting procedures. This is recognised as important to understand the total impact of on-farm energy use however it occurs outside of this project boundary.

3.2.5 Emission testing cycles selection

According to (Nagendran, 2003), diesel engine emission testing is generally conducted according to the broad classification as on- and off-road vehicles. The power range (e.g. light- or heavy-duty vehicles) may also be included in the classification. Depending on these classifications, different test cycles have been developed in Europe to simulate the steady state and the real operation cycle (transient) (Nagendran, 2003). These test cycles were designed to simulate the most common operational characteristics of diesel engine types with the wider population, which may not cover all.

In this study, the tractor had to be tested with three test cycles. Firstly, two tests were selected in order to determine the variation between the emissions of the steady-state and transient testing. Secondly, an additional test cycle was developed in order to provide an adequate understanding of the effects of various

applications on the emissions of agricultural tractors (the design of the cycle is described in section 4.5 in chapter 4).

The ESC test (described in section *2.5.2.1*) is deemed to simulate the transient operations of the tractor for two reasons. Firstly, the ESC test is a standard test that is designed for testing the conventional diesel engines and represents the wider range of the off-road diesel engine operations including agricultural tractors. Secondly, the alternative test (ETC test) is designed for on-road heavy-duty engines testing which simulates the real driving cycles of buses and trucks (Directive 1999/96/EC, 2000). Therefore, ESC test was found to be more appropriate to implement the comparison between the transient and steady state testing and the comparison between the general standard test to the machinery application-specific test in this study.

3.3 Specifications of Experimental Equipment

3.3.1 Tractor's specification

One of the primary objectives of this thesis is to calculate diesel emissions using the Australian emission factors that are in use for agricultural applications and then compare the figures with the results acquired in the laboratory. The criteria used to select the tractor, is as follows: The tractor must be in the popular power range that can be useful in wide range of farming systems, currently in use, and a relatively old production. Ideally, it should have power take off. At

the time of the selection, there were only two tractors available at University of Southern Queensland (USQ), a Belarus 920 tractor (Fig. 3.2) powered with 74.5 kW engine and a John Deere powered with a 24.8 kW engine. The final selection was, according to the availability and the power value, the Belarus 920. The specifications of the tractor and the engine are listed in Table 3.3 and Nebraska test report for this model is presented in Appendix D.

Table 3.3: Tractor and engine specifications (Leviticus et al., 1996)

Manufacturer	Minsk, Belarus
Model	920
Year of manufacture	1996
Operation hours	424 hr
Displacement	4.75 L
No. of cylinders	4
Bore/Stroke	110 × 125 mm
Compression ratio	16:1
Cooling system	liquid-cooled
Fuel injection system	Direct injection
Air injection system	Supercharged
Operating speed range	750–2300 rpm
Rated engine speed	2200 rpm
Brake engine power	74.5 kW (100 hp)
PTO torque at rated speed	890 Nm
PTO power	68.6 kW (92 hp)
PTO Type	independent

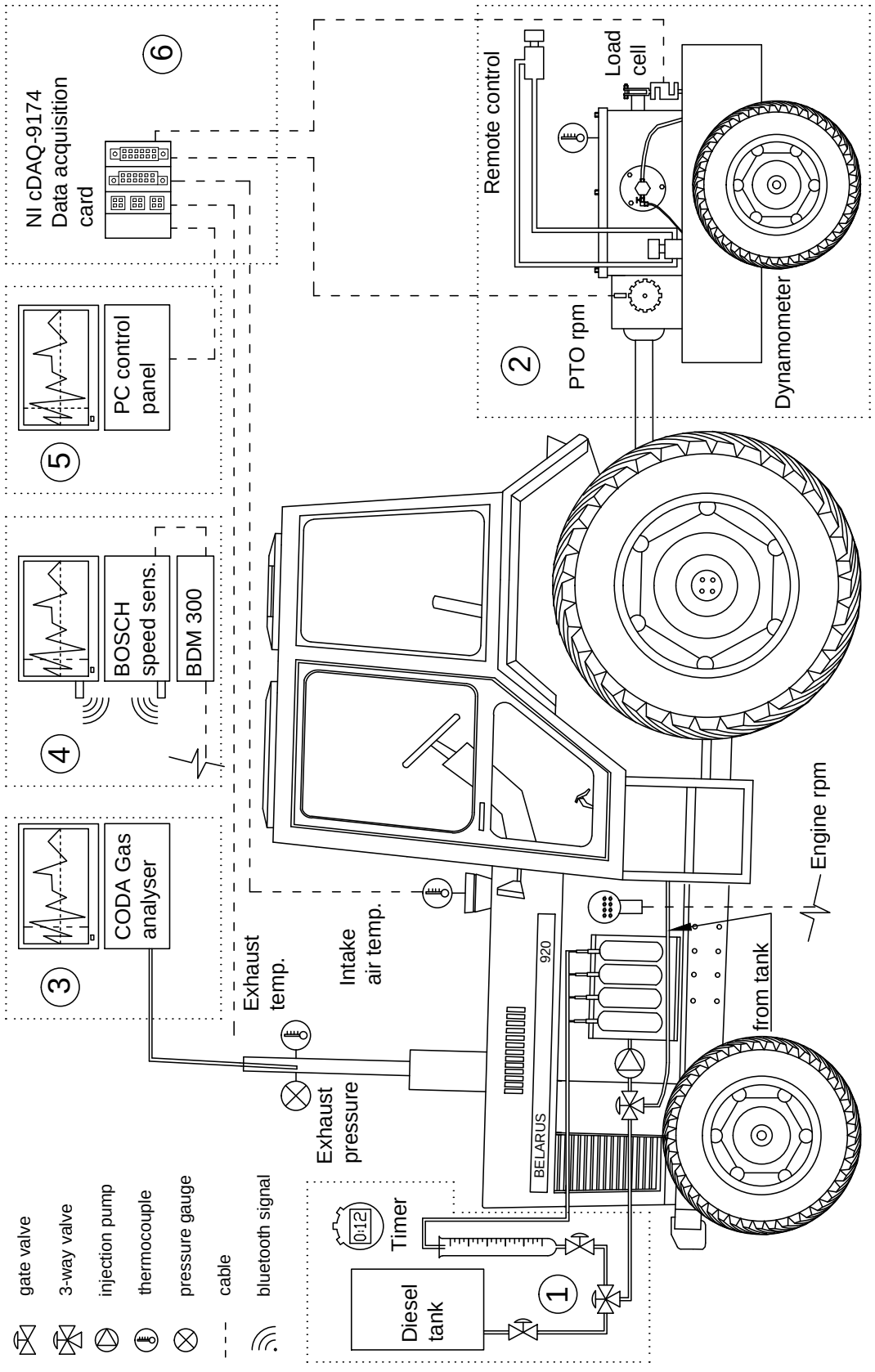

Figure 3.1: Schematic test instrumentation.

Figure 3.2: Belarus 920 Tractor with mechanically controlled governor

3.3.2 Gas analyser

To measure the exhaust gas emissions from the raw exhaust gas, a special standard has to be met. In this study the the BS ISO (No 16183:2002) for raw exhaust gas measurement of heavy duty engines was followed along with some other requirements form the European Union emission standards. A portable CODA gas analyser unit was used (Fig. 3.3a) for conducting the measurements. This device can measure the following gases: O_2, CO_2, HC (n-hexane and propane) CO and NO_x and is consistent with ASM and OIML standards (full specifications are listed in Appendix B).

The probe was fitted into the exhaust pipe directly with some modifications to ensure the accuracy of the measurements and to sustain high temperatures.

(a) gas analyser

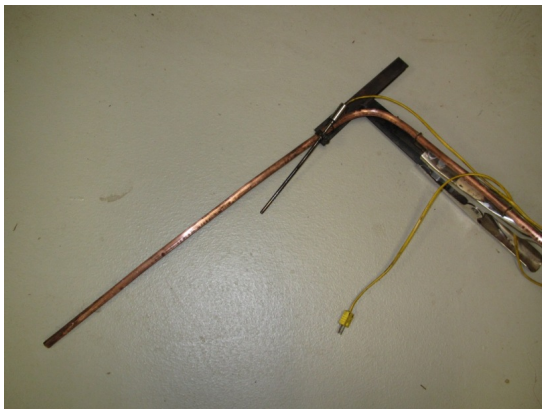

(b) modified probe

(c) modified probe

Figure 3.3: CODA gas analyser portable unit.

These modifications were made to comply with the European Standards (Directive 1999/96/EC, 1999) instructions for the position and the temperature of the sampling location (if raw exhaust gas sampling is performed in ESC test) which needs to be 0.5 m upstream of exhaust pipe opening and sufficiently close to the

engine to ensure the temperature of the exhaust gas is not less than 70 ℃ (see Fig. 3.3b).

Table 3.4: CODA specification.

Description	**Gases**			
	CO	**CO_2**	**NO_x**	**O_2**
Measurement Range	0–15 %	0–20 %	0–5000 ppm	0–25 %
Measurement Resolution	0.001 %	0.01 %	1 ppm	0.01 %
Response Time	2 seconds	2 seconds	5.5 seconds	40 seconds

Table 3.5: Accuracy of CODA measurements.

Gases	**Range**	**Accuracy**
CO	0–10 %	± 3 %
	10.001–15 %	± 5 %
CO_2	0–16 %	± 3 %
	16.01–20 %	± 5 %
NO_x	0–4000 ppm	± 4 %
	4001–5000 ppm	± 5 %
O_2	0–25 %	± 5 %

In this study, the raw exhaust gaseous emission was sampled and analysed. Therefore, the probe of the gas analyser was fitted directly inside the exhaust pipe before operating the analyser (Fig. 3.3b). A special arrangement was made to the probe to sustain the over heating effect and to comply with the standards. Two particulate filters were used to protect the gaseous emission sensors (Fig. 3.3a). These filters were replaced before commencing each test.

3.3.3 PTO Dynamometer

The dynamometer used in the experimental work for this project was a mobile PTO dynamometer form AW model Nebraska 400 (Fig. 3.4). The torque is developed by a friction-based brake system. A rotating shaft attached to the brake drum of the brake system can be coupled to the PTO of the tractor. To apply the desired torque, the brake system is activated by controlling the flow of a hydraulic system which is mechanically driven by the PTO shaft. The brake unit is placed in a housing free of rotation and connected to a load cell to measure the generated torque values (Fig. 3.4b). The housing is filled with water to control the generated heat. The temperature of the brake system was kept constant throughout the tests by using a variable water flow rate according to the manufacturer's recommendations to ensure accurate measurements.

This dynamometer was modified to meet the requirements of this project. The major modification was made to the data acquisition method. Torque values in the original design of the PTO dynamometer were obtained using analogue display with very slow response, therefore, a labview code was developed to acquire (display and record) the instantaneous torque values (one reading per second) in higher resolution(refer to section 3.3.7). The load cell and the data acquisition system were calibrated twice using two methods. Firstly, it was calibrated by applying known values of constant loads directly to the load cell while it was suspended by a chain (Fig. 3.6). Secondly, the load cell was calibrated against constant torque values after connecting it to the dynamometer (Fig 3.5). An accuracy of $\pm$4N.m for the torque readings was achieved.

(a) PTO dynamometer

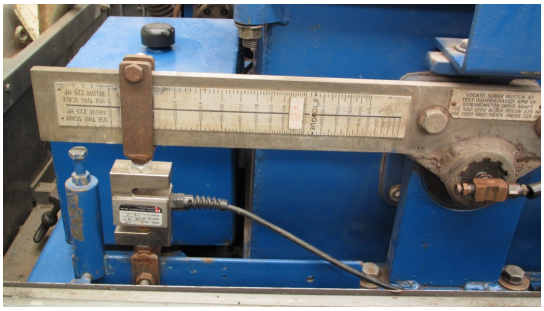

(b) load cell

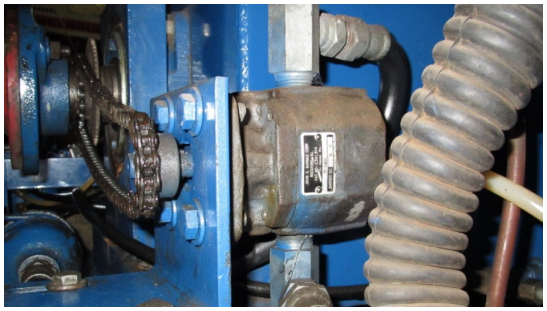

(c) hydraulic pump

Figure 3.4: AW Dynamometer: model Nebraska 400 with hydraulic brake system.

Figure 3.5: Torque calibration for the load-cell.

Figure 3.6: Direct force load-cell calibration.

3.3.4 Fuel consumption metering system

Initially, the fuel consumption measurement system consisted of two fuel-flow sensors. One sensor was placed in the feed line to measure the amount of fuel pumped to the injector. Another sensor was placed in the over-flow fuel line. The readings of the sensors were recorded simultaneously using a Labview program. To obtain the net fuel consumption, the readings of the second sensor was to be subtracted from the simultaneous readings of the first sensor. However, a difficulty was encountered in avoiding the pulsation effects of the engine's fuel injection pump on the measurements which led to shift into using a manual volumetric fuel consumption measurement method. The second system (Fig. 3.7)

consisted of an additional tank to supply the engine with diesel and a 100 mL buret. The feed-in hose of the system was fitted to a three-way valve which was placed in the main feed-in line of the tractor before the injection pump. The over-flow fuel hose was fitted back to the buret to obtain the net fuel consumption (Fig. 3.1 part (1)). The volume of fuel consumed during 60 seconds was recorded and this process was repeated twice or three times if there was enough time. The volumetric flow rate was converted into mass flow rate by multiplying it by the diesel density (0.83 kg/L).

Figure 3.7: Fuel consumption measuring system.

3.3.5 Temperature, pressure and humidity measurements

To measure the temperature of the exhaust gas and air intake, two thermocouples (type k) were placed in effective positions in the exhaust manifold and the pure air inlet. They were connected to a NI 9219 data logger (Fig 3.9). They were calibrated with a standard thermometer at different temperatures. The thermocouple that was used to measured the exhaust gas temperature, was attached to the probe of the gas analyser (Fig. 3.3c) and second thermocouple was inserted inside the intake air manifold.

The absolute pressure, the relative humidity and the ambient temperature were recorded from sensors on the CODA gas analyser and USQ weather station (Appendix E).

3.3.6 Engine and PTO speed measuring methods

Two different approaches were deployed to measure the speed of the engine.The first method was direct observation by using a combined sensor that was developed by BOSCH. This sensor (model BDM 300 which works in conjunction with BEA 460) measures the engine speed based on the sound waves conveyed by two means. The first is structure of the engine and second is the air (Fig. 3.8). In the second method, engine speed is calculated from PTO speed readings by subroutine in the labview code using 2075/540 engine/PTO converting ratio (Fig. 3.10). The measured and the calculated values were found to be consistent with $\pm 3\,\%$ margin depending on the speed range.

(a) BDM 300

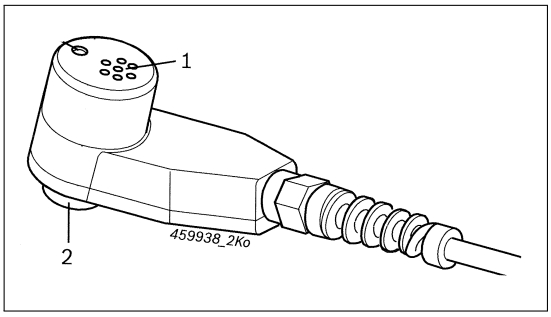

(b) combi sensor: 1) microphone for recording air-borne sound, 2) magnetic base for recording structure-borne sound

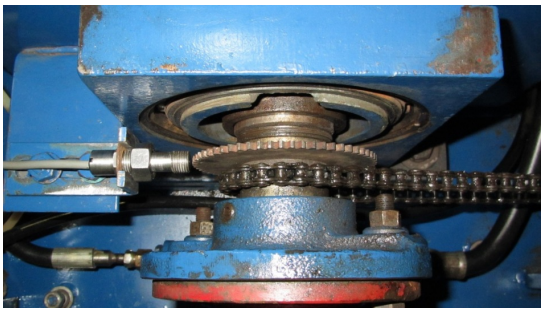

(c) Magnatic pick-up tachometer

(d) photo-tachometer

Figure 3.8: (a) and (b) Bosch BDM 300 rapid speed sensing from the structure-borne sound and airborne sound signal of the engine to measure engine speed, (c) tachometer to measure PTO speed and (d) photo-tachometer for calibration.

PTO speed was measured by using a tachometer with a magnetic pick-up which sends an analogue signal when every tooth crosses nearby its magnetic field. A subroutine in the labview code was set to convert the recoded signals over a period of time into speed expressed in min^{-1}. The accuracy of the measurements was within the permitted range of $\pm 5\,\mathrm{rpm}$. The calibration was done against a high accuracy photo-tachometer before conducting the test.

According to the operating procedure of the engine speed sensor, it was attached on the body of the tractor in a vicinity to the engine to pick up the sound waves. One consideration when using this sensor, is that the engine must be operated before operating the sensor to ensure the establishment of the communication

between the sensor and the PC for Data logging. For PTO speed measurement, the tachometer was permanently connected to the dynamometer as a part of the original design.

3.3.7 Data acquisition system (DAS)

Employing multiple sampling and measuring apparatus increased the confidence of the measured data. A difficulty was encountered in grouping the data because some sensors and analysers required their own proprietary software. Some sensors such as the thermocouples, load cell and the tachometers required to be brought to the standard sampling rates of the European Union directives. The problem was overcome by using three PCs in order to operate three major data acquisition programs as shown in Fig. 3.1. The first PC was used to run the CODA gas analyser. The second PC was used to operate the BOSCH speed sensors. The compatible software packages were provided with the analyser by the supplier.

For logging the data measured by other measuring devices (this includes temperature, torque and PTO speed measurement), a National Instrument cDAQ-9174 was used (Fig 3.9). It required a program in order to save and display the data on a PC. Therefore, a labview code was developed to serve this purpose (Fig. 3.10).

Figure 3.9: NI data acquisition card.

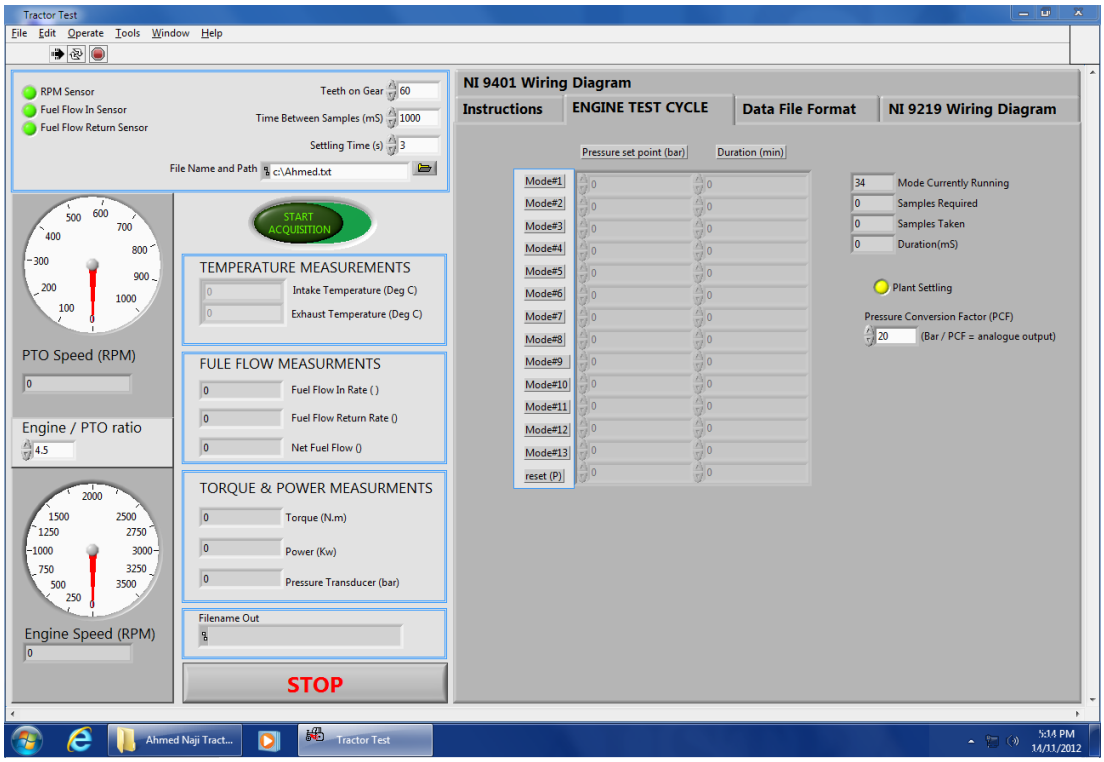

Figure 3.10: LabView user interface for data displaying and and recording.

3.3.8 Commissioning of test equipment

All instrumentation was designed for convenient installation and then removal prior and after each test. In particular, key consideration included the setup of the dynamometer and the tractor prior to testing

3.3.9 Commissioning of the dynamometer

The essence of the project is to apply variable sequences of loads on the engine and then monitor the subsequently produced emissions. Therefore, the dynamometer is an essential part and maintaining stable conditions of the dynamometer is very important for the reliability of the results. Installing the dynamometer consists of several steps starting with connecting it to the power-take-off of the tractor. An adapter was used for this purpose. Having the dynamometer connected, the cooling water tank was filled to the recommended level and the hydraulic oil level was checked as well. The dynamometer was secured with all guards for the rotating members for safety measures. A quick check was conducted before the tests for the load cell (Fig. 3.5).

3.3.10 Engine conditioning and temperature control

Before utilising the tractor for the test, the engine was maintained to ensure that it was in good mechanical condition. The lubricating oil was replaced, air intake filter was cleaned and radiator coolant level was topped up.

Before running the test, the engine was brought to the normal operating condition by a reiterating procedure. First of all, the engine was run at low idle speed for around 45 minutes to reach a steady state condition. This is considered to be a good engineering practice for warming up and cycling the lubrication oil. Then the engine was run at maximum power for 15 minutes in order to stabilise the engine parameters. Immediately after this procedure was completed, the test cycles were executed.

The cooling system of the engine is water based. It was designed to maintain the temperature within a permitted range. However, in the case of over heating the engine, an additional fan was used to assist the cooling system and stabilise the temperature. When these test were performed, all the parameters that affect the exhaust gas emission were kept, as much as practical, constant. This does not include the torque and engine speed which are considered the key factors in this study.

Chapter 4

EXPERIMENTAL WORK

4.1 Introduction

This chapter describes the test procedure that was followed to conduct the experimental work. The mathematical procedure to analyse the observed data acquired the individual tests are also presented in this chapter, supported by a sample of the calculation.

4.2 Engine Performance at Maximum Operating Conditions

One of the requirements of the tests prescribed in this chapter is that the employed engine had to be mapped for the full load and maximum power curve. This is necessary for calculating the tested torque and speed values of each test. The engine map would cover the area from no load at maximum speed to maximum

load. According to Directive 1999/96/EC (2000), the reported information by the manufacturer would be adequate for this purpose if it is within ±3 % of the measured curves. The deployed tractor is a 1996 model and has been in service for 15 years. Therefore, performing a test to define the full-load and power curves against engine speed was very necessary for this project.

4.2.1 Test procedure

Directive 80/1269/EEC (1980) on the engine power of motor vehicles was followed to define the required parameters of this test when a simple static loading pattern was followed. The first step of the test involved setting the injection-pump at full speed without any further alteration. The injection timing and the governor were kept unmodified maintaining the manufacturer's production specifications.

The initial tractor test started at 2300 rpm and no load, then the torque was increased by even steps of 100 Nm until the maximum power was reached at the rated speed. Then the torque was increased to achieve an even reduction in speed until the speed dropped below 1000 rpm so that the maximum torque can be determined. The same procedure was repeated at 2200 rpm to verify test reliability. In every step, the speed was maintained at a range of ±10 rpm, while torque, fuel consumption and inlet air and exhaust gas temperature were simultaneously recorded. The average values were reported in section 4.2.2. Each measurement were recorded after ensuring the engine speed, torque and exhaust gas temperature reached constant values.

4.2.2 Test results

The test was repeated three times in order to obtain reliable measurements. The torque and speed were measured at the PTO and averaged. The PTO power curve is plotted in Fig 4.1. The rated engine power of a tractor is typically measured at the PTO as stated by Grisso et al. (2004). Therefore, the power obtained at the PTO of Belarus 920 was regarded as the net power of the engine in Fig. 4.2 and was used in the calculations. The speed and torque values of the engine were determined by multiplying PTO torque and speed by the engine/PTO convention ratio of 2075/540. This ratio was measured in this experiment and it was found to be comparable with the Nebraska test report (1996). The brake power was corrected for temperature and atmospheric pressure by multiplying the power at any speed by the correction factor K_d which was determined by Equation 4.1 (Directive 80/1269/EEC, 1980).

$$K_d = \left(\frac{99}{P_s}\right) \times \left(\frac{T}{298}\right)^{0.7} \tag{4.1}$$

where:

$\boldsymbol{T}$ is the absolute temperature of the intake air in Kelvin;

$\boldsymbol{P_s}$ is the dry atmospheric pressure in kPa.

The maximum power measured at the PTO (net engine power) was around 51 kW at 559 rpm (engine speed of 2150 rpm). This shows a deviation of 18 kW (26 %) and 50 rpm (2.3 %) from the maximum power and rated speed values, respectively,

that were reported by the manufacturer and measured by the Nebraska test. The age of the tractor is the possible reason for this deviation. In addition, the declared maximum power and rated speed are measured for the best production of this tractor model (cited in Liljedahl et al., 1989, p. 429).

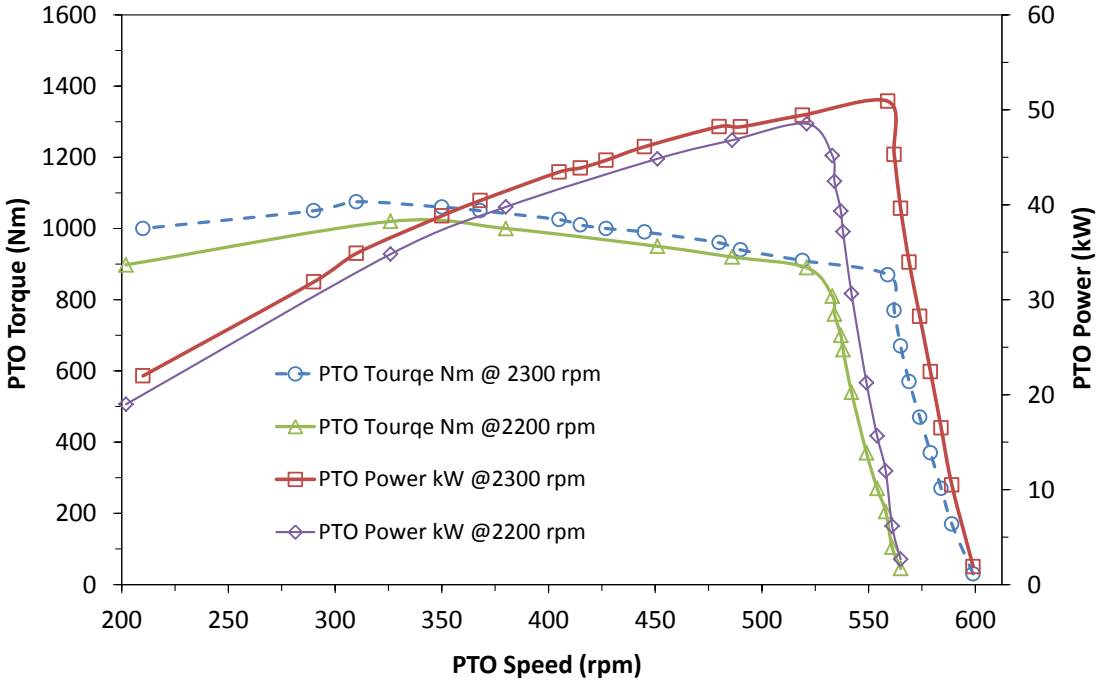

Figure 4.1: PTO power and torque curves against PTO speed at maximum operating conditions at 2300 rpm and 2200 rpm for Belarus 920.

Other parameters, that are important for quantifying tractor performance, include the torque rise, the governed speed range and specific fuel consumption. From the torque curve, this tractor showed a 7 % of speed regulation before the governor opened to the maximum fuel delivery. According to Baillie and Vasey (1969), up to 10 % is acceptable. Whilst, for the torque rise, the results showed 13 % at 1612 rpm and 17.6 % at 1433 rpm ($^3/_4$ and $^2/_3$ of the measured rated speed respectively). Torque rise of about 10 % at two-thirds of the rated speed is regarded as an acceptable performance of a tractor (Baillie and Vasey, 1969). The hourly rates of fuel consumption and the corresponding power use were processed

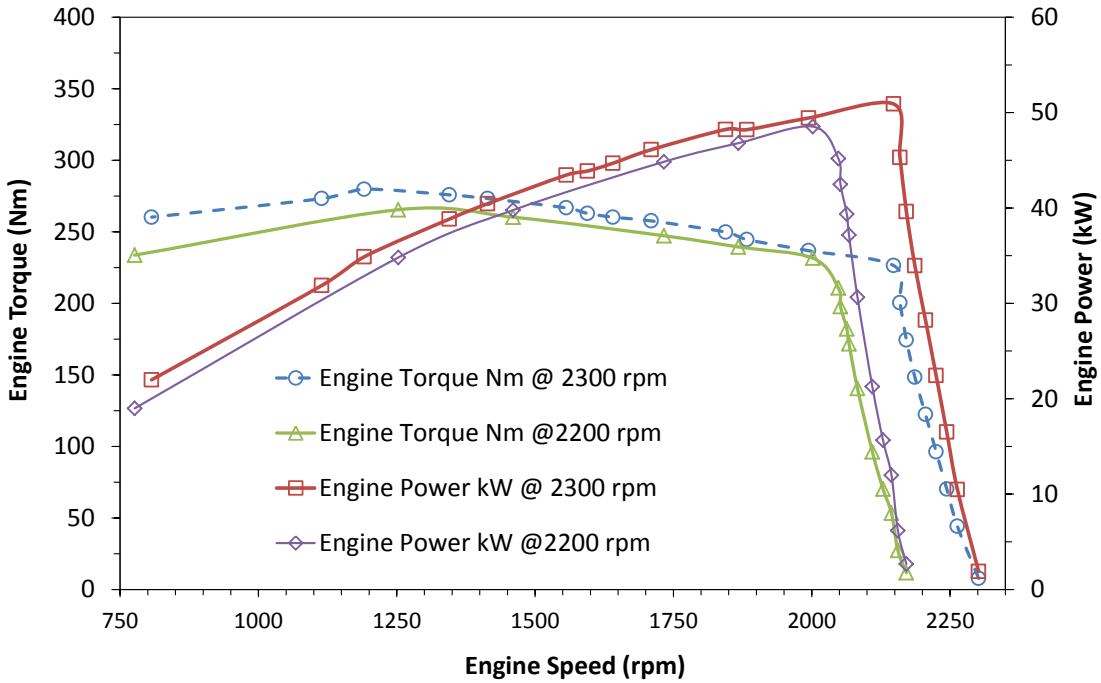

Figure 4.2: Engine power and torque curves against engine speed at maximum operating conditions at 2300 rpm and 2200 rpm for Belarus 920.

to obtain the specific fuel consumption (SFC). The minimum and relatively stable SFC for the Belarus 920 was 264 ± 2 g/kWh and it was obtained at 83 % of the maximum power. According to Serrano et al. (2007), this is considered an excellent performance for optimising the fuel consumption without affecting the work rate. Grisso et al. (2008) reported that the typical range for SFC of tractors is 207.4 to 484.5 g/kWh.

4.3 Steady-State Emission Testing

4.3.1 Emissions of full-load test

At full-load test, measurements of the exhaust gas emission components were taken. The measurement was recorded in order to represent the emission of Belarus 920 as function of engine power while other variables were stabilised. Moreover, these values were used as a reference for the comparison between the values of the transient testing for validation.

The first component of the exhaust gas emission that was examined was CO_2. Figure 4.3 shows the relationship between engine power (kW) and CO_2 formation (kg/h). The CO_2 emissions from the Belarus during the steady state test exhibited a linear correlation with respect to engine power with fit value R^2 of 0.9785. The correlation of CO_2 emission with power presented a higher R^2 value than Bane's (2002) results with an R^2 value of 0.964.

NO_x emissions are presented in Figure 4.4 against engine power. NO_x had similar results to CO_2 as they both increased when engine power increased but with less regularity. NO_x emissions were not linear neither polynomial with power. This is due to the multiple factors that influence NO_x formation. They correlated in polynomial line with an R^2 value of 0.9139 which was higher than Bane's (2002) NO_x results.

CO emissions from the maximum-load steady state tests did not correlate to power, torque nor engine speed. The plot of CO versus engine power was fitted

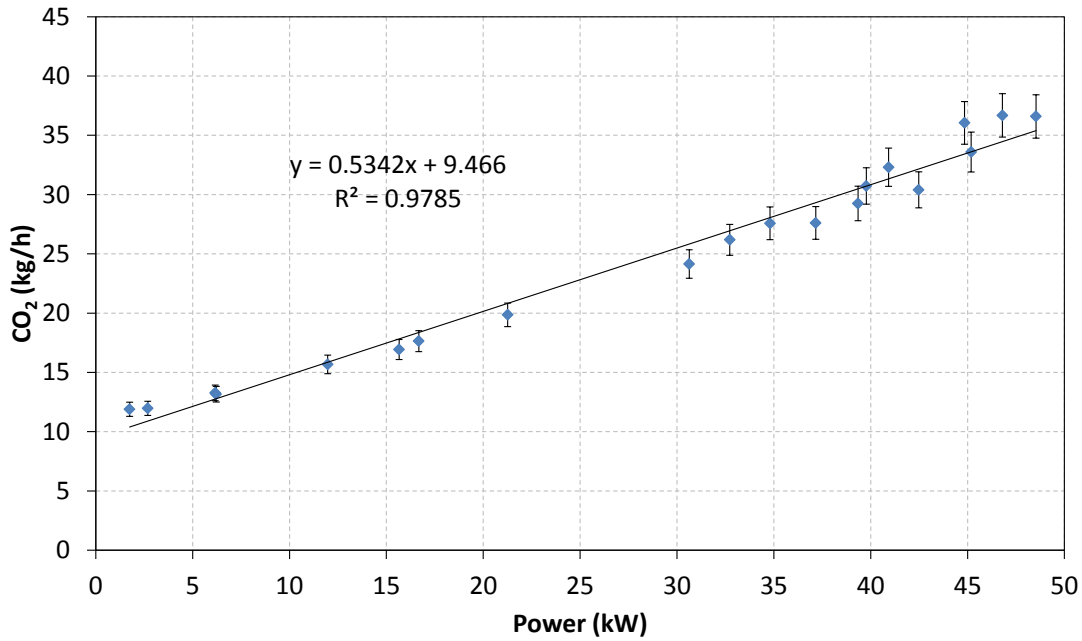

Figure 4.3: CO_2 emissions versus engine power at full-load test.

with a linear line. The data points were essentially scattered and did not show any obvious trend. However, CO showed a linear relation with engine power if only the data of CO at full-fuel delivery were plotted (Fig 4.6). A very different

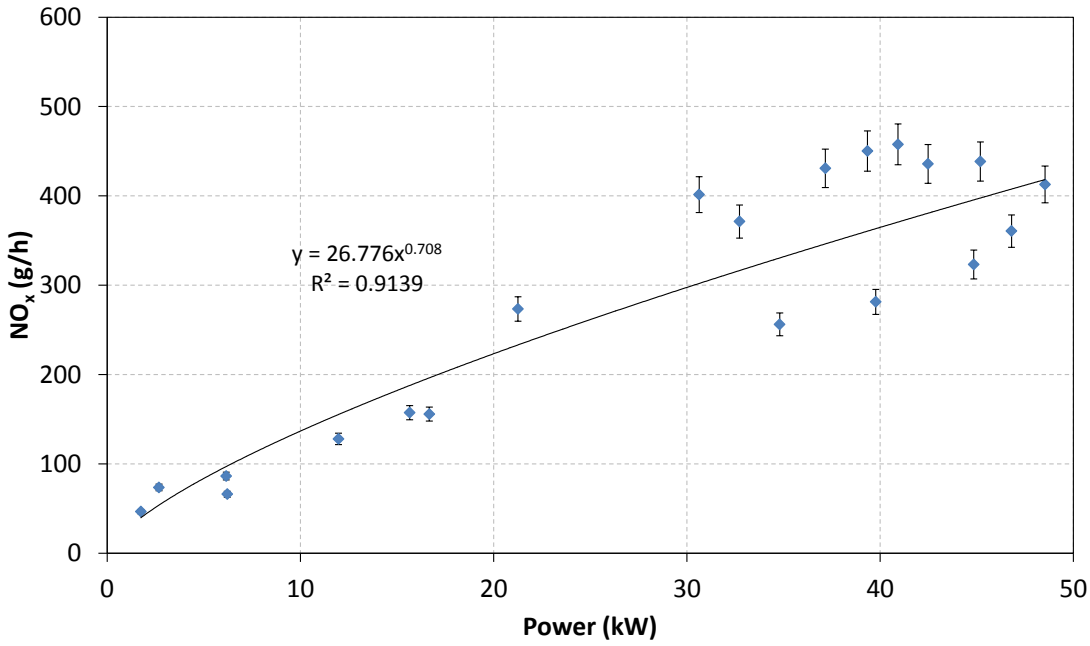

Figure 4.4: NO_x emission versus engine power with polynomial fit line.

relation was exhibited when the emission of CO, during the governed engine speed, was plotted versus engine power (Fig. 4.5).

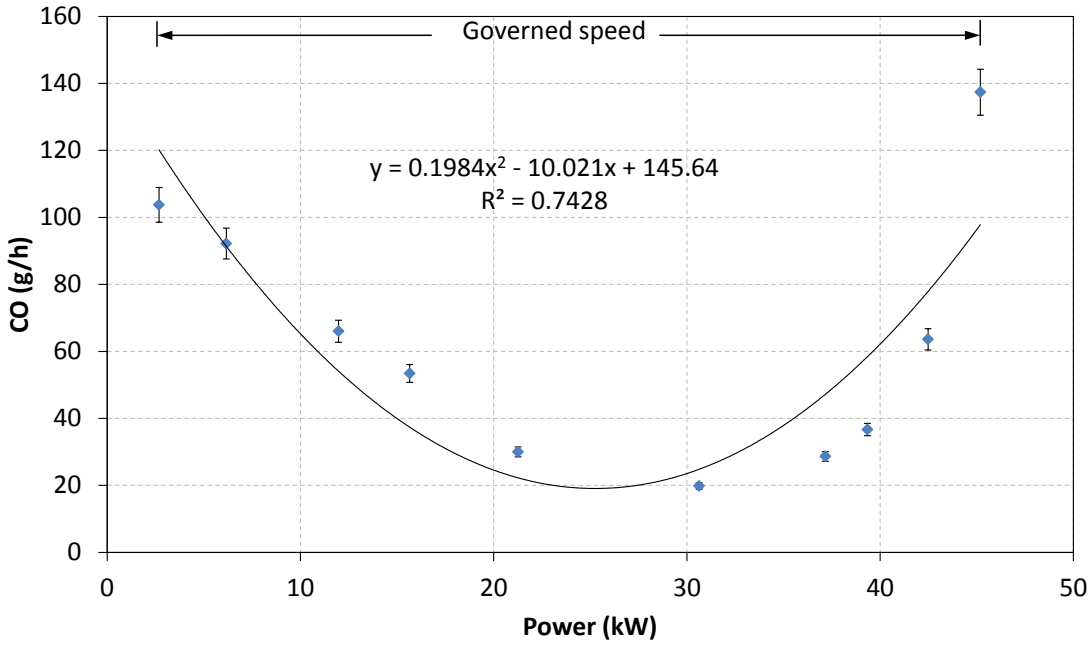

Figure 4.5: CO emissions vs. engine power of full-load test.

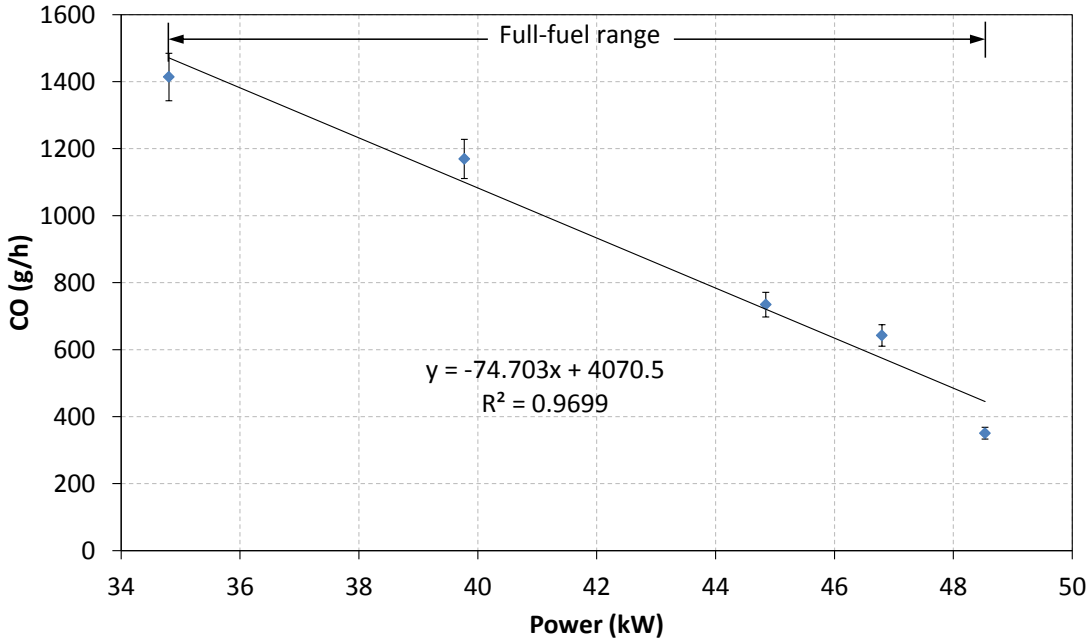

Figure 4.6: CO emissions vs. engine power of full-load test.

4.3.2 Steady-state emission models

Emission is typically estimated from the fuel consumed in the Australian Greenhouse Accounts, as explained in section 2.3.2. In the previous researches (eg. Serrano et al., 2007; Grisso et al., 2004), the calculation of fuel consumption of agricultural tractors was based on engine or PTO power utilisation. Therefore, for ease of calculation and to exclude the influence of all the factors except the power, the direct correlation between the emission of the steady-state test under maximum operation conditions and engine power was studied.

For the emissions that were examined in this test, equations were formulated for each type. Equations 4.2, 4.3, 4.4 and 4.5 were fitted to the collected data as a formula of engine power to calculate each emission species for later comparison with transient test results and the Australian standards.

$$\mathrm{CO}_2 = 0.5342 \times P + 9.466 \tag{4.2}$$

$$\mathrm{NO}_x = 26.776 \times P^{0.708} \tag{4.3}$$

$$\mathrm{CO}_G = 0.1984P^2 - 10.021 \times P + 145.64 \tag{4.4}$$

$$\mathrm{CO}_F = -74.703 \times P + 4070.5 \tag{4.5}$$

where:

$\mathbf{CO}_G$ is the CO emission at the governed range of the engine speed (g/h)

$\mathbf{CO}_F$ is the CO emission at full-fuel delivery (g/h)

$\boldsymbol{P}$ is the engine power (kW)

The equation were used to calculate the emissions from the engine power values of the different modes of ESC and Constant Speed tests. In this case the comparison between the emission is based on the changes in the engine's power. The equations were validated with the measured emissions of the standard steady-state test ECE R-49. The validation procedure is explained in Appendix A.

4.3.3 ECE R-49 test procedure

The tractor was tested with the ECE R-49 test. The purpose of this test is to confirm the emissions compliance with the method that was used at the time of production. This test consists of 10 modes of steady-state loading at two engine speeds. The speeds were determined according to the procedure described in the Directive 88/77/EEC (1988) of the European Union for diesel engine emissions regulations. The rated speed of the Belarus 920 was 2150 rpm and the intermediate speed was 1300 rpm (60 % of the rated speed). During the test, the engine was run three times at low idle speed and no load was applied. The cycle is explained in Fig. 4.7 and Table 4.1.

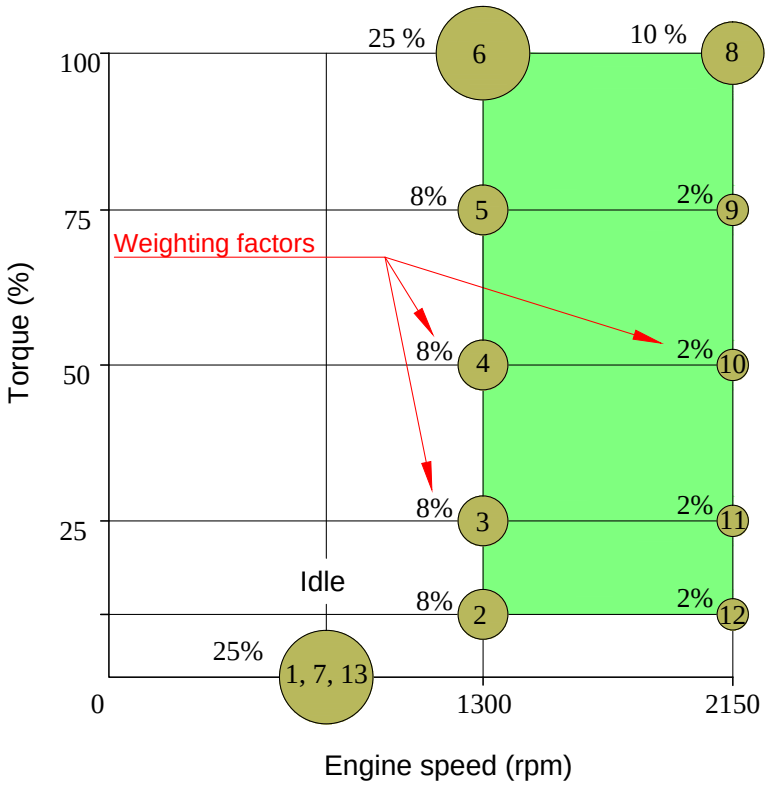

Figure 4.7: Schematic ECE R-49 test diagram for the Belarus 920.

4.3.4 Data analysis procedure

The concentrations of gaseous emissions were measured several times (6 – 7 readings) per second for the entire cycle in ppm. The readings for the last 60 seconds, which is about 360 readings, of every mode in the cycle were averaged and then converted into mass flow rates for each gas using Equations 4.6, 4.8 and 4.7 as exhaust gas density was considered to be 1.293 kg/m^3 at 0 °C and 101.3 kPa (Directive 1999/96/EC, 2000). The averaged specific emissions and the standard deviation for CO_2, NO_x and CO for all the individual modes are presented in Table 4.2.

$$CO_{2(mass)} = 0.001519 \times CO_{2(conc)} \times \dot{m}_{exhw} \tag{4.6}$$

Table 4.1: ECE R-49 test cycle.

Mode No.	**Engine speed type**	**Engine speed (rpm)**	**Torque (%)**	**Torque (Nm)**
1	idle	750	—	—
2	intermediate	1300	10	106
3	intermediate	1300	25	265
4	intermediate	1300	50	530
5	intermediate	1300	75	795
6	intermediate	1300	100	1060
7	idle	750	—	—
8	rated	2150	100	870
9	rated	2150	75	653
10	rated	2150	50	435
11	rated	2150	25	218
12	rated	2150	10	87
13	idle	750	—	—

$$\mathrm{NO}_{x(mass)} = 0.001587 \times \mathrm{NO}_{x(conc)} \times K_{H,D} \times \dot{m}_{exhw} \tag{4.7}$$

$$\mathrm{CO}_{(mass)} = 0.000966 \times \mathrm{CO}_{(conc)} \times \dot{m}_{exhw} \tag{4.8}$$

Where $\mathrm{CO}_{2(\mathrm{conc})}$, $\mathrm{NO}_{x(\mathrm{conc})}$ and $\mathrm{CO}_{(\mathrm{conc})}$ are the average concentration in ppm and $\dot{m}_{exhw}$ is the exhaust gas mass flow rate in kg/h.

As the NO_x emission depends on the ambient air conditions, concentration of NO_x was corrected for the deviation from the base temperature and humidity

with correction factor $K_{H,D}$, as given in Equation 4.9.

$$K_{H,D} = \frac{1}{1 + A \times (H_a - 10.71) + B \times (T_a - 298)} \tag{4.9}$$

where:

$\boldsymbol{A}$ $= 0.309\, \dot{m}_{fuel}/\dot{m}_{aird} - 0.0266$

$\boldsymbol{B}$ $= -0.209\, \dot{m}_{fuel}/\dot{m}_{aird} + 0.00954$

$\boldsymbol{T_a}$ = temperature of the air, Kelvin

$\boldsymbol{H_a}$ = humidity of the air (g of water per kg dry air) and can be calculated by Equation 4.10

$$H_a = \frac{6.22 \times R_a \times p_a}{p_B - p_a \times R_a \times 10^{-2}} \tag{4.10}$$

where:

$\mathbf{R_a}$ is relative humidity of the air, %

$\mathbf{p_a}$ is saturation vapour pressure of the air, kPa

$\mathbf{p_B}$ is the total barometric pressure, kPa.

Table 4.2: The average specific emissions and the standard deviation of CO_2, NO_x and CO, power and fuel consumption for the 13 modes of the ECE R-49 test.

Mode No.	Power (kW)	Diesel flow rate (kg/h)	CO_2 (kg/kWh)	CO_2 STDEV	CO (g/kWh)	CO STDEV	NO_x (g/kWh)	NO_x STDEV
1	0.27	1.39	11.409	3.067	374.347	227.202	94.276	28.370
2	3.75	3.45	1.868	0.222	29.473	23.272	30.022	4.528
3	9.38	4.02	1.152	0.071	2.811	0.409	30.799	3.307
4	18.77	6.81	0.926	0.008	1.228	1.341	22.969	0.533
5	28.15	8.20	0.907	0.006	1.517	0.766	19.694	0.093
6	37.53	10.44	0.951	0.035	27.833	8.268	12.237	1.321
7	0.32	1.26	9.407	2.123	103.892	50.208	128.253	29.978
8	50.95	13.78	1.072	0.017	4.525	5.122	13.757	0.275
9	38.24	11.52	1.006	0.033	1.449	0.431	18.370	0.803
10	25.47	9.92	1.060	0.019	0.835	0.447	22.029	1.993
11	12.77	6.01	1.443	0.017	4.655	1.041	20.092	1.694
12	5.09	4.37	2.426	0.100	14.498	2.910	24.301	4.192
13	0.27	2.79	11.751	4.042	152.079	104.899	106.067	39.292

4.4 Transient Emission Testing

The European stationary cycle (ESC) was employed for the evaluation of the transient effects on emission generation. The cycle was performed on the tractor through the PTO terminal and repeated three times. The engine output data during this test was maintained in the range of ±2 % of the maximum torque and ±50 rpm for any particular torque engine speed respectively as specified in Directive 1999/96/EC (2000).

4.4.1 ESC test procedure

The ESC test consists of 13 modes of engine speed and torque combinations, which did not comprise a cold start phase. Determination of the tested speed and the torque depends on the maximum rated speed of a tractor's and rated power. Every mode has a weighting factor in the procedure of emission calculation according to Table 4.3. The cycle is depicted in Fig 4.8.

Determination of speed A, B and C (in Table 4.3) was based on Equations 4.11, 4.12 and 4.13 which are defined in Directive 1999/96/EC (2000, Appendix 3 of Annex III). The values were informed by engine performance test.

$$\text{Speed A} = n_{lo} + 25\%(n_{hi} - n_{lo}), \tag{4.11}$$

$$\text{Speed B} = n_{lo} + 50\%(n_{hi} - n_{lo}), \tag{4.12}$$

$$\text{Speed C} = n_{lo} + 75\%(n_{hi} - n_{lo}) \tag{4.13}$$

Table 4.3: ESC test cycle used after July 2000 (EEA, 2006).

Mode	Engine Speed	Torque (%)	Weighting Factor	Time (min)
1	idle	0	0.15	4
2	A	100	0.08	2
3	B	50	0.10	2
4	B	75	0.10	2
5	A	50	0.05	2
6	A	75	0.05	2
7	A	25	0.05	2
8	B	100	0.09	2
9	B	25	0.10	2
10	C	100	0.08	2
11	C	25	0.05	2
12	C	75	0.05	2
13	C	50	0.05	2

Where $\boldsymbol{n_{hi}}$ is the highest engine speed at 70 % of the maximum power and it was 1114 rpm at a power of 31 kW. While, $\boldsymbol{n_{lo}}$ is the lowest engine speed at 50% of the maximum power and it was 807 rpm at a power of 22 kW. n_{hi} and n_{lo} determination for the Belarus 920 are illustrated in Fig. 4.9.

According to Directive 1999/96/EC (2000), the ambient condition has to be checked for test validity before testing the emissions. The test validation value F for diesel engine is calculated by Equation 4.14 (Directive 1999/96/EC, 2000).

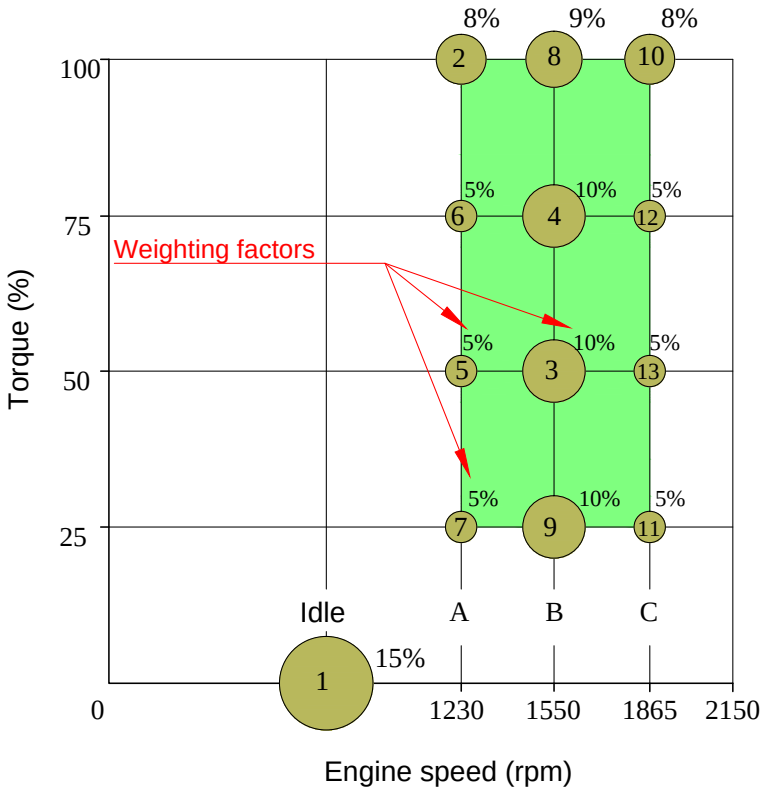

Figure 4.8: ESC schematic test cycle for the Belarus 920.

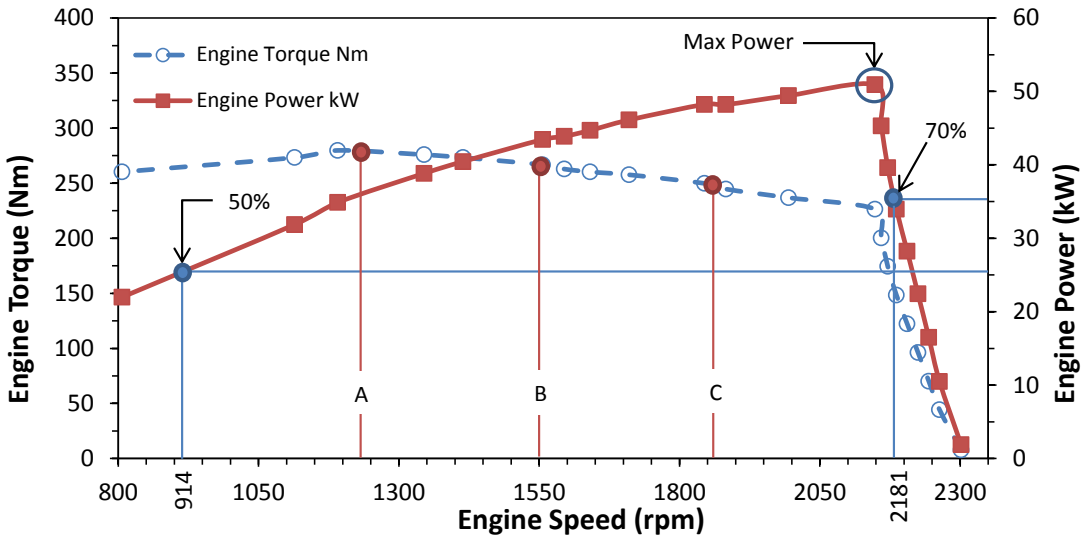

Figure 4.9: Engine power and torque against engine speed at maximum operating conditions showing the calculations of control area for Belarus 920.

The test is valid if the value of F is within a range of 0.96–1.06.

$$\mathrm{F} = \left(\frac{99}{\mathrm{P}_s}\right) \times \left(\frac{\mathrm{T}_a}{298}\right)^{0.7} \tag{4.14}$$

Table 4.4: Implemented speeds and torque values in ESC test for Belarus 920.

Speeds	Implemented Torques			
	100%	**75%**	**50%**	**25%**
A = 1230 rpm	279.7 Nm	209.7 Nm	139.7 Nm	69.7 Nm
B = 1550 rpm	266.7 Nm	199.8 Nm	133.2 Nm	66.6 Nm
C = 1865 rpm	244.6 Nm	183.5 Nm	122.3 Nm	61.2 Nm

where:

$\mathbf{P}_s$ is the atmospheric pressure expressed in kPa,

$\mathbf{T}_a$ is the engine's inlet temperature (Kelvin).

The concentrations of the produced exhaust emissions were collected continuously during the test. However, the last 30 seconds of each mode were only averaged and processed. The concentrations of CO_2, NO_x and CO were measured in ppm and they were converted into hourly mass flow rates (g/h) by using Equations 4.6, 4.7 and 4.8 in section 4.3.4. The result of NO_x only (Directive 1999/96/EC, 2000) was corrected for ambient conditions (humidity, pressure and ambient temperature) in calculating the mass flow rate. The correction factor $K_{H,D}$ in Equation 4.7 was calculated using Equations 4.9 and 4.10 as described in subsection 4.3.4. The averaged specific emissions and the standard deviation for CO_2, NO_x and CO for all the individual modes are presented in Table 4.5.

Table 4.5: The average specific emissions and the standard deviation of CO_2, NO_x and CO, power and fuel consumption for the 13 modes of the ESC test.

Mode No.	Power (kW)	Diesel flow rate (kg/h)	CO_2 (kg/kWh)	CO_2 STDEV	CO (g/kWh)	CO STDEV	NO_x (g/kWh)	NO_x STDEV
1	0.5	0.89	9.981	3.153	381.218	151.734	68.513	21.074
2	36.0	8.50	0.854	0.061	25.975	20.473	10.546	1.701
3	21.6	6.34	0.973	0.022	1.361	0.320	21.782	1.188
4	32.4	8.20	0.907	0.017	2.372	0.528	15.730	1.307
5	18.0	4.64	0.888	0.008	0.925	0.103	19.039	1.807
6	27.0	6.58	0.860	0.009	2.483	1.119	15.433	1.788
7	9.0	3.02	1.128	0.023	13.044	17.399	23.232	1.198
8	43.3	10.59	0.939	0.040	6.438	11.390	10.689	1.328
9	10.8	3.85	1.190	0.028	3.487	0.688	25.749	1.493
10	47.8	13.32	1.016	0.002	10.275	1.110	10.771	0.942
11	11.9	4.15	1.289	0.034	3.981	1.040	20.078	1.246
12	35.8	9.21	0.925	0.004	1.339	0.208	15.502	1.219
13	23.9	6.68	0.971	0.016	0.900	0.502	19.237	1.442

4.5 Constant Speed Test Cycle

It was recognised by many researchers (eg. Lindgren, 2004; Nagendran, 2003; Ullman et al., 1999) that the standardised off-road diesel engine tests were designed to cover all the applications without considering the individual operational characteristics of their application (such as agricultural operations). Lindgren (2004) stated that averaging the variation of non-road machinery in one specific standardised test is not valid. The need for designing a test that can adapt the

variations of agricultural operations was found. In this study, a test cycle which was derived from the ESC test was suggested to simulate the actual on farm tractor behaviour.

4.5.1 Constant Speed test procedure

As the test was conducted through the PTO, the standard PTO speed was selected for testing. The standardised PTO speed for high power operations is 540 rpm (Baillie and Vasey, 1969; Abbaspour-Gilandeh et al., 2009; Işiktepe and Sümer, 2010). The equivalent engine speed of the Belarus 920 to 540 rpm was 2075 rpm. Therefore, the test was designed to be performed at one speed which was 2075 rpm. The changes that occurred in the speed were a result of the applied torque. This is the case in which the tractor is hindered by an obstacle or is facing a variation in the physical properties of the soil during an ordinary farming routine.

The controlled variable in the test was the engine torque. The common power range of PTO-driven implements was considered to be covered in the test. According to Scarlett (2001), the power supplied by the PTO for most of the operations is 50 to 95% of the maximum power of the tractor. The torque percentages that were employed in the test were 25, 50, 75 and 100 % of the maximum torque for the Belarus 920 and they were equivalent to 30, 60, 90 and 120 % of the maximum torque at the tested speed. That was to transmit a power range of 30–98 % of the maximum tractor power.

Table 4.6: 14-mode additional test cycle at constant speed.

Mode No.	Engine Speed (rpm)	Torque (%)	Torque (Nm)	Weighting Factors	Time (min)
1	2075	0	–	0.05	3
2	2075	100	276	0.08	2
3	2075	50	140.5	0.10	2
4	2075	75	210	0.10	2
5	2075	50	140.5	0.05	2
6	2075	75	210	0.05	2
7	2075	25	70	0.05	2
8	2075	100	276	0.09	2
9	2075	25	70	0.10	2
10	2075	100	276	0.08	2
11	2075	25	70	0.05	2
12	2075	75	210	0.05	2
13	2075	50	140	0.05	2
14	idle	0	–	0.1	3

This test contained a number of different loading modes and speeds. The same number of ESC modes was adopted plus one additional mode which represented the time of the implements engagement with the soil. The test started by setting the fuel injection pump to a speed of 2075 rpm with no load applied. Then, the same sequence of the ESC test was followed to apply the torques. Due to overloading of the engine in some modes throughout the cycle, the speed subsequently dropped. The drop in speed was recorded and utilised in the calculation of the

power produced. In the last mode, the speed was reduced to low idle speed and no load was applied. The test cycle is explained in Table 4.6.

4.5.2 Data analysis procedure

The procedure for finding the mass flow rates of the individual mode concentrations was the same as described in the two previous tests. The concentration data was averaged for the last 30 seconds and then converted into mass flow rates using Equations 4.6, 4.7 and 4.8.

Table 4.7: The average specific emissions of CO_2, NO_x and CO, power and fuel consumption for the 14 modes of the Constant Speed test.

Mode No.	Engine speed (rpm)	Engine torque (Nm)	Power (kW)	Diesel flow rate (kg/h)	BSFC (g/kWh)	CO_2 (kg/kWh)	CO (g/kWh)	NO_x (g/kWh)
1	2040	2.60	0.6	4.47	8048.08	20.73	258.02	132.58
2	1630	275.86	47.1	16.54	351.43	1.00	22.17	10.07
3	1990	140.53	29.3	9.89	337.89	0.99	1.20	19.53
4	1960	210.80	43.2	13.88	321.01	0.99	3.30	14.37
5	1990	140.53	29.3	9.82	335.43	1.00	1.28	19.42
6	1960	210.80	43.2	14.10	326.04	1.00	3.52	14.27
7	2030	70.27	14.9	6.60	441.91	1.30	3.07	19.43
8	1630	278.46	47.5	15.19	319.74	1.03	27.00	10.01
9	2030	70.27	14.9	6.42	430.08	1.28	3.04	18.79
10	1810	266.75	50.5	16.00	316.62	1.05	19.98	10.17
11	2040	70.27	15.0	6.49	432.61	1.30	2.64	18.77
12	1950	210.80	43.0	14.17	329.43	1.00	3.87	13.52
13	1980	140.53	29.1	9.54	327.59	0.98	1.29	18.25
14	750	5.20	0.4	1.16	2843.19	7.22	142.54	68.98

4.6 Weighted Specific Emission Calculations

To provide a mean of the comparison between the tests conducted during this study, it was suggested to calculate the specific emissions relative to the hourly work rate. The calculation of specific emissions factors for the ECE R-49, ESC and Constant Speed tests was done by using Equations 4.15, 4.16 and 4.17 (Directive 1999/96/EC, 2000, Appendix 3 of Annex III):

$$\overline{\mathrm{CO_2}} = \frac{\sum \mathrm{CO}_{2(mass)} \times \mathrm{WF}_i}{\sum \mathrm{P(n)}_i \times \mathrm{WF}_i} \tag{4.15}$$

$$\overline{\mathrm{NO}_x} = \frac{\sum \mathrm{NO}_{x(mass)} \times \mathrm{WF}_i}{\sum \mathrm{P(n)}_i \times \mathrm{WF}_i} \tag{4.16}$$

$$\overline{\mathrm{CO}} = \frac{\sum \mathrm{CO}_{(mass)} \times \mathrm{WF}_i}{\sum \mathrm{P(n)}_i \times \mathrm{WF}_i} \tag{4.17}$$

where:

$\mathbf{WF}_i$ is the weighting factor for mode number i,

$\mathbf{P(n)}_i$ is the engine power for mode number i.

4.7 Example of Calculation Procedure

The sample calculation presented in this section, is for the ESC test. Table 4.8 presents the measured data that used for calculating of the individual mode results. This sample calculation procedure is identical for all modes in all tests.

Table 4.8: Sample of data from ESC test shows the mass flow rates of fuel, intake air and exhaust gas and the concentrations of the exhaust gas emission components in ppm of mode 10 of the cycle.

P (kW)	T_a (K)	H_a (kg)	$\dot{m}_{airw}$ (kg/h)	$\dot{m}_{fuel}$ (kg/h)	$\dot{m}_{exh}$ (kg/h)	CO_2 (ppm)	CO (ppm)	NO_x (ppm)
47.75	297.15	5.79	268.22	13.31	281.53	113364	2023.3	1134.7

H_a was calculated using Equation 4.10,

$$H_a = \frac{6.22 \times R_a \times p_a}{p_B - p_a \times R_a \times 10^{-2}}$$

where the measured relative humidity of the air (R_a) was 40 % and the barometric pressure (P_B) was 101.4 kPa. The saturation vapour pressure of the air (P_a) for 20℃ is 2.3392 kPa which was obtained from (Çengel and Boles, 2007, Table A-4, p.916).

- *Calculation of the NO_x humidity correction factor $K_{H,D}$ (Equation 4.9):*

$$A = 0.309 \times 13.31/268.22 - 0.0266 = -0.0112$$

$$B = 0.209 \times 13.31/268.22 + 0.00954 = 0.0199$$

$$K_{H,D} = \frac{1}{1 + A \times (H_a - 10.71) + B \times (T_a - 298)}$$

$$K_{H,D} = \frac{1}{1 - 0.0112 \times (5.79 - 10.71) + 0.0199 \times (297.15 - 298)} = 0.9438$$

- *Calculation of emission mass flow rates:*

$$\mathrm{CO}_{2(mass)} = 0.001519 \times \mathrm{CO}_{2(conc)} \times \dot{m}_{exhw}$$

$$\mathrm{CO}_{2(mass)} = 0.001519 \times 113364 \times 268.22 = 48480.12\,\mathrm{g/h}$$

$$\mathrm{NO}_{x(mass)} = 0.001587 \times \mathrm{NO}_{x(conc)} \times K_{H,D} \times \dot{m}_{exhw}$$

$$\mathrm{NO}_{x(mass)} = 0.001587 \times 1134.7 \times 268.22 = 478.54\,\mathrm{g/h}$$

$$\mathrm{CO}_{(mass)} = 0.000966 \times \mathrm{CO}_{(conc)} \times \dot{m}_{exhw}$$

$$\mathrm{CO}_{(mass)} = 0.001519 \times 113364 \times 268.22 = 48480.12\,\mathrm{g/h}$$

- *Calculation of the specific emissions:*

The following example calculation is for NO_x and it is identical for the other components.

The emission mass flow rates were multiplied by the respective weighting factors, as listed in Table 4.3. The summation of the results were calculated to find the weighted mean mass flow rate over the cycle.

$$\overline{\mathrm{NO}_x} = \frac{\sum \mathrm{NO}_{x(mass)} \times \mathrm{WF}_i}{\sum \mathrm{P(n)}_i \times \mathrm{WF}_i}$$

$$\begin{aligned}\sum \mathrm{NO}_{x(mass)} \times \mathrm{WF}_i = &(23.36 \times 0.15) + (382.48 \times 0.08) + (444.19 \times 0.10) \\ &+ (484.10 \times 0.10) + (311.62 \times 0.05) + (367.61 \times 0.05) \\ &+ (196.36 \times 0.05) + (408.8 \times 0.09) + (206.55 \times 0.10) \\ &+ (478.53 \times 0.08) + (231.97 \times 0.05) + (507.66 \times 0.05) \\ &+ (420.89 \times 0.05) \\ = &\, 329.87\,\mathrm{g/h}\end{aligned}$$

The engine power for each individual mode was multiplied by the same respective weighting factors that are listed in Table 4.3. The summation of the results were calculated to find the weighted mean power over the cycle.

$$\begin{aligned}\sum \mathrm{P(n)}_i \times \mathrm{WF}_i = &(0.5 \times 0.15) + (36.01 \times 0.08) + (21.61 \times 0.10) \\ &+ (32.42 \times 0.10) + (17.99 \times 0.05) + (27.00 \times 0.05) \\ &+ (8.97 \times 0.05) + (43.27 \times 0.09) + (10.80 \times 0.10) \\ &+ (47.75 \times 0.08) + (11.93 \times 0.05) + (35.81 \times 0.05) \\ &+ (23.87 \times 0.05) \\ = &\, 23.43\,\mathrm{kW}\end{aligned}$$

$$\overline{\mathrm{NO}_x} = \frac{329.87}{23.43} = \ 14.07\,\mathrm{g/kWh}$$

Chapter 5

RESULTS AND DISCUSSION

5.1 Introduction

This chapter presents the emissions results measured from the Belarus 920 during the steady state (ECE R-49), transient cycle (ESC) and the additional test at constant speed (described in chapter 4). Both the measured and the calculated emissions that is based on the steady state equations (from Subsection 4.3.2) using the power measured during the transient cycle and the additional cycle are analysed. The steady state emission are compared to the transient emissions of each cycle.

5.2 Emissions of ECE R-49 Test

The average of the weighted specific emissions of three repeated runs are presented in Table 5.1. The results show that the measured emissions, if compared to the emission component limits set by Directive 88/77/EEC (1988), were 0.22 g/kWh

higher for NO_x and 1.96 g/kWh higher for CO. Considering the age of the tractor, these results are practically acceptable as there is an expectation that performance will deteriorate over time. Moreover, The characteristics of the tested fuel was slightly different from the fuel specified by Directive 1999/96/EC (2000) (refer to Appendix C). The result here give confidence in the engine to test different methodologies.

Table 5.1: ECE R-49 results compared to European Union limits (Directive 88/77/EEC, 1988).

Gaseous emissions	**Belarus 920 (A)**	**EU limits (B)**	**Differences %** $\left(\frac{\mathrm{A}-\mathrm{B}}{\mathrm{B}} \times \mathbf{100}\%\right)$
$\mathbf{NO_x}$	16.02 g/kWh	15.8 g/kWh	1.39 %
CO	14.26 g/kWh	12.3 g/kWh	15.93 %
$\mathbf{CO_2}$	1043.11 g/kWh	—	—

From the difference in the percentages between the measured specific emission and EU limits presented in Table 5.1, some could speculate that transient test emission would have a similar increasing trend, if not higher.

5.3 Comparison of Transient and Steady-State Emissions

The first objective of this project is to study the differences in emission amounts due to the variation between steady state and transient testing. Therefore, equa-

tions based on steady-state test was formulated in order to compute the emissions from engine power. The steady-state calculated emissions were compared to the measured emissions during the transient testing.

5.3.1 Emissions of ESC test related to EU limits

The weighted specific emission of three repeated tests were averaged and listed in Table 5.2. The results were then compared to the European Union (EU) emissions standards, for NO_x and CO only, that were specified for heavy-duty diesel engines type A for the years between 2000 and 2005. The emissions of the Belarus 920 tractor produced during the ESC test were exceedingly over the limits of the EU emissions standards. They were more than three times that of the EU emissions standards for NO_x and nearly four times for CO. Such a substantial increase is a result of the transient effects on the produced emission. The results showed an evident inability of the old technology comply with limits of the transient test.

Table 5.2: ESC results compared to European Union limits (Directive 1999/96/EC, 2000).

Gaseous emissions	**Belarus 920 (A)**	**EU limits (B)**	**Differences** $\left(\frac{\mathrm{A}-\mathrm{B}}{\mathrm{B}} \times \mathbf{100}\%\right)$
$\mathbf{NO_x}$	15.09 g/kWh	5.0 g/kWh	201 %
CO	7.99 g/kWh	2.1 g/kWh	280 %
$\mathbf{CO_2}$	975.86 g/kWh	—	—

5.3.2 Transient versus calculated steady state

The emissions of CO_2, NO_x and CO were time aligned with the beginning of the test by considering the response time (in Table 3.4) of the CODA gas analyser for each individual component. The calculated emissions that were obtained using Equations 4.2 to 4.5 in Subsection 4.3.2 from the measured power during the ESC test were plotted in the same figures.

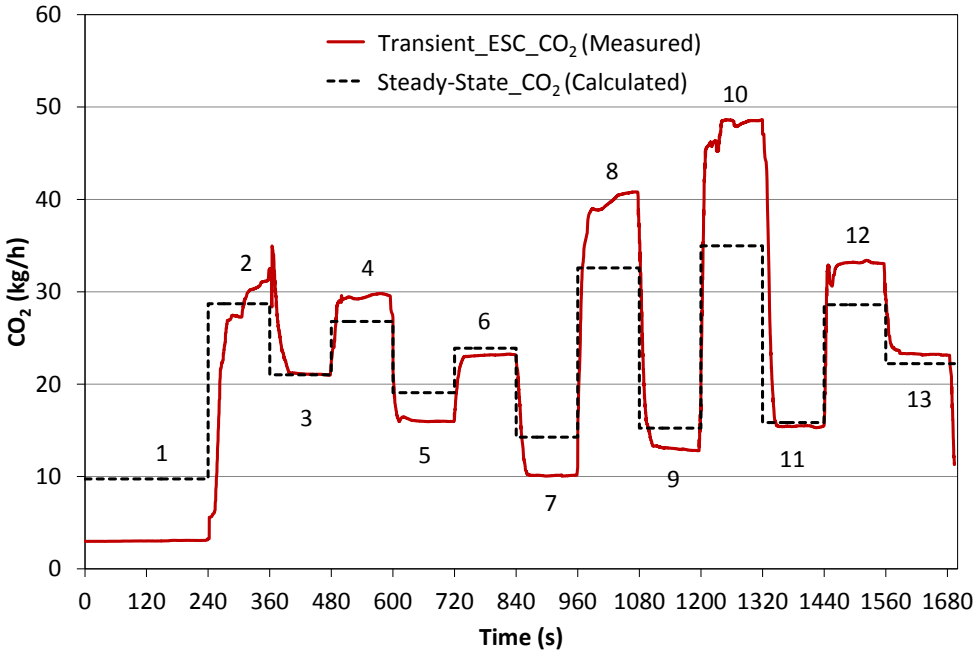

Figure 5.1: Comparison between steady state and transient (ESC) CO_2 emissions against testing time (s). The values of (1, 2, ..., 13) refer to changes in engine speeds and torques presented in Table 4.3.

Figure 5.1 presents the measured CO_2 in kg/h for the ESC test and the power-based calculated steady state emission. Both measured and calculated CO_2 emissions showed a rather similar trend with a slight increase or decrease in the emission values for most of the modes. The calculated CO_2 emission was slightly higher where the negative change in engine torque occurred. On the other hand measured emissions were higher in the modes with positive torque changes. In

modes 8 and 10, where engine speed and engine torque had both been increased, a considerable increase in measured CO_2 over the calculated occurred.

Figure 5.2 presents both measured and the power-related steady state calculated NO_x emissions in g/h for the ESC test. The measured NO_x transient emission showed an evident deviation from the calculated steady state emission. This occurred because, firstly, the steady state equation for the NO_x emission was less accurate in predicting the emission amount than CO_2. Secondly, NO_x formation is influenced by a range of other factors as well as the effect of engine brake power. However, the steady state equation predicted the trend of the emission changes (increase or decrease) for the cycle except for mode 3, where the torque reduced and the speed increased, measured NO_x emission exhibited opposite tendency.

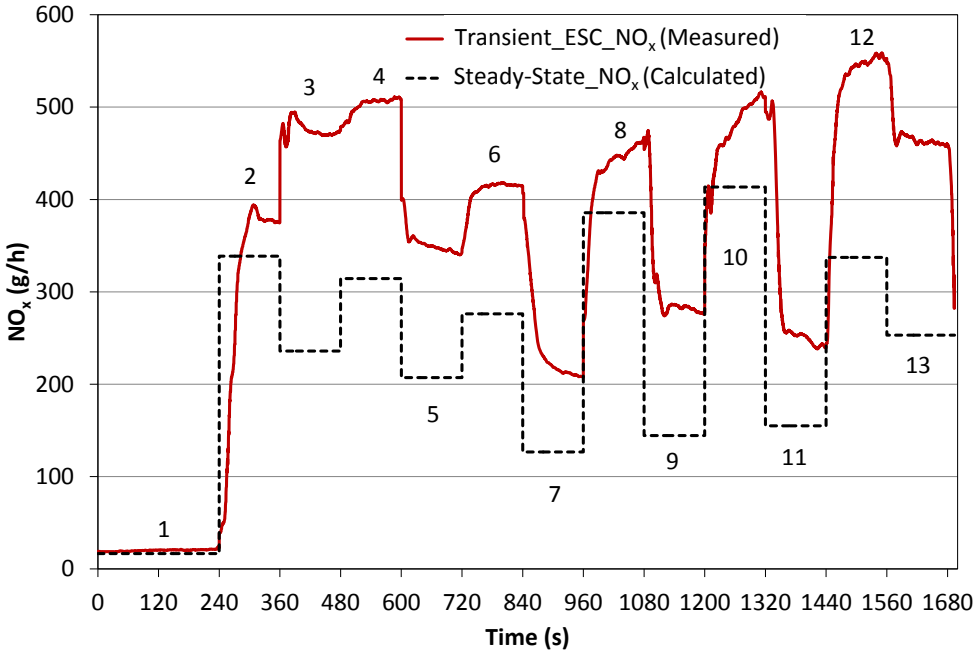

Figure 5.2: Comparison between steady state and transient (ESC) NO_x emissions against testing time (s). The values of (1, 2, ..., 13) refer to changes in engine speeds and torques presented in Table 4.3.

Measured and calculated CO emissions for the ESC test are presented in Fig. 5.3.

The measured CO emission was very close to the calculated steady state emission except in some segments (mode 2 and 8) of the cycle which were evidently due to the influence of the transient effects. This result is in agreement with Ericson et al.'s (2005) findings when they compared their model to predict transient emission from steady state-based equations with measured emissions during TNO part 3 test cycle.

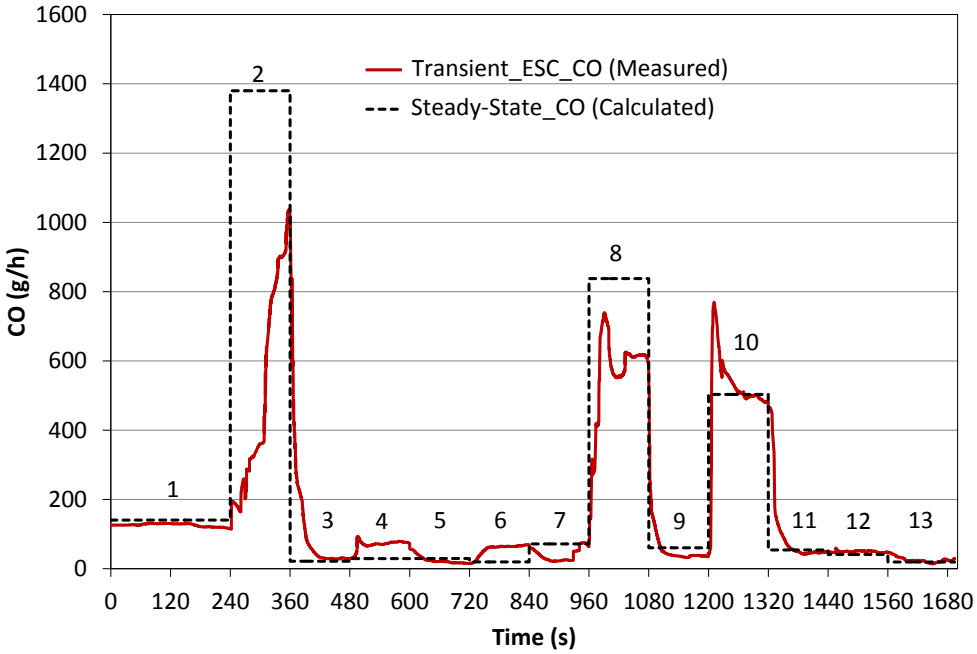

Figure 5.3: Comparison between steady state and transient (ESC) CO emissions against testing time (s). The values of (1, 2, ..., 13) refer to changes in engine speeds and torques presented in Table 4.3.

The weighted specific emission for the entire cycle of both transient and steady-state emissions of all gaseous components are presented in Table 5.3. An over counting of 44.26 % for CO emission was found for the resulting percent differences between steady state and transient emissions. Whilst, steady state based emissions were lower by 3.73 % for CO_2 and 33 % for NO_x.

Table 5.3: Belarus 920 steady-state emission compared to the transient emission.

Gases	Steady State	Transient	Differences %
NO_x	10.02 g/kWh	15.09 g/kWh	33.58
CO	11.54 g/kWh	7.99 g/kWh	−44.26
CO_2	939.43 g/kWh	975.86 g/kWh	3.73

5.3.3 Constant Speed versus calculated steady state

Figure 5.4 presents the measured CO_2 in kg/h for the Constant Speed test and the power-based calculated steady state emission. Both measured and calculated CO_2 emissions showed a rather similar trend with considerable differences in the emission values for most of the positive loading modes. The calculated emission was insensitive to the speed variation when the power was close to the zero as in mode 1 and 14.

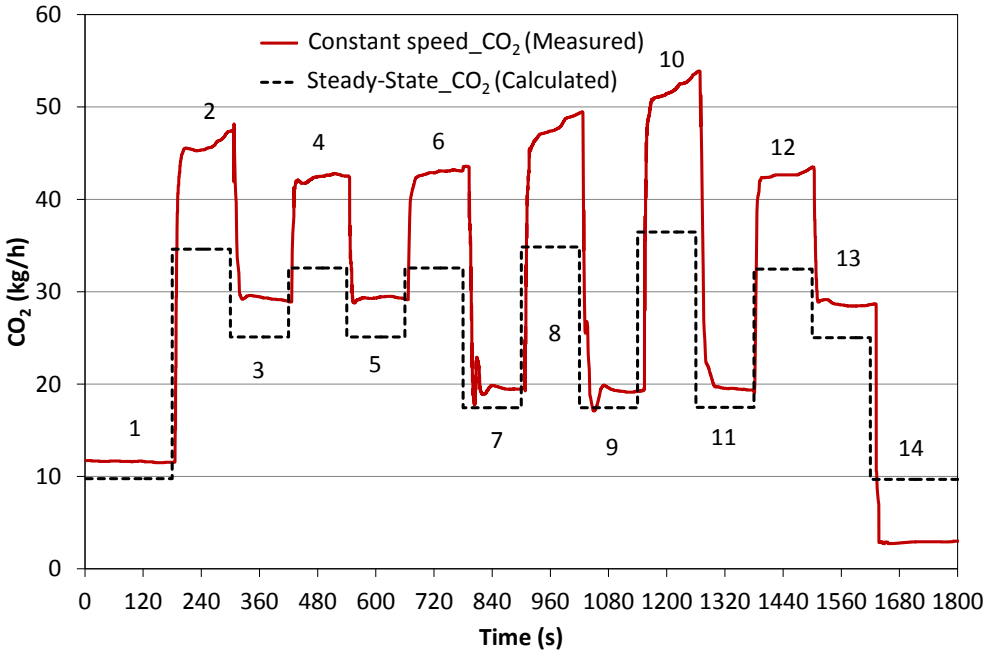

Figure 5.4: Comparison between steady state and Constant Speed test CO_2 emissions against testing time (s). The values of (1, 2, ..., 14) refer to changes in engine speeds and torques presented in Table 4.6.

Figures 5.5 and 5.6 present the emissions of both measured and the power-related steady state for the NO_x and CO emissions in g/h for Constant Speed test. The measured NO_x emissions showed an enormous variations from the calculated steady state emission. While, CO measured emissions had a marginal differences in all the modes except modes 2, 8 and 10 which had considerable differences where the engine was overloaded.

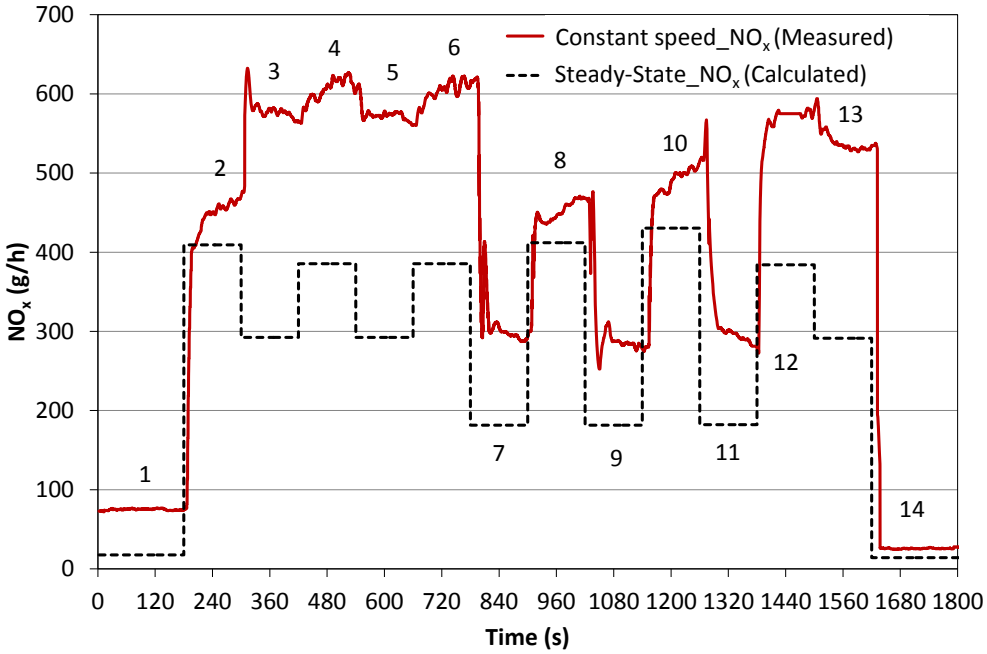

Figure 5.5: Comparison between steady state and Constant Speed test NO_x emissions against testing time (s). The values of (1, 2, ..., 14) refer to changes in engine speeds and torques presented in Table 4.6.

The weighted specific emission for the entire cycle of both the Constant Speed test and steady-state emissions of all gaseous components are compared in Table 5.4. From the result, CO_2 emission for the Constant Speed test was found to be 19.74 % higher than the calculated steady state. Interestingly, the difference between the measured NO_x and the steady state in this test was similar to that between measured NO_x and the steady state in the ESC test. Emission of CO was found higher than the steady state in contrast with the ESC test.

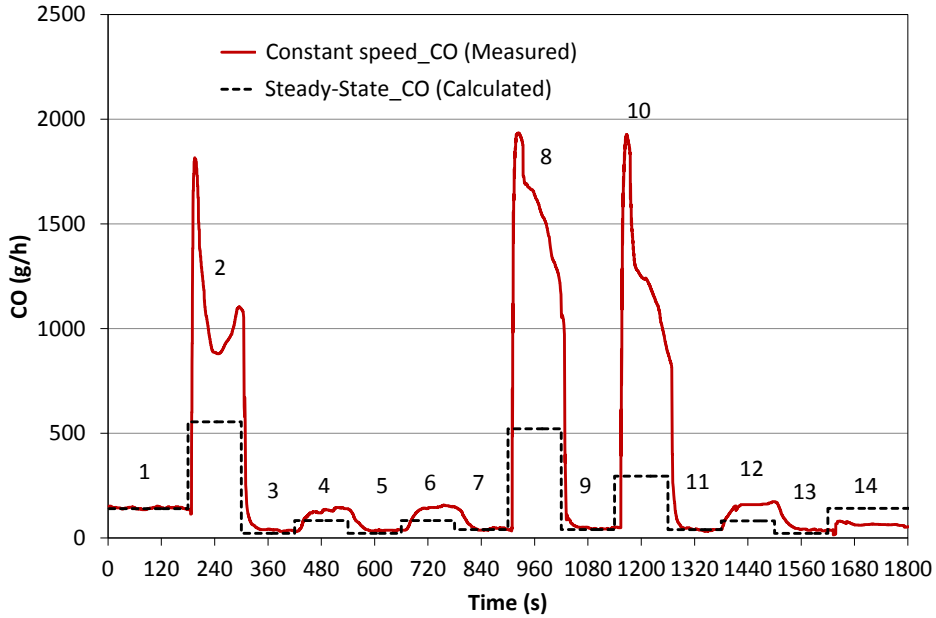

Figure 5.6: Comparison between steady state and Constant Speed test CO emissions against testing time (s). The values of (1, 2, ..., 14) refer to changes in engine speeds and torques presented in Table 4.6.

Table 5.4: Belarus 920 calculated steady-state emission compared to the Constant Speed test emission.

Gases	**Steady State**	**Constant Speed Test**	**Differences %**
$\mathbf{NO}_x$	9.39 g/kWh	14.14 g/kWh	33.59 %
CO	5.57 g/kWh	11.44 g/kWh	51.25 %
$\mathbf{CO_2}$	853.71 g/kWh	1063.7 g/kWh	19.74 %

5.4 Variation in the Emissions Due to Machinery Application

Studying the effect of machinery application on the emission is on of the objectives of this study. The tractor was tested under various loads at one constant speed (2075 rpm) in order to simulate the on-field loading patterns of agricultural tractors. The resulted emission then compared to the standard ESC test to determine the difference.

5.4.1 Constant Speed versus ESC result

The emissions of CO_2, NO_x and CO for Constant Speed and ESC tests were time aligned together. The ESC test emission was shifted 60 seconds backward to match with beginning of the modes in the constant speed test by deleting the first 60 seconds of the ESC test data set. Figure 5.7 presents CO_2 emissions. The results of Constant Speed test were apparently higher than the results of the ESC test because the engine was operated at higher speed and under higher torques.

Figure 5.8 presents the emissions of NO_x for constant speed and ESC. The figure shows that both tests had a similar general trend. The tests had identical result in modes 8, 9 and 10. In modes 8 and 10, the produced powers were similar, therefore, resulting in close amounts of NO_x emitted in these modes. In mode 9, ESC test had a lower power value than the Constant Speed test (10 kW in the ESC and 15 kW in the Constant Speed test), however they had close results. The

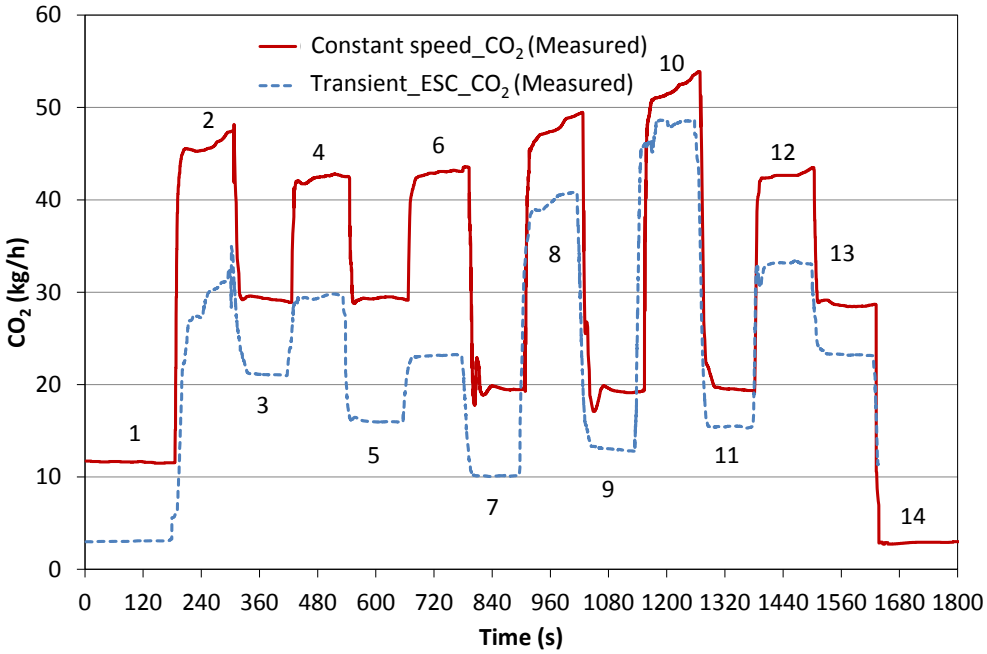

Figure 5.7: Comparison between ESC and Constant Speed test CO_2 emissions against testing time (s). The values of (1, 2, ..., 14) refer to changes in engine speeds and torques presented in Tables 4.3 and 4.6.

exhaust gas mean temperature in mode 9 of ESC was 239 °C and 309 °C in mode 9 of the Constant Speed test. Hence, the similarity in the results was a factor of the differences in engine power and engine temperature for both tests.

Figure 5.9 presents the emission of CO for the ESC and Constant Speed tests. The chart shows no significant differences in the resulted emission of these tests as the emissions of most of the modes ranged between 25 to 160 g/h. However, it emphasises the effects of overloading the engine on the fuel combustion quality. It had a significant role in increasing the emission of CO by nearly three times as can be seen in mode 3, 8 and 10 when the engine was overloaded by subjecting high torque equivalent to 120 % of the its capacity at this speed.

The weighted specific emission for the entire cycle of both the Constant Speed test and transient test (ESC) of all gaseous components are compared in Table 5.5.

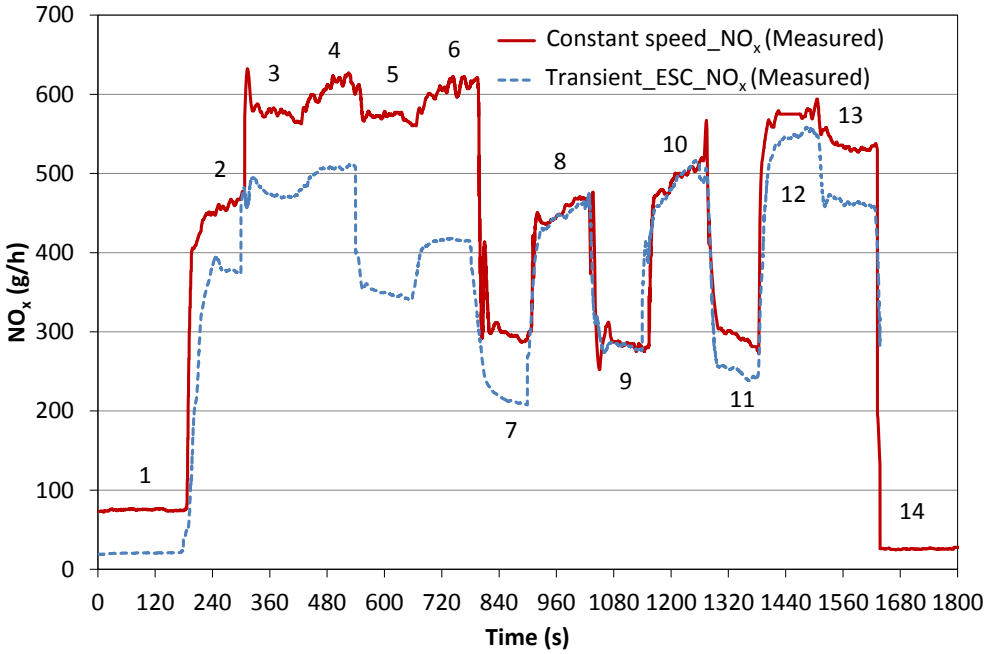

Figure 5.8: Comparison between ESC and Constant Speed test NO_x emissions against testing time (s). The values of (1, 2, ..., 14) refer to changes in engine speeds and torques presented in Tables 4.3 and 4.6.

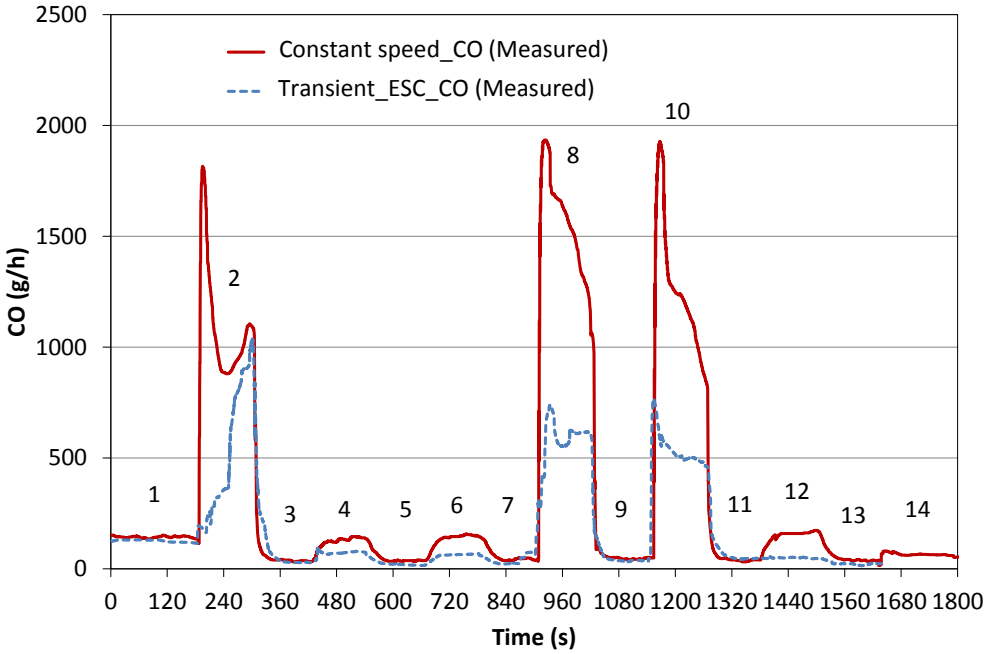

Figure 5.9: Comparison between ESC and Constant Speed test CO emissions against testing time (s). The values of (1, 2, ..., 14) refer to changes in engine speeds and torques presented in Tables 4.3 and 4.6.

From the table, CO_2 emission for the Constant Speed test was found to be 8.25 % higher than the ESC test. The higher result for CO_2 is due to the difference in

Table 5.5: Belarus 920 transient test emission compared to the Constant Speed test emission.

Gases	**Transient (ESC)**	**Constant Speed Test**	**Differences %**
NO_x	15.09 g/kWh	14.14 g/kWh	−6.65
CO	7.99 g/kWh	11.44 g/kWh	30.15
CO_2	975.86 g/kWh	1063.7 g/kWh	8.25

engine speed and torque and consequently higher fuel consumption. The constant speed test produced 6.65 % less NO_x and 30.15 % more CO than the ESC test. According to Juostas and Janulevičius (2009), incomplete combustion of the fuel in diesel engines leads to an increase in CO; While NO_x tends to decrease because incomplete combustion generates less heat thereby a lower temperature in the combustion chamber. The specific emission of NO_x does not seem to match the measured result in g/h presented in Fig 5.8. That is because of the generated power during the cycle in constant speed test was 26.4 % higher than the ESC test.

The increase in CO emission was due to the increase in applied torque. At higher torque the engine may suffer incomplete combustion. According to Juostas and Janulevičius (2009), changes in fuel consumption at the normal conditions has no influence on CO emission because in diesel engines, the fuel is burnt with an abundant access of air.

5.5 Australian Emission Factors Versus the Measured

In the Australian National Greenhouse Gas Accounts (NGA) factors, estimating the annual emission quantity of agricultural tractors is based on the total quantity of fuel consumed. The emission value is obtained by multiplying total fuel amount by the respective emission factor (kg CO_2-e/GJ) and the energy content (GJ/kL) from Table 2.2 as in Equation 2.1 (as explained in Section 2.3.2). This method is designed to have a general application so it can cover the broader range of greenhouse emissions inventories (DCCEE, 2011). The total time integrated fuel consumption during each test cycle is listed in Table 5.6. The CO_2-e emissions form the accumulated diesel consumption of each cycle were calculated. It was found that the real measurement of CO_2 emissions yielded about 10 to 13 percent higher results than the calculated CO_2-e emission using the Australian emission factors (EF) (Fig. 5.10).

Table 5.6: Accumulated fuel consumed during the test cycles and the respective estimated emission using Australian EF compared to the measured CO_2 emissions.

Description	**ECE R-49**	**ESC**	**Constant Speed**
Total test duration (min)	78	28	30
Total fuel consumption (L)	8.395	3.488	4.903
Total CO_2 emission (kg CO_2-e)	22.618	9.397	13.209
Total measured CO_2 (kg)	25.596	10.348	14.816

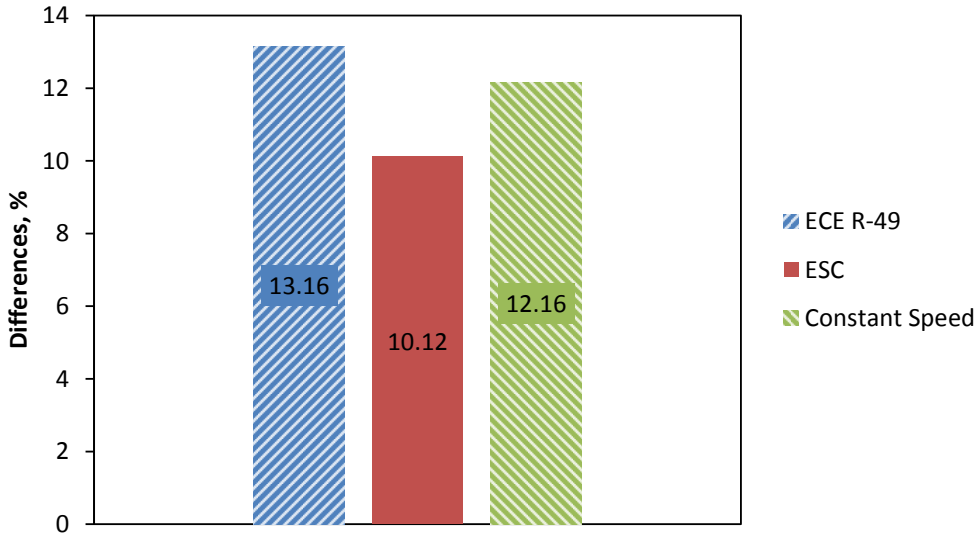

Figure 5.10: The percentages of the differences between the measured CO_2 emission and the Australian EF-based calculated emission.

5.6 General Discussion

5.6.1 Transient and Steady State

The result showed that the test cycle characteristics have a considerable impact on exhaust emissions. However, some factors are more important than others. Figure 5.11 shows the influence of transient effects on emissions from the diesel engine of the agricultural tractor. It is clear that the emissions estimation based on steady state did not match the real measurement of the test cycles. Although CO_2 has less sensitivity for transient as its magnitude is governed by the amount of fuel consumption, it showed a significant variation in the Constant Speed test.

The transient test (ESC) clearly resulted in higher emissions for both CO_2 and NO_x and lower CO than the calculated steady state. This comparison was supported when the results of real measurement of steady state against engine torque

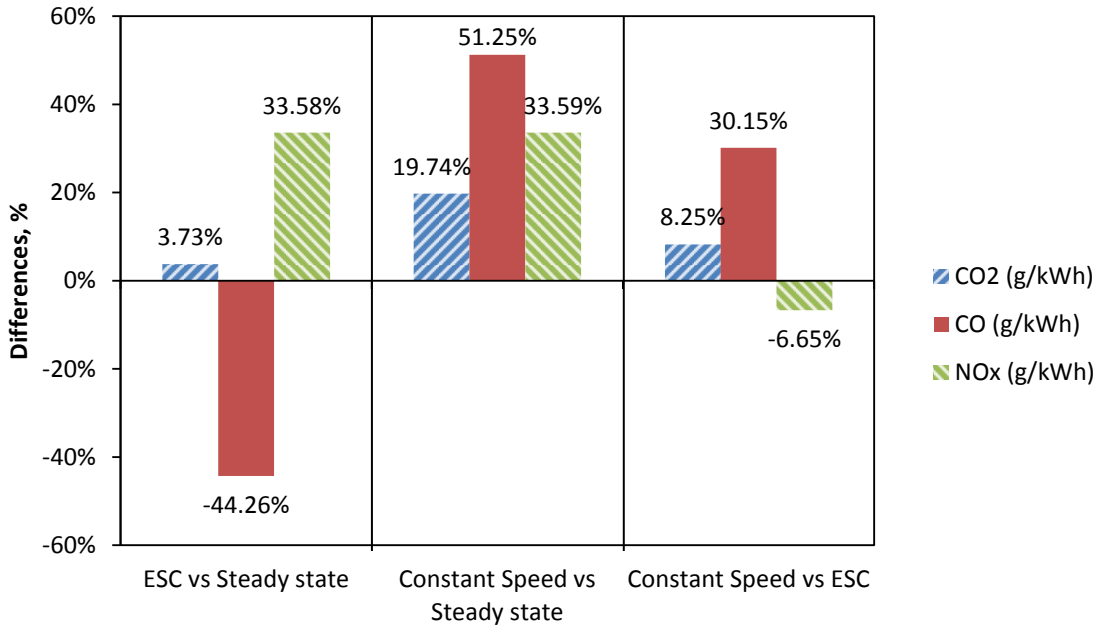

Figure 5.11: Measured emissions during the ESC and Constant Speed test cycles versus calculated emissions.

and speed were compared to the ESC test results as shown in Figs. 5.12, 5.13 and 5.14. CO_2 and NO_x emissions for the ESC test generated at 100 % torque were higher than steady state emission at the same torque and speed ranges due to the influence of transient changes on emission levels.

The percentage of the difference between test Constant Speed test and ESC test showed that considering the application-specific characteristics in the test have an influence on the resulted emissions. The obtained CO result from Constant Speed test was 30 % higher than the ESC. This shows an agreement with the percentage of the difference between CO emission factors of HD on-road vehicles and agricultural tractors, which is 30 % as well, reported by Ntziachristos and Samaras (2009) and Winther and Samaras (2009).

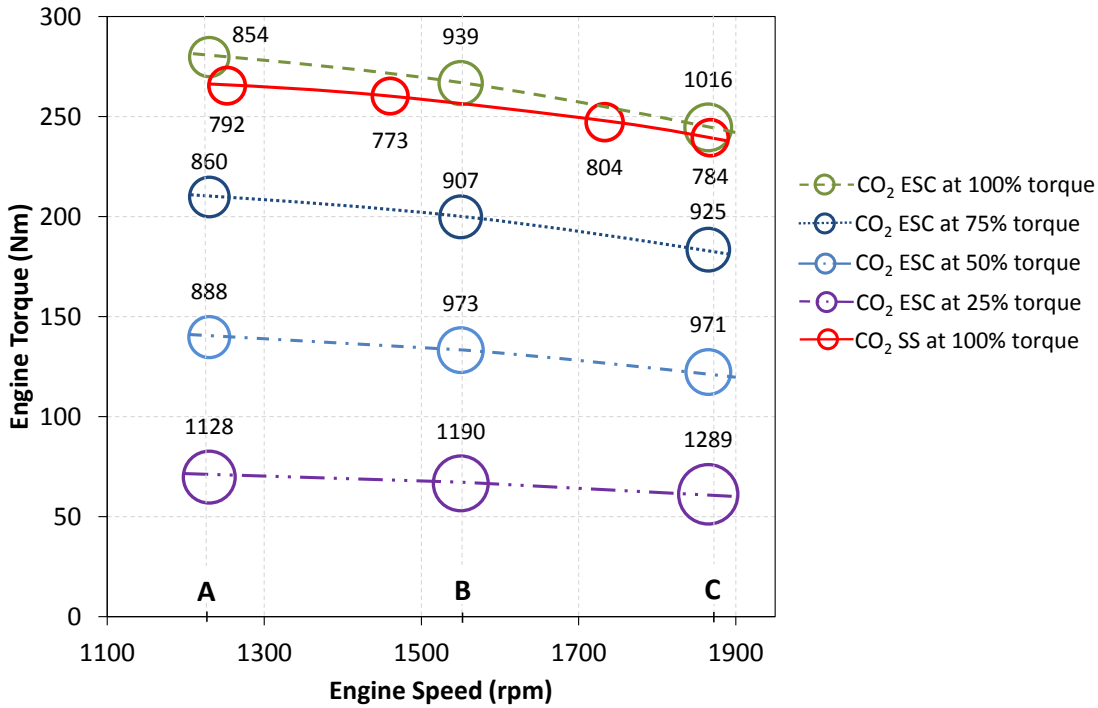

Figure 5.12: Comparison between CO_2 (g/kWh) of steady-state and ESC tests. A, B and C are the speeds listed in Table 4.4. The circle size represents the quantity of the emission.

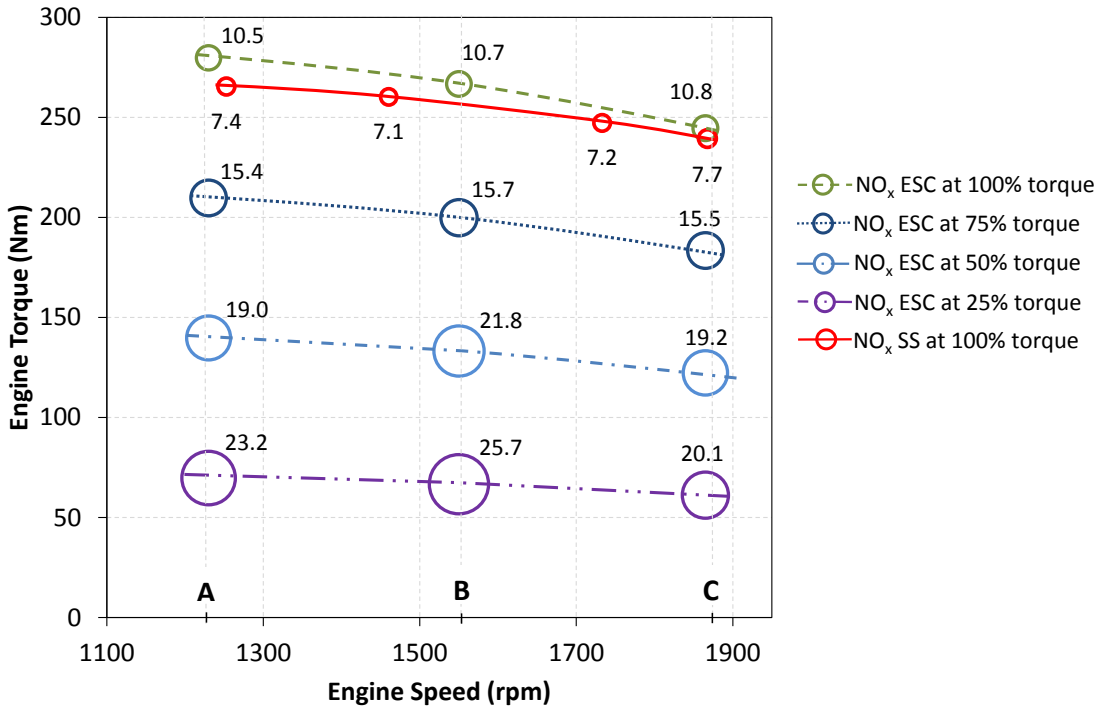

Figure 5.13: Comparison between NO_x (g/kWh) of steady-state and ESC tests. A, B and C are the speeds listed in Table 4.4. The circle size represents the quantity of the emission.

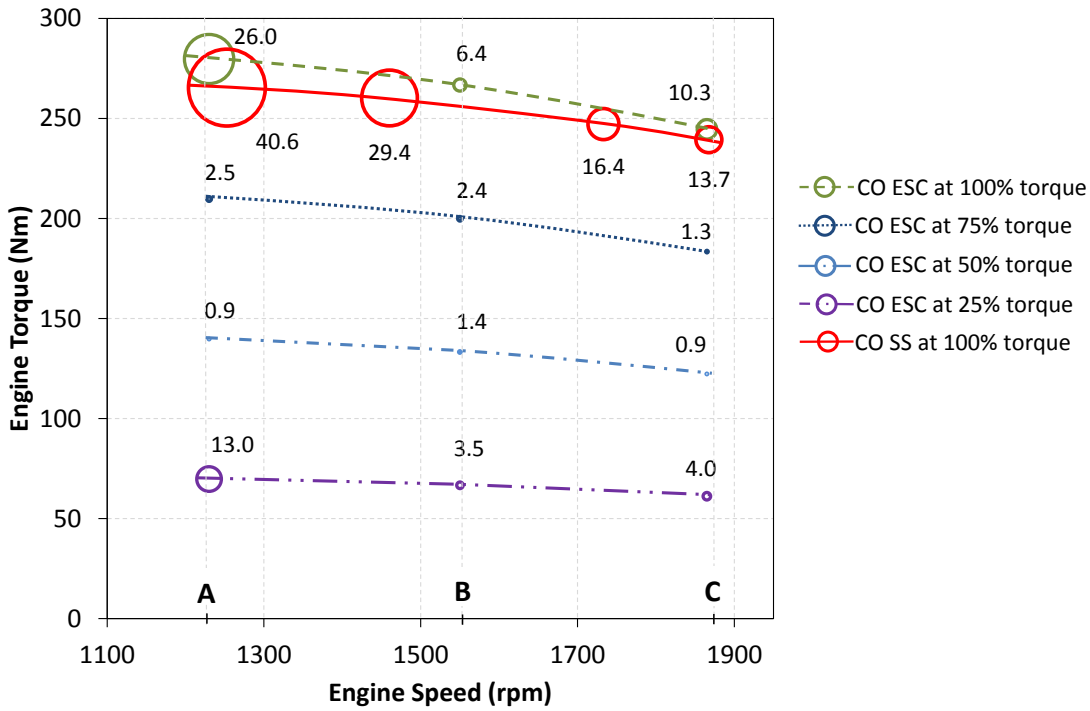

Figure 5.14: Comparison between CO (g/kWh) of steady-state and ESC tests. A, B and C are the speeds listed in Table 4.4. The circle size represents the quantity of the emission.

Chapter 6

CONCLUSION AND FUTURE WORK

6.1 Conclusion

The primary objective of this study is to assess the adequacy of the emission factors that are currently used in Australia for agricultural machinery. The source of the emission factors for agricultural applications were investigated and it was found that they were derived from old researches that did not consider the transient behaviour. The recent updates were based on transient emission testing of a heavy-duty diesel engine for on-road track applications.

This research work includes two types of steady state and two transient engine testing methods in terms of emissions production. A test was also developed to represent the transient behaviour of agricultural tractors in particular. A comparison was made between the resulted emissions of steady state and the transient and then the resulted emission of all employed tests and emissions were calculated using the Australian emission factors.

A commercial tractor (Belarus 920) was evaluated with the ECE R-49 steady

state test for emission levels. It was found that the results of the regulated emissions (NO_x and CO) for the Belarus 920 slightly exceeded the acceptable limits of the European emission standards (Directive 88/77/EEC). The NO_x and CO emissions were 1.39 % and 15.93 %, respectively higher than the limits. The variation in fuel properties of the diesel that was used in the test and the age of the tractor are believed to be the reasons for the increase.

Chapter 5 presented a comparative study between transient tests and steady state in terms of specific emissions. The results demonstrated that calculating the emission of CO_2 depending on power value resulted in 3.73 % less emission than the measured for the ESC test. The margin was larger for NO_x emission with 33.58 %. CO results showed a 44.26 % over-counting for steady state based calculated CO emission. This result suggested that transient effects that were generated in the ESC test had an evident influence on the quantity of exhaust gas emissions. Transient conditions in engine speed and torque have a major effect on emissions of CO_2, NO_x and CO.

It was found that the test design has an enormous impact on the emissions levels in heavy duty diesel engines. While the emissions of the Belarus 920 tractor might be acceptable in the ECE R-49 steady state test when compared to the European standard, the results of the ESC test exhibited a three times and four times rise over the standards for NO_x and CO respectively. Thus, this study developed a test comparable to the on-farm tractor applications. The test cycle consisted of variable loads ranging from 30 to 120 % of the maximum torque at fixed fuel injection pump setting. The results of all emissions in this test were

considerably higher than ESC results.

CO_2 emissions were calculated for the ECE R-49 , ESC, and Constant Speed tests based on fuel consumption using the Australian emission factors. The calculations showed 11.8 % (on average) less emissions than real measurements indicating there is a need for revising the emission factors or the followed methodology.

6.2 Further Work

Despite the significant findings of this study, further investigations are recommended in the following areas.

- Diesel was only used in conducting the steady state and transient experiments in this project. Nowadays, the world's attention is directed towards the alternative fuels such as biofuel. Therefore, studying the emissions of different types of fuel for tractors, such us biodiesel, is one of the objectives for a future research area.

- The sample in this study may be increased in the future to include models of agricultural tractors with variable PTO power and more sophisticated engines enforced by the resent developments such as common rail, turbocharged, intercooled, EGR and catalyst converter. Also, other types of agricultural machinery such as harvesters and irrigation water pumps may be included.

- The study can be extended to include on-farm direct emission measurements

of various farming operations, crop types, and seasons.

References

Abbaspour-Gilandeh, Y., Rahimi-Ajdadi, F., Asli-Ardeh, E. A. and Sharabiani, V. R. (2009), Application of Artificial Neural Network for Predicting Fuel Consumption of Tractor, p. unpaginated.

ABS (2012), '7121.0 - Agricultural Commodities, Australia, 2010-11, LAND USE', http://www.abs.gov.au. [accessed 20-July-2012].

Al-lwayzy, S. H., Yusaf, T. F. and Jensen, T. A. (2012), Evaluating Tractor Performance and Exhaust Gas Emissions Using Biodiesel from Cotton Seed Oil, *in* 'IOP Conference Series: Materials Science and Engineering', Vol. 36, IOP Publishing.

Baillie, C. and Chen, G. (2011), Energy, Greenhouse Gas Emissions and Irrigated Agriculture [online], *in* R. Hegarty, T. Banhazi and C. Saunders, eds, 'Society for Engineering in Agriculture Conference: Diverse Challenges, Innovative Solutions', Engineers Australia, Barton, Canberra, pp. 48–57.

Baillie, W. F. and Vasey, G. H. (1969), 'Graphical Representation of Tractor Performance', *The Journal of The Institution of Engineers, Australia* **41** (6), 83–92.

Bane, B. R. (2002), A Comparison of Steady State and Transient Emissions from a Heavy-Duty Diesel Engine, Master's thesis, West Virginia University.

Bünger, J., Krahl, J., Munack, A., Ruschel, Y., Schröder, O., Emmert, B., Westphal, G., Müller, M., Hallier, E. and Brüning, T. (2007), 'Strong Mutagenic Effects of Diesel Engine Emissions Using Vegetable Oil as Fuel', *Archives of Toxicology* **81** , 599–603. 10.1007/s00204-007-0196-3.
URL: `http://dx.doi.org/10.1007/s00204-007-0196-3`

Çengel, A. Y. and Boles, M. A. (2007), *Thermodynamics: An Engineering Apptoach*, 6th edn, MacGraw-Hill Higher Education.

Chen, G. and Baillie, C. (2007), Development of EnergyCalc-A Tool to Assess Cotton On-Farm Energy Uses, Technical Report National Centre for Engineering in Agriculture Publication 1002565/1, USQ, Toowoomba, QLD.

Chen, G. and Baillie, C. (2009), 'Development of a Framework and Tool to Asses On-Farm Energy Uses of Cotton Production', *Energy Conversion and Management* **50**(5), 1256–1263.

Chow, J. (2001), 'Diesel Engines: Environmental Impact and Control', *Journal of the Air & Waste Management Association* **51**(9), 1258–1270.

Dalal, R., Allen, D., Livesley, S. and Richards, G. (2008), 'Magnitude and Biophysical Regulators of Methane Emission and Consumption in the Australian Agricultural, Forest, and Submerged Landscapes: A Review', *Plant and Soil* **309**, 43–76.
URL: `http://dx.doi.org/10.1007/s11104-007-9446-7`

Dalgaard, T., Halberg, N. and Porter, J. (2001), 'A Model for Fossil Energy Use in Danish Agriculture Used to Compare Organic and Conventional Farming', *Agriculture, Ecosystems & Environment* **87**(1), 51–65.

DCCEE (2008), *National Greenhouse and Energy Reporting (Measurement) Technical Guidelines 2008 v1.1*, Office of Legislative Drafting and Publishing, Attorney-General's Department, Canberra, Australia.

DCCEE (2010*a*), *National Greenhouse Account (ANG) Factors*, Department of Climate Change and Energy Efficiency, Canberra, Australia.

DCCEE (2010*b*), *National Greenhouse and Energy Reporting (Measurement) Determination 2008*, Office of Legislative Drafting and Publishing, Attorney-General's Department, Canberra, Australia.

DCCEE (2011), *National Greenhouse Account Factors*, Department of Climate Change and Energy Efficiency, Canberra, Australia.

Desantes, J. M., Benajes, J. V., Molina, S. A. and Herndez, L. (2005), 'Multi-Objective Optimization of Heavy Duty Diesel Engines Under Stationary Conditions', *Proceedings of the Institution of Mechanical Engineers, Part D: Journal of Automobile Engineering* **219** (1), 77–87.

Diesel Net: Emission Test Cycle, European Transient Cycle (2010), `http://www.dieselnet.com/standards/cycles/etc.html`. [accessed 12-April-2010].

Directive 1999/96/EC (2000), 'Directive of the European Parliament and of the Council of 16 December 1999', *Official Journal of the European Communities*

(L 44), 1 – 155.

URL: `http://eur-lex.europa.eu/`

Directive 80/1269/EEC (1980), 'Council Directive of 16 December 1980 on the Approximation of the Laws of the Member States Relating to the Engine Power of Motor Vehicles', *Official Journal of the European Communities* (L 375), 46 – 67.

URL: `http://eur-lex.europa.eu/`

Directive 88/77/EEC (1988), 'Council Directive of 3 December 1987 on the Approximation of the Laws of the Member States Relating to the Measures to Be Taken Against the Emission of Gaseous Pollutants From Diesel Engines for Use in Vehicles', *Official Journal of the European Communities* (L 36), 33 – 61.

URL: `http://eur-lex.europa.eu/`

Dyer, J. and Desjardins, R. (2003), 'Simulated Farm Fieldwork, Energy Consumption and Related Greenhouse Gas Emissions in Canada', *Biosystems Engineering* **85** (4), 503 – 513.

EEA (2006), EMEP/CORINAIR Emission Inventory Guidebook - 2006, Technical Report No 11/2006.

Ericson, C., Westerberg, B. and Egnell, R. (2005), Transient Emission Predictions with Quasi Stationary Models, *in* 'Powertrain & Fluid Systems Conference & Exhibition', Society of Automotive Engineers, San Antonio, TX, USA.

Filipovic, D., Kosutic, S., Gospodaric, Z., Zimmer, R. and Banaj, D. (2006), 'The Possibilities of Fuel Savings and the Reduction of CO_2 Emissions in the Soil

Tillage in Croatia', *Agriculture, Ecosystems & Environment* **115** (14), 290 – 294.

Fleming, J. R. (1998), *Historical Perspectives on Climate Change*, Oxford University Press, New York, USA.

Forster, P., Ramaswamy, V., Artaxo, P., Berntsen, T., Betts, R., Fahey, D., Haywood, J., Lean, J., Lowe, D., Myhre, G., Nganga, J., Prinn, R., Raga, G., Schulz, M. and Dorland, R. V. (2007), Changes in Atmospheric Constituents and in Radiative Forcing, *in* S. Solomon, D. Qin, M. Manning, Z. Chen, M. Marquis, K. Averyt, M.Tignor and H. Miller, eds, 'Climate Change 2007: The Physical Science Basis. Contribution of Working Group I to the Fourth Assessment Report of the Intergovernmental Panel on Climate Change', Cambridge University Press. Cambridge, United Kingdom and New York, NY, USA.

Fritz, A. and Pitchon, V. (1997), 'The Current State of Research on Automotive Lean NO_x Catalysis', *Applied Catalysis B: Environmental* **13** (1), 1 – 25.

Garnett, T. (2011), 'Where Are the Best Opportunities for Reducing Greenhouse Gas Emissions in the Food System (Including the Food Chain)?', *Food Policy* **36** , s23 – s32.

Giakoumis, E. G. and Alafouzos, A. I. (2010), 'Comparative Study of Turbocharged Diesel Engine Emissions During Three Different Transient Cycles', *International Journal of Energy Research* **34** (11), 1002–1015.
URL: `http://dx.doi.org/10.1002/er.1625`

Grisso, R., Kocher, M. and Vaughan, D. (2004), 'Predicting Tractor Fuel Consumption', *Biological Systems Engineering: Papers and Publications* **20** (5), 553–561.

Grisso, R., Vaughan, D. and Roberson, G. (2008), 'Fuel Prediction for Specific Tractor Models', *Applied Engineering in Agriculture* **24**(4), 423–428.

Hansson, P. A., Lindgren, M., Nordin, M. and Pettersson, O. (2003), 'A Methodology for Measuring the Effects of Transient Loads on the Fuel Efficiency of Agricultural Tractors', *Applied Engineering in Agriculture* **19** (3), 251–257.

Hediger, W. (2006), Modeling GHG Emissions and Carbon Sequestration in Swiss Agriculture: An Integrated Economic Approach, *in* 'International Congress Series', Vol. 1293, Elsevier, pp. 86–95.

Houghton, J., Meiro Filho, L., Callander, B., Harris, N., Kattenburg, A. and Maskell, K. (1996), *Climate Change 1995: The Science of Climate Change*, Cambridge University Press, Cambridge, UK.

Işiktepe, M. and Sümer, S. K. (2010), 'Comparing Operational Characteristics of 540 rpm and 750 rpm PTO in Tractors Through Laboratory Tests', *Anadolu Tarm Bilimleri Dergisi* **25** (3), 168–174.

IPCC (1997*a*), *Revised 1996 IPCC Guidelines for National Greenhouse Gas Inventories: Greenhouse Gas Inventory Reference Manual*, Vol. 3, IPCC/OECD/IEA, Paris, France.

IPCC (1997*b*), *Revised 1996 IPCC Guidelines for National Greenhouse Gas*

Inventories: Greenhouse Gas Inventory Reporting Instructions, Vol. 1, IPCC/OECD/IEA, Paris, France.

IPCC (2000), *Good Practice Guidance and Uncertainty Management in National Greenhouse Gas Inventories*, Japan.

IPCC (2006), *2006 IPCC Guidelines for National Greenhouse Gas Inventories, Prepared by the National Greenhouse Gas Inventories Programme*, Published: IGES, Japan.

Jokiniemi, T. and Ahokas, J. (2011), 'Energy Saving in Farming Field Operations', **9** (Special Issue I), 63–67.

Juostas, A. and Janulevičius, A. (2009), 'Evaluating Working Quality of Tractors by Their Harmful Impact on the Environment', *Journal of Environmental Engineering and Landscape Management* **17** (2), 106–113.

Kean, A. J., Sawyer, R. F. and Harley, R. A. (2000), 'A Fuel-Based Assessment of Off-Road Diesel Engine Emissions', *Journal of the Air & Waste Management Association* **50** (11), 1929–1939.

Klingstedt, F., Arve, K., Ernen, K. and Murzin, D. Y. (2006), 'Toward Improved Catalytic Low-Temperature NO_x Removal in Diesel-Powered Vehicles', *Accounts of Chemical Research* **39** (4), 273–282.
URL: `http://pubs.acs.org/doi/abs/10.1021/ar050185k`

Lacis, A. A., Wuebbles, D. J. and Logan, J. A. (1990), 'Radiative Forcing of Climate by Change in the Vertical Distribution of Ozone', *Jornal of Geophysical Research* **95** (D7), 9971 – 9981.

Le Treut, H., Somerville, R., Cubasch, U., Ding, Y., Mauritzen, C., Mokssit, A., Peterson, T. and Prather, M. (2007), Historical Overview of Climate Change, *in* S. Solomon, D. Qin, M. Manning, Z. Chen, M. Marquis, K. Averyt, M. Tignor and H. Miller, eds, 'Climate Change 2007: The Physical Science Basis. Contribution of Working Group I to the Fourth Assessment Report of the Intergovernmental Panel on Climate Change', Cambridge University Press, Cambridge, United Kingdom and New York, NY, USA.

Leviticus, L. I., Bashford, L. L., Grisso, R. D. and Kocher, M. F. (1996), Test 1716: Belarus 900, 905, 920 and 925 Diesel 18-Speed, Technical report, University of Nebraska, Lincoln, Nebraska, USA.

Liljedahl, J. B., Turnquist, P. K., Smith, D. W. and Hoki, M. (1989), *Tractors and Their Power Units*, 4th edn, Van Nostrand Reinhold, New York, USA.

Lindgren, M. (2004), Engine Exhaust Gas Emission from Non-road Mobile Machinery: Effects of Transient Load Conditions, PhD thesis, Swedish University of Agricultural Sciences, Uppsala.

Lindgren, M. and Hansson, P. (2004), 'Effects of Transient Conditions on Exhaust Emissions from Two Non-Road Diesel Engines', *Biosystems engineering* **87** (1), 57–66.

Myher, G., Highwood, E. J., Shine, K. P. and Stordal, F. (1998), 'New Estimates of Radiative Forcing Due to Well Mixed Greenhouse Gases', *Geophysical Research Letters* **25** (14), 2715 – 2718.

Nagendran, V. (2003), Characterization of Exhaust Emissions from Catalyzed

Trap-Equipped Non-Road Heavy-Duty Diesel Engines, PhD thesis, West Virginia University.

Nakicenovic, N., Alcamo, J., Davis, G., de Vries, B., Fenhann, J., Gaffin, S., Gregory, K., Grubler, A., Jung, T. Y., Kram, T., La Rovere, E. L., Michaelis, L., Mori, S., Morita, T., Pepper, W., Pitcher, H. M., Price, L., Riahi, K., Roehrl, A., Rogner, H.-H., Sankovski, A., Schlesinger, M., Shukla, P., Smith, S. J., Swart, R., van Rooijen, S., Victor, N. and Dadi, Z. (2000), *Special Report on Emissions Scenarios : a special report of Working Group III of the Intergovernmental Panel on Climate Change*, Cambridge University Press, Cambridge.

Nelson, R. G., Hellwinckel, C. M., Brandt, C. C., West, T. O., De La Torre Ugarte, D. G. and Marland, G. (2009), 'Energy Use and Carbon Dioxide Emissions from Cropland Production in the United States, 1990–2004', *Journal of Environmental Quality* **38** (2), 418–425.

Ntziachristos, L. and Samaras, Z. (2009), *EMEP/EEA Air Pollutant Emission Inventory Guidebook 2009*, European Environment Agency, chapter Passenger Cars, Light-Duty Trucks, Heavy-Duty Vehicles Including Buses and Motorcycles, pp. 1–136. Updated May 2012.

Pulkrabek, W. (2004), *Engineering Fundamentals of the Internal Combustion Engine*, second edn, Pearson Prentice-Hall, New Jersey, USA.

Rakopoulos, C. D. and Giakoumis, E. G. (2009), *Diesel Engine Transient Operation: Principles of Operation and Simulation Analysis*, Springer, Athens, Greece.

Ramaswamy, V., Boucher, O., Haigh, J., Hauglustaine, D., Haywood, J., Myhre, G., Nakajima, T., Shi, G. and Solomon, S. (2001), Radiative forcing of climate change, *in* J. Houghton, Y. Ding, D. Griggs, M. Noguer, P. P.J. van der Linden, X. Dai, K. Maskell and C. Johnson, eds, 'Climate Change 2001: The Scientific Basis. Contribution of Working Group I to the Third Assessment Report of the Intergovernmental Panel on Climate Change', Cambridge University Press, Cambridge, United Kingdom and New York, NY, USA.

Raupach, M. and Fraser, P. (2011), Climate and Greenhouse Gases, *in* H. cleugh, M. S. Smith, M. Battaglia and P. Graham, eds, 'Climate Change: Science and Solutions for Australia', CSIRO Publishing, Collingwood, Australia.

Salam, M. U., Riethmuller, G. P., Maling, T., Short, N., Bowling, J. and Fisher, J. (2010), 'Farm Energy Calculator'.

Scarlett, A. (2001), 'Integrated Control of Agricultural Tractors and Implements: A Review of Potential Opportunities Relating to Cultivation and Crop Establishment Machinery', *Computers and electronics in agriculture* **30** (1-3), 167–191.

Schimel, D., Alves, D., Enting, I., Heimann, M., Joos, R., Raynaud, D., Wigley, T., Prather, M., Derwent, R., Ehhalt, D., Eraser, R., Sanhueza, E., Zhou, X., Jonas, R., Charlson, R., Rodhe, H., Sadasivan, S., Shine, K., Fouquart, Y., Ramaswamy, V., Solomon, S., Srinivasan, J., Albritton, D., Derwent, R., Isaksen, L., Lal, M. and Wuebbles, D. (1996), *Climate Change 1995: The Science of Climate Cliange*, Cambridge University Press, Cambridge, UK, chapter Radiative Forcing of Climate Change, pp. 65–132.

Seinfeld, J. H. and Pandis, S. N. (2006), *Atmospheric Chemistry and Physics: From Air Pollution to Climate Change*, 2nd edn, J. Wiley & Sons, Hoboken, New Jersey, USA.

Serrano, J. M., Peça, J. O., da Silva, J. M., Pinheiro, A. and Carvalho, M. (2007), 'Tractor Energy Requirements in Disc Harrow Systems', *Biosystems Engineering* **98** (3), 286–296.

Shell (2009), Shell Diesoline 10: Automotive Diesel Fuel, Technical report. PDS Number: 200004320.

Shine, K. P., Derwent, R. G., Wuebbles, D. J. and Morcrette, J.-J. (1990), *Climate Change: The IPCC Scientific Assessment*, Cambridge University Press, chapter Radiative Forcing of Climate, pp. 41 –68.

Srivastava, D. C. and Oyama, T. (2009), 'Evaluating the Emission Reduction Targets in UNFCCC Kyoto Protocol by Applying Primary Energy Data Analyses', *Journal of Asian Public policy* **2** (1), 36 – 56.

Stone, R. (1999), *Introduction to Internal Combustion Engines*, 3rd edn, Society of Automotive Engineers, Warrendale, PA, USA.

Tschoeke, H., Graf, A., Stein, J., Krüger, M., Schaller, J., Breuer, N., Engeljehringer, K. and Schindler, W. (2010), Diesel Engine Exhaust Emissions, *in* K. Mollenhauer and H. Tschoeke, eds, 'Handbook of Diesel Engines', Springer, Heidelberg Berlin, pp. 417 – 485.

Tyndall, J. (1861), 'The Bakerian Lecture: On the Absorption and Radiation of Heat by Gases and Vapours, and on the Physical Connexion of Radiation,

Absorption, and Conduction', *Philosophical Transactions of the Royal Society of London* **151** , pp. 1–36.

URL: `http://www.jstor.org/stable/108724`

Ullman, T., Webb, C. and Doorlag, M. (1999), 'Non-Road Engine Activity Analysis and Transient Cycle Generation', *SAE International* pp. 1–11.

Wark, K., Warner, C. F. and Davis, W. T. (1998), *Air Pollution: Its Origin and Control*, 3rd edn, Addison Wesley Longman.

Weaver, C. (1988), Feasibility and Cost-Effectiveness of Controlling Emissions from Diesel Engines Used in Real, Marine, Farm, and Other Mobile Off-Highway Equipment., Technical report, Report under EPA Contract No. 68-01-7288, Radian Corporation.

Winther, M. and Samaras, Z. (2009), *EMEP/EEA Air Pollutant Emission Inventory Guidebook 2009*, European Environment Agency, chapter Non-road Mobile Sources and Machinery, pp. 1–72. Updated June 2010.

Xinqun, G., Dou, D. and Winsor, R. (2010), Non-Road Diesel Engine Emissions and Technology Options for Meeting Them, *in* 'Agricultural Equipment Technology Conference', number 34 *in* 'ASABE DISTINGUISHED LECTURE SERIES', Orlando, Florida, USA, pp. 1–24.

Yastreboff, M. (2013), 'Diesel Net Emission Test cycles, CUEDC (Diesel)', `http://www.dieselnet.com/standards/cycles/etc.html`. [accessed 09-January-2013].

Appendix A

Validation of Steady-State Emission Equations

A.1 Introduction

The purpose of this appendix is to provide detail information about the steady-state model for emission calculation from the engine power. The followed procedure in testing the accuracy of the equations consists two statistical analysis methods.

A.2 Differences of the Total Emission

First of all, calculating the percentage of the difference for the total amount of each gas. The amount of each gas was calculated by multiplying the mass flow rate (g/h) of the measured and the calculated emissions by the duration of the mode (Table A.1). Then the percentages differences of the summation was determined as in Table A.2. The percentage of the differences showed insignificant variation between the measured and the calculated emissions for CO_2 and NO_x. The calculated CO_2 using the steady-state modelled equation was higher than the measured CO_2 by 1.78 % and NO_x was lower by 4.25 %. However, the percentage of CO difference was very high which needed extra verification.

Table A.1: model validation

Mode No.	CO_2 ave. (g/h)	CO_2 ave. (g)	CO_2 ave. (g/h) Cal	CO_2 ave. (g) Cal	NO_x ave. (g/h)	NO_x ave. (g)	NO_x ave. (g/h) Cal	NO_x ave. (g) Cal	CO ave. (g/h)	CO ave. (g)	CO ave. (g/h) Cal	CO ave. (g) Cal
1	2883.10	288.31	3492.31	349.23	23.95	2.39	25.56	2.56	71.65	7.17	142.99	14.30
2	7011.25	701.13	6790.22	679.02	112.69	11.27	135.78	13.58	68.11	6.81	110.82	11.08
3	10812.35	1081.23	12113.75	1211.38	289.01	28.90	241.95	24.20	27.03	2.70	69.08	6.91
4	17374.01	1737.40	20986.31	2098.63	431.07	43.11	374.57	37.46	10.74	1.07	27.45	2.75
5	25526.28	2552.63	29858.86	2985.89	554.42	55.44	483.68	48.37	51.66	5.17	20.77	2.08
6	35694.57	3569.46	38731.41	3873.14	459.33	45.93	579.87	57.99	1044.69	104.47	1266.54	126.65
7	2896.11	289.61	3543.82	354.38	39.42	3.94	28.75	2.88	40.63	4.06	142.45	14.25
8	54623.09	5462.31	51415.68	5141.57	700.90	70.09	703.08	70.31	76.84	7.68	150.09	15.01
9	38477.36	3847.74	39399.75	3939.97	702.51	70.25	586.73	58.67	52.13	5.21	52.56	5.26
10	26996.51	2699.65	27328.44	2732.84	561.19	56.12	454.16	45.42	21.28	2.13	19.11	1.91
11	18424.79	1842.48	15312.51	1531.25	256.51	25.65	293.79	29.38	51.61	5.16	50.04	5.00
12	12360.80	1236.08	8058.65	805.86	123.82	12.38	164.63	16.46	79.57	7.96	99.73	9.97
13	2885.38	288.54	3498.75	349.87	25.82	2.58	25.97	2.60	53.11	5.31	142.93	14.29

Table A.2: ECE R-49 measured emissions compared to power-based calculated emissions for Belarus 920.

Gaseous emissions	**Calculated (A)**	**Measured (B)**	**Differences %** $\left(\frac{\mathrm{A}-\mathrm{B}}{\mathrm{B}} \times \mathbf{100}\%\right)$
$\mathbf{NO}_x$	409.85 g	428.06 g	-4.25 %
CO	229.46 g	164.91 g	39.14 %
$\mathbf{CO_2}$	26053.05 g	25596.56 g	1.78 %

A.3 Analysis of Variance (ANOVA)

The data were analysed using SPSS 17.0 for Windows software. A one-way analysis of variance f-test (ANOVA) were preformed on the measured and calculated sets of data for all types of the examined emissions. The test results are presented in Table A.3 and they showed insignificant differences between the measured and the calculated emission of ECE R-49 test as p was greater than 0.05.

Table A.3: ANOVA one-way analysis of variance (f-test) results

ANOVA

		Sum of Squares	df	Mean Square	F	Sig.
CO	Between Groups	223.754	1	223.754	.281	.601
	Within Groups	19084.043	24	795.168		
	Total	19307.797	25			
NO_x	Between Groups	12.751	1	12.751	.021	.885
	Within Groups	14302.573	24	595.941		
	Total	14315.324	25			
CO_2	Between Groups	8014.572	1	8014.572	.003	.956
	Within Groups	61469025.285	24	2561209.387		
	Total	61477039.857	25			

A regression analysis between the measured and the calculated emission was preformed by using Microsoft Excel. The results are presented in Figures A.1, A.2 and A.3. The results showed very high R^2 value for all emissions types.

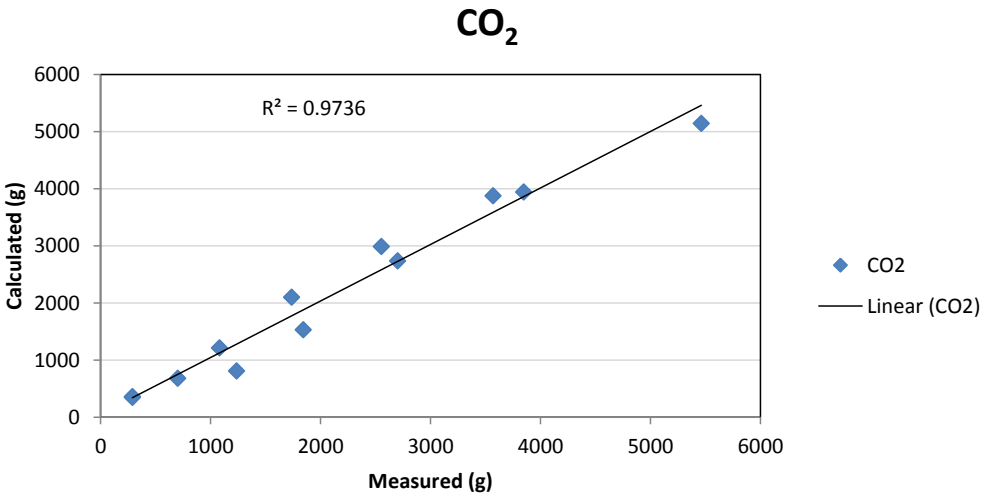

Figure A.1: CO_2 regression result

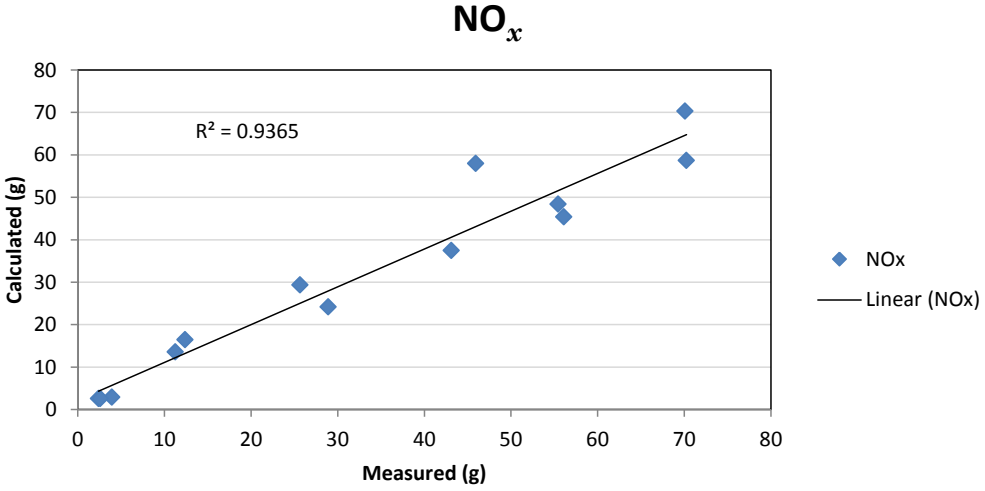

Figure A.2: NO_x regression result

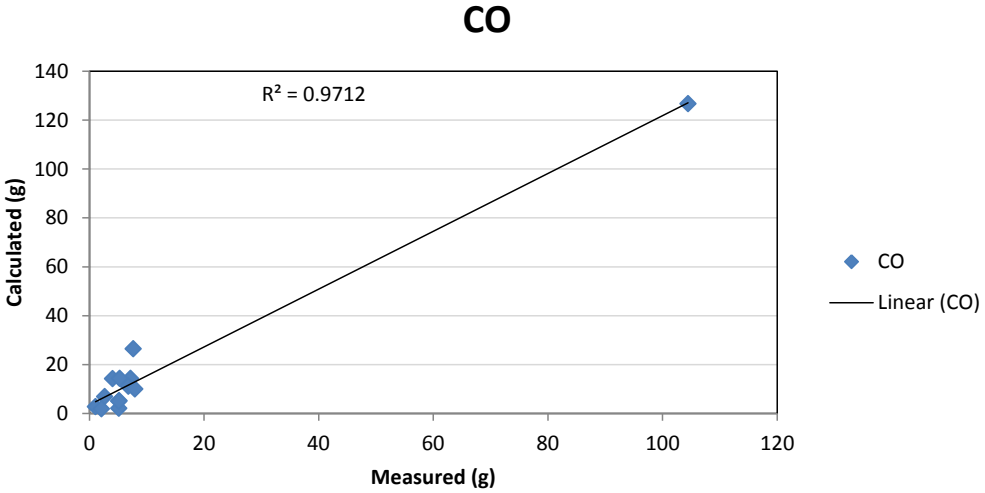

Figure A.3: CO regression result

Appendix B

CODA gas analyser specifications

Exhaust Gas Analyser

Coda Products

Manufacturers and Suppliers of Quality Diagnostic Equipment to the Motor Industry

SPECIFICATIONS:

Measurement Method: NDIR (Non-Dispersive Infrared and Electro-chemical

Measured Gases: HC as either n-Hexane or Propane; CO Carbon Monoxide; CO_2 Carbon Dioxide: O_2 Oxygen; NO, Nitric Oxide.

Measurement Range:

HC:	0 to 30,000 ppm (n-Hexane)
CO:	0 to 15%
CO_2:	0 to 20%
O_2:	0 to 25%
NO:	0 to 5,000 ppm

Measurement Resolution:

HC:	1 ppm
CO:	0.001%
CO_2:	0.01%
O_2:	0.01%
NO:	1 ppm

Measurement Accuracy:

HC:	0 to 2,000 ppm (n-Hexane)	±4 ppm abs. ±3% rel:
	2,001 to 15,000 ppm	±5% rel.
	15,001 to 30,000 ppm	±8% rel.
CO:	0 to 10%	±0.02% abs. ±3% rel.
	10.001 to 15.00%	±5% rel.
CO_2:	0 to 16%	±0.3% abs. ±3% rel.
	16.01% to 20.00%	±5% rel.
O_2:	0 to 25%	±0.1% abs. ±5% rel.
NO:	:0 to 4,000 ppm	±20 ppm abs ±4% rel.
	4,001 to 5,000 ppm	±5% rel.

Operating Altitude: -300m to +2,500m (-1,000 ft to + 8,000 ft.

Size: Length, 400 mm; Width, 360 mm; Height, 180 mm.

Weight: 5 Kilograms.

Input Power: 10.0 to 16.00 volts DC.

Response Time:

HC:	≤ 2 seconds
CO:	≤ 2 seconds
CO_2:	≤ 2 seconds
O_2:	≤ 40 seconds, 21% to <0.1
NO:	≤ 5.5 seconds

Warm-Up Time: < 20 seconds

Standards: Europe, OIML Class 0 & 1; USA (EPA) EPA, ASM; USA California, ASM/BAR 97

Operating Temperature: 0°C to 50°C (32°F to 122°F)

Operating Humidity: 0 to 95% RH (non-condensing)

Warranty: One Year Parts & Labour Return to Base Warranty

All Coda products are proudly owned, designed and manufactured in Australia.
For more information on this product and other quality products please contact your local distributor or :
Coda Products Pty Ltd, 97 Denison Street, Hamilton NSW 2303, Australia
Telephone: 61 2 4962 2575 Fax: 61 2 4969 3875 E-Mail: sales@coda.com.au Web: www.coda.com.au

Appendix C

Fuels Data Sheets


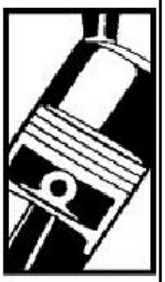



SHELL DIESOLINE 10

AUTOMOTIVE DIESEL FUEL

DESCRIPTION

Shell Diesoline 10 is a special purpose light distillate fuel for use in high speed diesel engines (i.e. those operating at greater than 800 rpm), in services involving frequent and relatively wide variations in loads and speeds. It is used in automotive (both on and off road) and industrial applications. Shell Diesoline 10 is formulated to deliver adequate lubricity, to help protect fuel pumps and injectors from wear. The cloud point is controlled on a regional and seasonal basis to for the purposes of delivering operability across Australia. Shell Diesoline 10 is an Ultra Low Sulphur Diesel fuel. The sulphur content is controlled to less than 10 mg/kg,

Shell Diesoline 10 is produced to conform to the Australian Fuel Quality Standards Act 2000 (Cth) (with cold properties controlled by Australian Standard AS3570 – 1998).

SUMMARY OF BENEFITS

Shell Diesoline 10 is an Ultra low sulphur diesel fuel designed for modern high-speed compression ignition engines. The diesel meets all the requirements of the Australian Fuel Quality Standards Act 2000 (Cth) and has a maximum sulphur content of 10 ppm. This fuel is suitable for use in modern engines that are fitted with exhaust aftertreatment devices
Shell Diesoline 10 meets all the requirements of NSW Coal Mine Health and Safety Act 2002, Clause 73(1) of the Coal Mine Health and Safety Regulation 2006 for Diesel fuel used in underground mine operations (Amended June 2009).

HEALTH & SAFETY

Shell Diesoline 10 is unlikely to present any significant health or safety hazard when properly used in the recommended application. For further guidance on Product Health & Safety refer to the appropriate Shell Material Safety Data Sheet (MSDS).


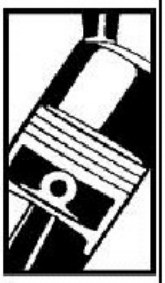



TYPICAL CHARACTERISTICS

DESCRIPTION	UNITS	METHODS	TYPICAL
Density @15°C	kg/L	D1298/D4052	0.830 [0.82 – 0.85]
Viscosity @40 °C	mm^2/s	D445	3.05
Flash Point	°C	D93	79
Sulphur	mg/kg	D2622/D5453	8
Cetane Index	-	D4737	49
Distillation - 95%	°C	D86	340
Water	% volume	D95	<0.05
Ash	% mass	D482	<0.01
Sediment	% mass	D473	<0.01
Filterability Test	% mass	D2068	1.05
Strong Acid Number	mg KOH/g	D974	Nil
Total Acid Number	mg KOH/g	D664	<0.1
Copper Corrosion	-	D130	1a
Lubricity (HFRR test)	Microns	IP 450	400

Document Information	
PDS Number:	200004320
Date Revised:	03/07/2009

PRODUCT SPECIFICATION

BP ULTIMATE DIESEL

Supply Area : Australia

Product Code : ULT

Application : A diesel fuel containing a performance additive. Not for Aviation use. This fuel complies with the requirements of the West Australian Environment Protection (Diesel & Petrol) regulations of 2001, Queensland EPA regulations of 2000 and the Fuel Quality Standards Determination (Diesel) 2001. SA Environment Protection (Motor Vehicle Fuel Quality) Policy 2002. It meets the requirements of BS EN 590 and ASTM D975 for lubricity and AS3570 of 1998 for cloud point.

TEST	UNIT	LIMIT	TYPICAL	METHOD
Appearance @ 20 °C		Clear and bright	Clear and bright	Visual
Haziness		1 max.	1	ASTM D4176 Proc 2
Colour		2 max	1	ASTM D1500
Density @ 15°C	kg/L	0.85 max	0.83	ASTM D4052
API Gravity @ 15°C		41-33	36	
Cetane Index		46 min	52	ASTM D4737
Flash Point	°C	61.5 min	66	ASTM D93
Viscosity - kinematic @ 40°C	cSt	2.0 - 4.5	3.0	ASTM D445
Cloud Point OR	°C	Table 1		ASTM D2500
Cold Filter Plugging Point	°C	Table 1		IP 309
Carbon Residue on 10% bottoms - Ramsbottom or - Conradson	% mass % mass	0.2 max 0.16 max	0.01	ASTM D524 ASTM D189
Ash	% mass	0.01 max	<0.001	ASTM D482
Water and Sediment	% vol	0.05 max	<0.01	ASTM D2709
Acid -total -strong	mg KOH/g mg KOH/g	0.5 max Nil	<0.1 Nil	ASTM D974 ASTM D974
Sulphur-total	mg/kg	10 max	5	ASTM D4294
Copper Corrosion 3h @ 100°C		2 max	1	ASTM D130
Distillation 95% recovered	°C	361 max	350	ASTM D86
Lubricity wear scar diameter Note 1	mm	0.46 max	0.40	ASTM D6079
Oxidation Stability	mg/L	25 max	5	ASTM D2274

PRODUCT SPECIFICATION

BP ULTIMATE DIESEL

TEST	UNIT	LIMIT	TYPICAL	METHOD
Conductivity	pS/m	50 min	100	ASTM D 2624
Energy per unit mass	MJ/kg		45.6	BS 2869
Energy per unit volume	MJ/L		38.0	
Filter blocking tendency		2.0 max	1.01	IP 387

Notes

1) includes a lubricity additive
2) includes a detergent additive to clean fouled injectors
3) includes an additive to protect against corrosion
4) includes an additive to reduce foaming and splash back.
5) Product may be supplied to cloud point spec or cold filter plugging point CFPP spec

TABLE 1 -MAXIMUM CLOUD POINT at time of supply into local Terminal.

Supply Location	Jan	Feb	Mar	Apr	May	Jun	Jul	Aug	Sept	Oct	Nov	Dec
Darwin, Gove,	15	15	12	9	8	8	8	10	14	15	15	15
Adelaide	8	6	4	2	1	1	1	2	4	5	6	9
Brisbane	11	7	3	0	-1	-1	-1	0	2	7	9	13
Gladstone Mackay	15	12	7	4	2	2	2	4	7	12	15	15
Townsville	15	15	11	7	6	6	6	8	11	15	15	15
Cairns	15	15	12	7	7	7	7	9	12	15	15	15
South West Australia	8	6	0	0	0	0	0	0	3	5	8	8
Geraldton	8	6	0	0	0	0	0	0	3	5	8	8
Broome, Wyndham	15	15	12	9	8	8	8	10	14	15	15	15
Port Hedland, Dampier, NW Cape	15	15	9	6	5	5	5	7	11	15	15	15
Melbourne	9	6	3	1	0	0	0	1	2	4	6	8
Geelong	9	6	3	-1	-2	-2	-2	1	2	4	6	8
Sydney Newcastle	9	5	2	0	-1	-1	-1	0	2	5	7	9
Tasmania	3	1	-1	-2	-3	-3	-3	-3	-1	0	2	3

Cold flow improvers may be used to get better cold temperature performance. When cold flow improvers are used the maximum cloud point may be relaxed according to the difference between the cloud point and cold filter plugging point as in the following table.

Difference between specified cloud point and cold filter plugging point.	0-3	4	5 to 6	7 to 8	9 or more
Permitted Cloud point increase above the specification	0	+1	+2	+3	+4

BP guarantees that this product is fit for the purposes described above, and meets all legislative requirements. BP reserves the right to vary this specification from time to time without notice provided the product continues to meet legislative requirements

ANNEX IV

TECHNICAL CHARACTERISTICS OF REFERENCE FUEL PRESCRIBED FOR APPROVAL TESTS AND TO VERIFY CONFORMITY OF PRODUCTION

1. DIESEL FUEL ([1])

Parameter	Unit	Limits ([2])		Test Method	Publication
		Minimum	Maximum		
Cetane number ([3])		52	54	EN-ISO 5165	1998 ([4])
Density at15 °C	kg/m³	833	837	EN-ISO 3675	1995
Distillation:					
— 50 % point	°C	245	—	EN-ISO 3405	1998
— 95 % point	°C	345	350	EN-ISO 3405	1998
— final boiling point	°C	—	370	EN-ISO 3405	1998
Flash point	°C	55	—	EN 27719	1993
CFPP	°C	—	– 5	EN 116	1981
Viscosity at 40 °C	mm²/s	2,5	3,5	EN-ISO 3104	1996
Polycyclic aromatic hydrocarbons	%m/m	3,0	6,0	IP 391 (*)	1995
Sulphur content ([5])	mg/kg	—	300	pr. EN-ISO/DIS 14596	1998 ([4])
Copper corrosion		—	1	EN-ISO 2160	1995
Conradson carbon residue (10 % DR)	%m/m	—	0,2	EN-ISO 10370	
Ash content	%m/m	—	0,01	EN-ISO 6245	1995
Water content	%m/m	—	0,05	EN-ISO 12937	1995
Neutralisation (strong acid) number	mg KOH/g	—	0,02	ASTM D 974-95	1998 ([4])
Oxidation stability ([6])	mg/ml	—	0,025	EN-ISO 12205	1996
(*) New and better method for polycyclic aromatics under development	%m/m	—	—	EN 12916	[1997] ([4])

([1]) If it is required to calculate the thermal efficiency of an engine or vehicle, the calorific value of the fuel can be calculated from:
Specific energy (calorific value) (net) in MJ/kg = $(46{,}423 - 8{,}792d^2 + 3{,}170d)(1 - (x + y + s)) + 9{,}420s - 2{,}499x$
where,
d = the density at 15 °C
x = the proportion by mass of water (% divided by 100)
y = the proportion by mass of ash (% divided by 100)
s = the proportion by mass of sulphur (% divided by 100).

([2]) The values quoted in the specification are 'true values'. In establishment of their limit values the terms of ISO 4259, *Petroleums products – Determination and application of precision data in relation to methods of test*, have been applied and in fixing a minimum value, a minimum difference of 2R above zero has been taken into account; in fixing a maximum and minimum value, the minimum difference is 4R (R = reproducibility). Notwithstanding this measure, which is necessary for statistical reasons, the manufacturer of a fuel should nevertheless aim at a zero value where the stipulated maximum value is 2R and at the mean value in the case of quotations of maximum and minimum limits. Should it be necessary to clarifiy the question as to whether a fuel meets the requirements of the specification, the terms of ISO 4259 should be applied.

([3]) The range for cetane number is not in accordance with the requirement of a minimum range of 4R. However, in the case of dispute between fuel supplier and fuel user, the terms in ISO 4259 can be used to resolve such disputes provided replicate measurements, of sufficient number to achieve the necessary precision, are made in preference to single determinations.

([4]) The month of publication will be completed in due course.

([5]) The actual sulphur content of the fuel used for the test shall be reported. In addition, the sulphur content of the reference fuel used to approve a vehicle or engine against the limit values set out in row B of the Table in section 6.2.1. of Annex I to this Directive shall have a maximum sulphur content of 50 ppm. The Commission will as soon as possible, but no later than 31 December 1999, bring forward a modification to this Annex reflecting the market average for fuel sulphur content in respect of the fuel defined in Annex IV to Directive 98/70/EC.

([6]) Even though oxidation stability is controlled, it is likely that shelf life will be limited. Advice should be sought from the supplier as to storage conditions and life.

Appendix D

Nebraska Test Report for Belarus 920

1-1-1996

Test 1716: Belarus 900, 905, 920 and 925 Diesel 18-Speed

Tractor Museum
University of Nebraska-Lincoln, TractorMuseumArchives@unl.edu

NEBRASKA OECD TRACTOR TEST 1716—SUMMARY 211
BELARUS 925 DIESEL
ALSO BELARUS 900, 905 and 920 DIESEL
18 SPEED

POWER TAKE-OFF PERFORMANCE

Power HP (kW)	Crank shaft speed rpm	Gal/hr (l/h)	lb/hp.hr (kg/kW.h)	Hp.hr/gal (kW.h/l)	Mean Atmospheric Conditions
MAXIMUM POWER AND FUEL CONSUMPTION					
Rated Engine Speed (PTO speed–952 rpm)					
92.37 *(68.88)*	2200	5.40 *(20.45)*	0.410 *(0.249)*	17.10 *(3.37)*	
VARYING POWER AND FUEL CONSUMPTION					
92.37 *(68.88)*	2200	5.40 *(20.45)*	0.410 *(0.249)*	17.10 *(3.37)*	Air temperature
81.48 *(60.76)*	2279	4.79 *(18.14)*	0.412 *(0.251)*	17.00 *(3.35)*	75°F *(24°C)*
61.26 *(45.68)*	2294	3.81 *(14.41)*	0.436 *(0.265)*	16.09 *(3.17)*	Relative humidity
41.17 *(30.70)*	2312	2.91 *(11.01)*	0.496 *(0.302)*	14.15 *(2.79)*	56%
20.75 *(15.47)*	2331	2.05 *(7.79)*	0.694 *(0.422)*	10.10 *(1.99)*	Barometer
0.78 *(0.58)*	2354	1.33 *(5.02)*	11.983 *(7.289)*	0.59 *(0.12)*	29.03"Hg *(98.31 kPa)*

Maximum Torque 270 lb.-ft. *(366 Nm)* at 1600 rpm
Maximum Torque Rise 22.5%
Torque rise at 1800 engine rpm 17%

DRAWBAR PERFORMANCE
(Unballasted—Front Drive in Automatic mode)
FUEL CONSUMPTION CHARACTERISTICS

Power Hp (kW)	Drawbar pull lbs (kN)	Speed mph (km/h)	Crank-shaft speed rpm	Slip %	Fuel Consumption lb/hp.hr (kg/kW.h)	Hp.hr/gal (kW.h/l)	Temp.°F (°C) cool-ing med	Air dry bulb	Barom. inch Hg (kPa)
Maximum Power 9th(4H) Gear									
85.40 *(63.68)*	5544 *(24.66)*	5.78 *(9.30)*	2204	4.88	0.447 *(0.272)*	15.69 *(3.09)*	179 *(81)*	66 *(19)*	29.04 *(98.34)*
75% of Pull at Maximum Power—9th(4H) Gear									
67.25 *(50.15)*	4152 *(18.47)*	6.07 *(9.78)*	2283	3.59	0.476 *(0.289)*	14.75 *(2.90)*	169 *(76)*	68 *(20)*	29.04 *(98.34)*
50% of Pull at Maximum Power—9th(4H) Gear									
45.72 *(34.09)*	2766 *(12.30)*	6.20 *(9.97)*	2302	2.43	0.527 *(0.320)*	13.31 *(2.62)*	159 *(71)*	70 *(21)*	29.04 *(98.34)*
75% of Pull at Reduced Engine Speed—12th(7L) Gear									
67.35 *(50.23)*	4151 *(18.46)*	6.09 *(9.79)*	1785	3.82	0.455 *(0.277)*	15.41 *(3.04)*	178 *(81)*	71 *(22)*	29.03 *(98.31)*
50% of Pull at Reduced Engine Speed—12th(7L) Gear									
45.71 *(34.09)*	2773 *(12.33)*	6.18 *(9.95)*	1791	2.66	0.473 *(0.288)*	14.81 *(2.92)*	164 *(73)*	71 *(22)*	29.03 *(98.31)*

Location of Test: Tractor Testing Laboratory, University of Nebraska, Lincoln, Nebraska 68583-0832

Dates of Test: September 12-23, 1996

Manufacturer: Minsk Tractor Works, 29 Dolgobrodskaya Minsk, Belarus 220668

FUEL OIL AND TIME: Fuel No. 2 Diesel **Cetane No.** 53.9 **Specific gravity converted to 60°/60° F *(15°/15°C)*** 0.8422 **Fuel weight** 7.012 lbs/gal *(0.840 kg/l)* **Oil SAE** 10W30 **API service classification** SH/CG-4 **To motor** 2.944 gal *(11.144 l)* **Drained from motor** 2.622 gal *(9.943 l)* **Transmission and final drive lubricant** SAE 80W90 gear lubricant **Front axle lubricant** SAE 80W90 gear lubricant **Hydraulic lubricant** SAE 10 **Total time engine was operated** 22.5 hours.

ENGINE: Make MTZ Diesel **Model** D-243 **Type** four cylinder vertical with turbocharger **Serial No.** 198810 **Crankshaft** lengthwise **Rated rpm** 2200 **Bore and stroke** (as specified) 4.331" × 4.921" *(110.0 mm × 125.0 mm)* **Compression ratio** 16.0 to 1 **Displacement** 290 cu in *(4750 ml)* **Starting system** 12 volt **Lubrication** pressure **Air cleaner** paper element **Oil filter** full flow centrifugal **Oil cooler** radiator for crankcase oil **Fuel filter** two paper elements **Muffler** none **Exhaust** vertical **Cooling medium temperature control** one thermostat.

ENGINE OPERATING PARAMETERS: fuel rate: 36.8-38.8 lb/h *(16.7-17.6 kg/h)* **high idle:** 2325-2375 rpm **Turbo boost** nominal 11.0 psi *(76 kPa)* as measured 10.0 psi *(69 kPa)*

CHASSIS: Type front wheel assist **Serial No.** 404869 **Tread width** rear 60.0" *(1524 mm)* to 82.7" *(2100 mm)* front 59.5" *(1510 mm)* to 70.9" *(1800 mm)* **Wheel base** 96.5" *(2450 mm)* **Hydraulic control system** direct engine drive with throwout lever (engaged during test) **Transmission** selective gear fixed ratio **Nominal travel speeds mph *(km/h)*** first 1.28 *(2.06)* second 1.69 *(2.72)* third 2.19 *(3.52)* fourth 2.88 *(4.63)* fifth 3.71 *(5.97)* sixth 4.56 *(7.34)* seventh 4.91 *(7.90)* eighth 5.40 *(8.69)* ninth 6.03 *(9.70)* tenth 6.32 *(10.17)* eleventh 7.14 *(11.49)* twelfth 7.76 *(12.49)* thirteenth 8.35 *(13.43)* fourteenth 9.19 *(14.79)* fifteenth 10.26 *(16.51)* sixteenth 12.15 *(19.55)* seventeenth 17.09 *(27.50)* eighteenth 22.60 *(36.37)* reverse 2.63 *(4.24)*, 3.49 *(5.62)* 4.42 *(7.12)* 5.95 *(9.57)* **Clutch** single dry disc operated by foot pedal **Brakes** dry disc operated by two foot pedals which can be locked together **Steering** hydrostatic **Power take-off** 540 rpm at 2075 engine rpm or 1000 rpm at 2310 engine rpm **Unladen tractor mass** 8510 lb *(3860 kg)*.

DRAWBAR PERFORMANCE

(Unballasted—Front Drive in Automatic mode)

MAXIMUM POWER IN SELECTED GEARS

Power Hp *(kW)*	Drawbar pull lbs *(kN)*	Speed mph *(km/h)*	Crank-shaft speed rpm	Slip %	Fuel Consumption lb/hp.hr *(kg/kW.h)*	Hp.hr/gal *(kW.h/l)*	Temp.°F (°C) cool-ing med	Air dry bulb	Barom. inch Hg *(kPa)*
				5th(3L) Gear					
77.25 *(57.60)*	8775 *(39.03)*	3.30 *(5.31)*	2206	11.88	0.494 *(0.300)*	14.21 *(2.80)*	168 *(76)*	62 *(17)*	28.69 *(97.16)*
				6th(4L) Gear					
83.09 *(61.96)*	7301 *(32.47)*	4.27 *(6.87)*	2205	7.28	0.461 *(0.280)*	15.23 *(3.00)*	174 *(79)*	61 *(16)*	29.02 *(98.27)*
				7th(3H) Gear					
84.70 *(63.16)*	6888 *(30.64)*	4.61 *(7.42)*	2201	6.50	0.451 *(0.274)*	15.56 *(3.06)*	173 *(78)*	62 *(17)*	29.04 *(98.34)*
				8th(5L) Gear					
84.20 *(62.79)*	6157 *(27.39)*	5.13 *(8.25)*	2203	5.70	0.453 *(0.275)*	15.48 *(3.05)*	175 *(79)*	65 *(18)*	29.04 *(98.34)*
				9th(4H) Gear					
85.40 *(63.68)*	5544 *(24.66)*	5.78 *(9.30)*	2204	4.88	0.447 *(0.272)*	15.69 *(3.09)*	179 *(81)*	66 *(19)*	29.04 *(98.34)*
				10th(6L) Gear					
82.72 *(61.68)*	5083 *(22.61)*	6.10 *(9.82)*	2213	4.58	0.461 *(0.280)*	15.21 *(3.00)*	179 *(81)*	68 *(20)*	29.03 *(98.31)*
				11th(5H) Gear					
82.67 *(61.65)*	4493 *(19.99)*	6.90 *(11.10)*	2200	4.05	0.461 *(0.280)*	15.23 *(3.00)*	181 *(83)*	69 *(21)*	29.02 *(98.27)*
				12th(7L) Gear					
81.41 *(60.71)*	4051 *(18.02)*	7.54 *(12.13)*	2203	3.59	0.465 *(0.283)*	15.09 *(2.97)*	181 *(83)*	69 *(21)*	29.02 *(98.27)*
				13th(6H) Gear					
82.36 *(61.42)*	3792 *(16.87)*	8.15 *(13.12)*	2210	3.44	0.461 *(0.280)*	15.21 *(3.00)*	180 *(82)*	69 *(21)*	29.02 *(98.27)*

TRACTOR SOUND LEVEL WITH CAB	Front Wheel Drive Automatic dB(A)	2WD dB(A)
At 75% load in 9th(4H) Gear	90.0	89.0
Bystander in 18th(9H) Gear	—	91.5

TIRES AND WEIGHT — **Tested Without Ballast**

Rear Tires—No., size, ply & psi *(kPa)*: Two 16.9R38; 8; 16 *(110)*

Front Tires—No., size, ply & psi *(kPa)*: Two 13.6R20; 6; 20 *(140)*

Height of Drawbar: 20.0 in *(510 mm)*

Static Weight with Operator—Rear: 5766 lb *(2615 kg)*

—Front: 2908 lb *(1319 kg)*

—Total: 8674 lb *(3934 kg)*

REPAIRS AND ADJUSTMENTS: The transmission shifting linkage was adjusted prior to the maximum drawbar pull tests.

REMARKS: All test results were determined from observed data obtained in accordance with official OECD, SAE and Nebraska test procedures. This tractor did not meet manufacturers claim of 11.8 GPM *(44.7 l/m)* hydraulic flow. For the maximum power tests, the fuel temperature at the injection pump inlet was maintained at 148° F *(64° C)*. The performance figures on this summary were taken from a test conducted under the OECD Code II restricted standard test code procedure.

We, the undersigned, certify that this is a true and correct report of official Tractor No. **1716**, Summary 211, October 16, 1996.

LOUIS I. LEVITICUS
Engineer-in-Charge

L.L. BASHFORD
R.D. GRISSO
M.F. KOCHER
Board of Tractor Test Engineers

DRAWBAR PERFORMANCE
(Unballasted—Front Drive in 2WD mode)
FUEL CONSUMPTION CHARACTERISTICS

Power Hp *(kW)*	Drawbar pull lbs *(kN)*	Speed mph *(km/h)*	Crank-shaft speed rpm	Slip %	Fuel Consumption lb/hp.hr *(kg/kW.h)*	Hp.hr/gal *(kW.h/l)*	Temp.°F (°C) cool-ing med	Air dry bulb	Barom. inch Hg *(kPa)*
Maximum Power—9th(4H) Gear									
84.38	5587	5.66	2205	6.63	0.451	15.54	175	66	29.04
(62.92)	*(24.85)*	*(9.11)*			*(0.274)*	*(3.06)*	*(79)*	*(19)*	*(98.34)*
75% of Pull at Maximum Power—9th(4H) Gear									
67.49	4218	6.00	2290	4.72	0.477	14.72	167	68	29.04
(50.32)	*(18.76)*	*(9.66)*			*(0.290)*	*(2.90)*	*(75)*	*(20)*	*(98.34)*
50% of Pull at Maximum Power—9th(4H) Gear									
46.02	2815	6.13	2304	3.35	0.524	13.38	159	69	29.04
(34.32)	*(12.52)*	*(9.87)*			*(0.319)*	*(2.64)*	*(70)*	*(21)*	*(98.34)*
75% of Pull at Reduced Engine Speed—12th(7L) Gear									
67.59	4222	6.00	1782	4.87	0.451	15.56	182	70	29.04
(50.40)	*(18.78)*	*(9.66)*			*(0.274)*	*(3.07)*	*(83)*	*(21)*	*(98.34)*
50% of Pull at Reduced Engine Speed—12th(7L) Gear									
45.95	2812	6.13	1793	3.35	0.466	15.06	164	71	29.03
(34.26)	*(12.51)*	*(9.87)*			*(0.283)*	*(2.97)*	*(73)*	*(22)*	*(98.31)*
MAXIMUM POWER IN SELECTED GEARS									
5th(3L) Gear									
63.52	7224	3.30	2281	14.53	0.524	13.39	162	64	28.67
(47.37)	*(32.13)*	*(5.31)*			*(0.319)*	*(2.64)*	*(72)*	*(18)*	*(97.09)*
6th(4L) Gear									
77.39	7132	4.07	2198	11.15	0.489	14.33	172	63	28.68
(57.71)	*(31.72)*	*(6.55)*			*(0.298)*	*(2.82)*	*(78)*	*(17)*	*(97.12)*
7th(3H) Gear									
81.09	6964	4.37	2214	11.66	0.476	14.73	164	61	29.03
(60.47)	*(30.98)*	*(7.03)*			*(0.290)*	*(2.90)*	*(73)*	*(16)*	*(98.31)*
8th(5L) Gear									
82.64	6184	5.01	2208	7.90	0.462	15.18	170	63	29.04
(61.63)	*(27.51)*	*(8.07)*			*(0.281)*	*(2.99)*	*(77)*	*(17)*	*(98.34)*
9th(4H) Gear									
84.38	5587	5.66	2205	6.63	0.451	15.54	175	66	20.04
(62.92)	*(24.85)*	*(9.11)*			*(0.274)*	*(3.06)*	*(79)*	*(19)*	*(98.34)*
10th(6L) Gear									
83.84	5255	5.98	2213	6.27	0.459	15.28	173	67	29.03
(62.52)	*(23.38)*	*(9.63)*			*(0.279)*	*(3.01)*	*(78)*	*(19)*	*(98.31)*
11th(5H) Gear									
82.59	4522	6.85	2212	5.02	0.461	15.22	177	69	29.02
(61.59)	*(20.11)*	*(11.02)*			*(0.280)*	*(3.00)*	*(80)*	*(21)*	*(98.27)*
12th(7L) Gear									
81.51	4108	7.44	2202	4.57	0.463	15.15	176	69	29.02
(60.79)	*(18.27)*	*(11.98)*			*(0.281)*	*(2.99)*	*(80)*	*(21)*	*(98.27)*
13th(6H) Gear									
82.43	3838	8.05	2203	4.19	0.461	15.22	175	69	29.02
(61.47)	*(17.07)*	*(12.96)*			*(0.280)*	*(3.00)*	*(79)*	*(21)*	*(98.27)*

THREE POINT HITCH PERFORMANCE (OECD Static Test)

CATEGORY: II		
Quick Attach: None		
Maximum Force Exerted Through Whole Range:	3125 lbs	*(13.9 kN)*
i) Opening pressure of relief valve:	NA	
Sustained pressure with relief valve open:	2710 psi	*(187 bar)*
ii) Pump delivery rate at minimum pressure and rated engine speed:	10.9 GPM	*(41.3 l/min)*
iii) Pump delivery rate at maximum hydraulic power:	8.1 GPM	*(30.7 l/min)*
Delivery pressure:	2440 psi	*(168 bar)*
Power:	11.5 HP	*(8.6 kW)*

HITCH DIMENSIONS AS TESTED—NO LOAD

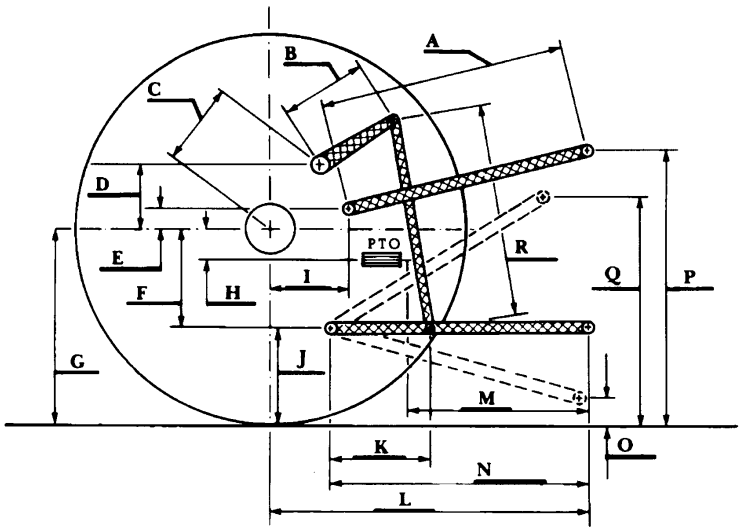

	inch	*mm*
A	22.0	*559*
B	10.2	*266*
C	17.3	*439*
D	10.6	*270*
E	6.0	*152*
F	10.4	*264*
G	27.4	*695*
H	4.8	*122*
I	19.0	*483*
J	17.0	*431*
K	18.2	*462*
L	38.9	*988*
M	22.5	*572*
N	31.7	*805*
O	8.0	*203*
P	41.0	*1041*
Q	31.8	*806*
R	17.8	*452*

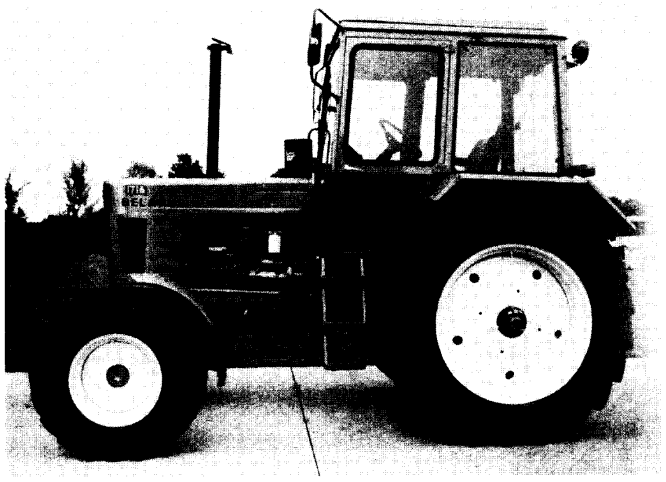

Belarus 925 Diesel

Agricultural Research Division
Institute of Agriculture and Natural Resources
University of Nebraska≈Lincoln
Darrell Nelson, Dean and Director

Appendix E

Weather report samples from USQ weather station

Toowoomba, QLD, 4350 Current Weather Conditions

[Select Refresh to Update]

Updated Automatically by Ambient Weather's Virtual Weather Station V14.00

Weather Links

- Detailed Conditions
- Daily Tabular Data

Conditions at 12:45pm on 14/11/12	25.3°C
Temperature	
Dew Point	6.0°C
Humidity	29%
Barometer - Sea Level	1017.0hPa Rate - 0.346hPa/hr
Wind Direction	E
Heat Index	24.8°C
Rainfall for Today	0.0mm
Evapotranspiration	0.0mm

Today's Extremes

High Temperature	25.3°C at 12:34pm
Low Temperature	16.2°C at 2:36am
High Heat Index	24.8°C at 12:34pm
Peak Wind Gust	0km/hr at 12:00am

Astronomical Data

Sunrise	4:54am
Sunset	6:21pm
Moonrise	4:49am
Moonset	6:44pm

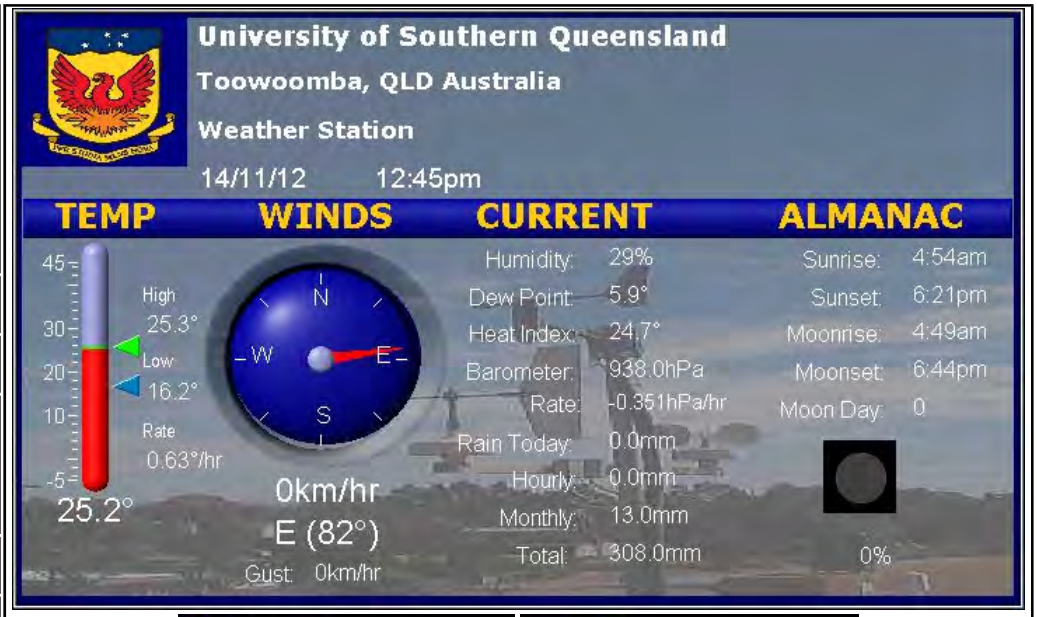

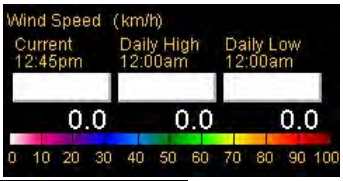

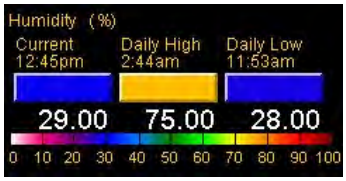

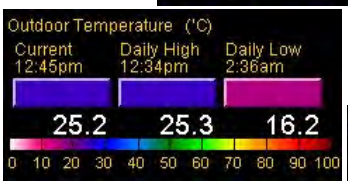

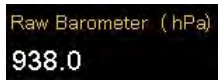

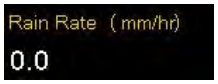

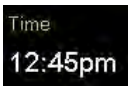

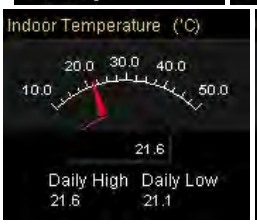

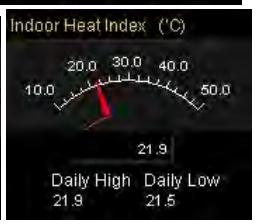

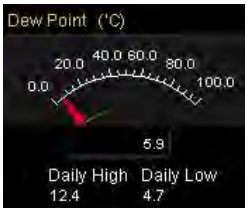

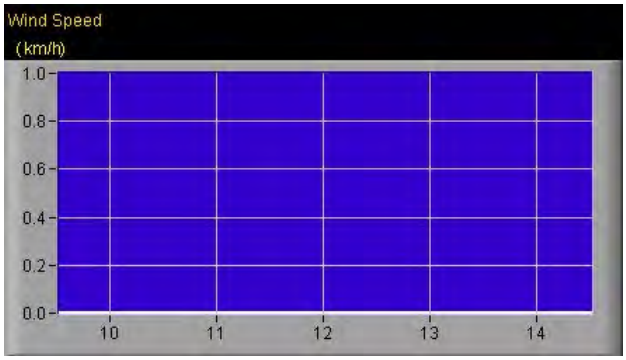

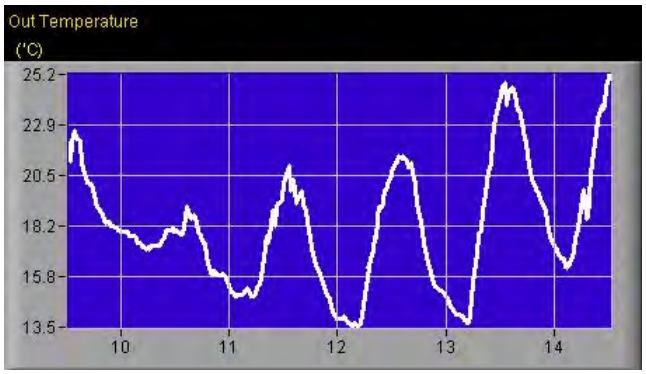

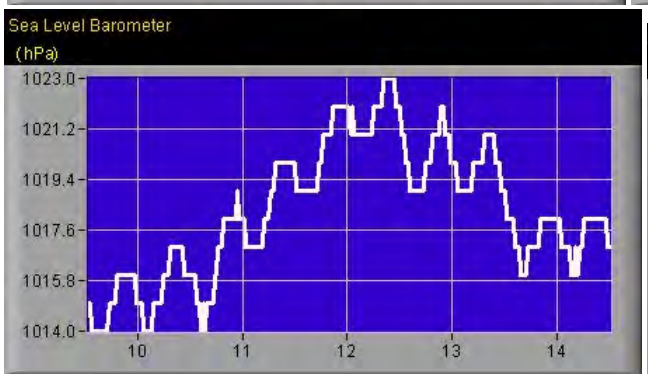

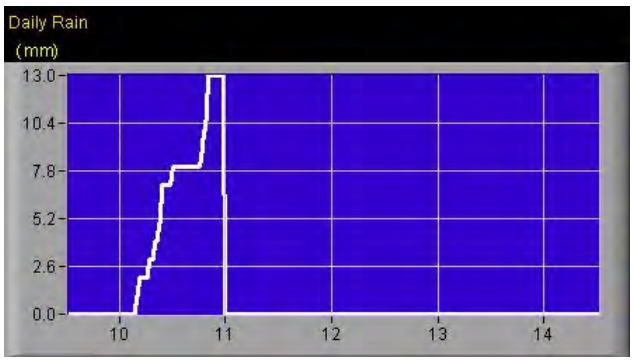

Weather Station

Physics, Department of Biological and Physical Sciences

University of Southern Queensland
Toowoomba(27.605S, 151.919E, Alt 693m), Australia.
Updated: 14/11/12 at 10:45am Sunrise: 4:54am Sunset: 6:21pm
NOTE: You may need to press reload / refresh to get the latest information

- More Weather Data (Including Graphs)
- Current UV levels in Toowoomba
- Cloud Monitoring at USQ
- USQ Physics Laboratory Indoor Weather Conditions
- Useful Links Page

Weather Station Forecast (Next 12 to 24 hours)

Current Weather Conditions (Last Updated: 10:45am at 14/11/12)

- Outdoor Temperature: **23.9°C** High: **24.0°C** at 10:41am **Lo: 16.2°C** at 2:36am
- Outdoor Heat Index: **23.5°C** High: 23.6°C at 10:41am Lo: 18.1°C at 2:36am
- Wind Chill: **23.9°C** Today's High: 24.0°C at 10:41am Lo: 16.2°C at 2:36am
- Barometric Pressure: **1018.0hPa** High: **1018.0hPa** at 12:00am Lo: **1016.0hPa** at 3:12am
- Barometric Trend: **Steady**
- Relative Humidity: **48%** High: 50% at 3:57am Lo: 48% at 12:00am
- Av Wind Speed (15 min): **0km/hr** Today's High: 0km/hr at 12:00am Lo: 0km/hr at 12:00am
- Av. Wind Speed (Previous Hour): **0km/hr**
- Wind Gust **0km/hr** Today's High: 0km/hr at 12:00am Lo: 0km/hr at 12:00am
- Current Wind Direction: **E**
- Av. Wind Direction (Previous Hour): **88°**
- Dew Point: **5.8°C** Today's High: 12.4°C at 12:00am Lo: 4.7°C at 9:57am
- Daily Rainfall: **0.0mm**

For more information: Kim Larsen

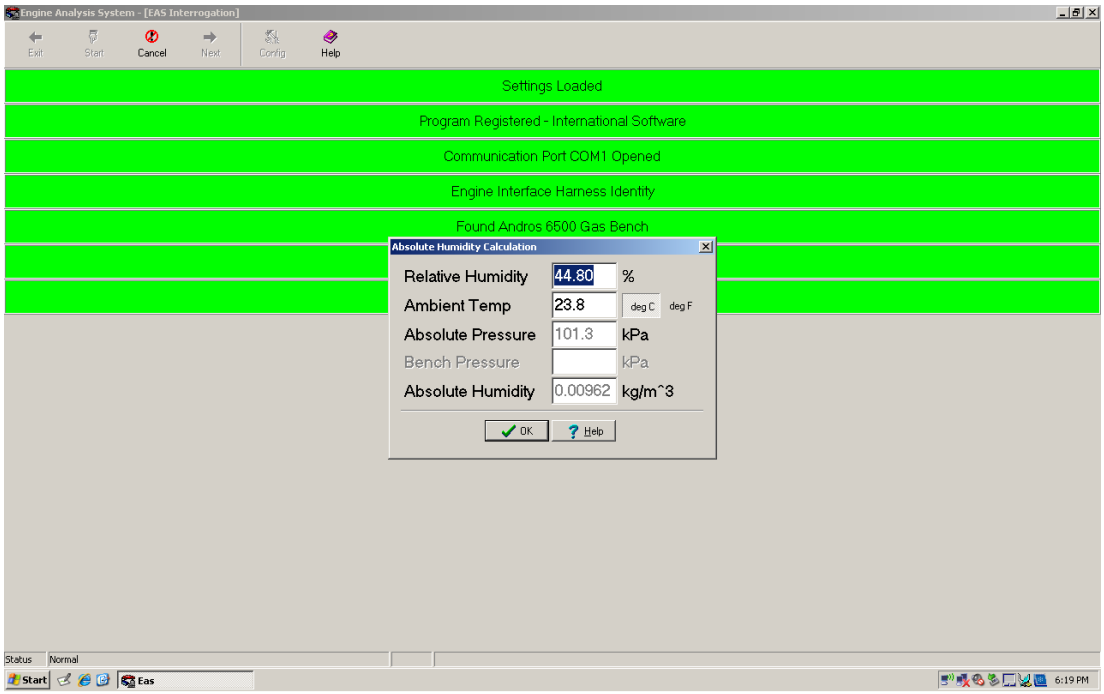

Figure E.1: CODA internal weather station readings sample.